University of Alberta

Voltage gated potassium currents in the Mauthner and MiD2cm cells of larval zebrafish

by

Daniel L. Brewster

A thesis submitted to the Faculty of Graduate Studies and Research
in partial fulfillment of the requirements for the degree of

Master of Science
in
Physiology, Cell and Developmental Biology

Biological Sciences

Spring 2012
Edmonton, Alberta

Abstract

The escape response in zebrafish is mediated in part by the Mauthner cell and its two homologues, MiD2cm and MiD3cm. In adult fish, the Mauthner cell fires a single action potential when activated while the homologues fire multiple action potentials. Their distinct firing properties are partially attributed to the differential expression of voltage gated potassium (Kv) channels. I am interested in determining the Kv channels associated with the Mauthner and MiD2cm cells, and if they contain Kv1.1. Immunohistochemistry and in situ hybridization confirmed the expression of Kv1.1 in the Mauthner and MiD2cm cells at 48 hours post fertilization. Electrophysiology showed these cells to contain A-type and delayed rectifier currents but with different current densities. Preliminary data has shown these cells have the same firing behavior as in adults but with distinct action potential waveforms. The presence of Kv1.1 and the distinct current properties are suspected of regulating the neuronal excitability.

Acknowledgements

First and foremost I would like to thank Declan Ali for being a great supervisor and providing me the opportunity to obtain my masters degree. I appreciate all your time, energy and resources that you invested in me and for your patience and guidance through the last three years of my schooling.

Thank you to my committee members Dr. Warren Gallin and Dr. Greg Goss for providing helpful insight, and keeping me on the straight and narrow; as well thanks to Dr. Clayton Dickson for stepping in as the external for my defence.

I would like to extend a big thanks to three labs:
To Mike Belosevic's lab, specifically Barb Katzenback, for teaching me RT-PCR. To Andrew Waskiewicz's lab, especially Laura Pillay, for assistance with in situ hybridizations. To Warren Gallin's lab, especially Carla Morgan and Rheanna Sand, for all their help and effort in trying to express Kv1.1 in oocytes.

To all my fellow labmates, Chris, Kessen, Nicole, Bipu, Marcus, Simon and Taylor for sharing the ups and downs of science. To the summer students over the years, especially Zach Mansour. To my fellow colleagues of Biological Sciences I thank you for all the good times we shared outside the lab that kept us sane.

To Barb for the last three years, listening and helping me through my masters and all our time spent together.

Finally and most importantly to my family, especially my parents, I thank you for your love and never ending support that cannot be summed up with words. This would not be possible without you.

Table of Contents

List of Tables

Results

Appendix I

List of Figures

Introduction

Results

List of Abbreviations

Å – angstrom

BEN – brainstem escape network

BSA – bovine serum albumin

Cm – membrane capacitance

CNS – central nervous system

DF – driving force

dpf – days post fertilization

DRG – dorsal root ganglia

E_K – Nernst potential of potassium

EHP – extrinsic hyperpolarizing potential

EPSP – excitatory postsynaptic potential

ER – endoplasmic reticulum

ETA – escape trajectory angle

GHK – Goldman Hodgkin Katz

hpf – hours post fertilization

I_K – potassium current

IPSP – inhibitory postsynaptic potential

K_{Ca} – calcium activated potassium channel

Kv/ VGKC – voltage gated potassium channel

LLC – long latency C-start

mV – millivolts

PBS – phosphate buffered saline

PBS-T – PBS with 0.1% Tween-20

PFA – paraformaldehyde

PTU – N-phenylthiourea

R_{input} – input resistance

Rm – membrane resistance

Ra – access resistance

RSN – reticulospinal neurons

SLC – short latency C-start

V_S – slope factor

Vm – membrane potential

V_{50} – midpoint of activation

1. Introduction

1.1 Overview

An integral part of an animal's life is survival against predatory attacks. Animals are innately hardwired with reflex behaviors that facilitate predator avoidance. Within higher vertebrates the startle response is a reflex behavior that causes contraction of body and facial muscles in response to various stimuli, which prepares the animal for a fight or flight response (Koch 1999). In lower vertebrates, such as teleost fish, a similar reflex behavior known as the escape response is initiated (Figure 1.1A) (Weihs 1973). It facilitates the contraction of trunk musculature causing the fish to turn and swim away from a predator (Kimmel et al 1980; Zottoli 1977). Both the startle and escape response are mediated by a simple neural circuit starting with sensory neurons that detect auditory, visual and/or touch stimuli. These sensory neurons project to the hindbrain of the organism where they activate reticulospinal neurons. These reticulospinal neurons activate motoneurons which stimulate the skeletal muscle causing it to contract and elicit the behavior (Korn & Faber 2005; Lingenhohl & Eckhard 1994).

Zebrafish have been used successfully as a model organism to study the nervous system and how it develops for several decades, on account of their simple neural circuitry, including that responsible for mediating the escape response (Lingenhohl & Eckhard 1994; Saint-Amant & Drapeau 1998). Another advantage of using zebrafish is that females lay a large number of eggs on a daily basis (Lewis & Eisen 2003; Saint-Amant & Drapeau 1998). These embryos, and

the chorion that protects them, are transparent which has allowed for the study and identification of individual neurons through the different stages of development using a variety of imaging/ staining techniques (Eisen 1991; Saint-Amant & Drapeau 1998). The ability to identify individual neurons enables a person to study the activity of one cell from embryo to embryo (Eisen 1991). This feature of identifiable neurons is evident in the hindbrain of zebrafish, in particular with regards to the reticulospinal neurons, which have all been identified and characterized based on morphology and the rhombomere segment within which they reside (Lee et al 1993; Metcalfe et al 1986). The Mauthner cell is a specific reticulospinal neuron that has been studied at great lengths since its discovery in the early 1900s on account of its large cell size and ease of identification (Zottoli 1977). Since the discovery that the Mauthner cell initiates the escape response in teleost fish (Zottoli 1977), ongoing research has continually advanced our understanding of its function and role in the escape response (Eaton et al 2001; Foreman & Eaton 1993). Advances in technology and techniques have allowed for the focus of study to shift from adult to embryonic/ larval zebrafish to understand the behavior, neural circuitry and the activity of individual neurons involved in the escape response from a developmental standpoint (Liu & Fetcho 1999; O'Malley et al 1996; Saint-Amant & Drapeau 1998).

Great strides have been made in understanding the ionic currents responsible for controlling the activity of neurons since Hodgkin and Huxley's experiments using the giant squid axon to record the sodium and potassium

currents and how they give rise to action potentials (Hodgkin & Huxley 1952a; b). Potassium currents play a great number of roles in affecting cellular excitability on account of their vast diversity arising from the large protein family, their ability to conduct different types of currents and the formation of heteromeric channels that alter their properties and kinetics (Gutman 2005). The different characteristics exhibited by each of the potassium channels contribute cell excitability (Pongs 2008).

Until now, the majority of research in young zebrafish has focused on their behavior and neural circuitry with little focus on the currents responsible for the activity of the individual neurons; largely because of the difficulty in recording from these cells (Chong & Drapeau 2007; Liu & Fetcho 1999; O'Malley et al 1996).

The objective of my thesis research was to determine the firing behavior of reticulospinal neurons that mediate the escape response in larval zebrafish and to identify the potassium currents responsible for facilitating the excitability of the neurons. The two aims of my thesis were:

1. To identify the types of voltage gated potassium currents present in the Mauthner and MiD2cm cells.

2. To determine the cellular excitability of the Mauthner and MiD2cm cells in larval zebrafish and to understand how the corresponding potassium currents contribute to regulating the firing behavior.

1.2 Larval zebrafish movement

Zebrafish are an advantageous model organism to study the nervous system because of how fast they develop and the ability to identify phenotypic changes involved in the neural control of their escape response or swimming behavior. In larval zebrafish the first signs of movement occur at 17 hours post fertilization (hpf) with the spontaneous coiling of the tail (Saint-Amant & Drapeau 1998). This spontaneous tail coiling is generated by motoneurons which undergo periodic depolarizations (Brustein et al 2003; Saint-Amant & Drapeau 2000). By 21 hpf the first signs of the escape response are observed as embryos respond to tactile stimuli to the head and tail with rapid coils of the tail followed by a slow relaxation. At 26 hpf swimming behavior is elicited in response to touch (Saint-Amant & Drapeau 1998).

Zebrafish hatch from their chorion between 48 and 72 hpf (Kimmel et al 1995). Newly hatched larvae are rather sedentary, but do elicit fast startle responses in accordance to a strong stimulus, which is observed as a C-bend that turns the fish away from the stimulus followed by several tail flicks to propel the fish away (Figure 1.1A) (Muller & van Leeuwen 2004). As zebrafish progress through the larval stage (> 48 hpf) their turning and swimming behaviors develop and mature. In larval zebrafish the turning behaviors are classified as either routine or escape. Routine turns are spontaneous, slow and lack a counterbend. The escape turn is induced by a stimulus such as touch or sound, which initiates a rapid single bend followed by a large counterbend. The swimming behaviors are classified into two categories: slow and burst. Slow swimming follows the routine

turn while burst swimming usually succeeds the escape turn. All four behaviors are elicited by descending inputs from the hindbrain that activate motoneurons in the spinal cord (Budick & O'Malley 2000). The escape turn is initiated by the Mauther neuron and its two homologues, MiD2cm and MiD3cm (Budick & O'Malley 2000; Chong & Drapeau 2007).

1.3 Development of the hindbrain and reticulospinal system

The development of the central nervous system (CNS) is a very elaborate process that requires great timing and precision. In vertebrates the CNS develops from neuroectodermal tissue of the gastrula (Greene & Copp 2009; Schoenwolf & Smith 1990; Stern 1992). Cells of the neuroectoderm form a neural tube in which the anterior part becomes divided into neuromeres (Kimmel 1993; Schoenwolf & Smith 1990). In zebrafish at 18 hpf, ten neuromeres are present, the three most anterior neuromeres develop into the diencephalon, telencephalon and mesencephalon (Kimmel 1993). The remaining seven form the rhombomere segments of the hindbrain while the posterior part of the neural tube becomes the spinal cord (Hannemann et al 1988; Kimmel 1993; Kimmel et al 1988). The rhombomeres are separated from one another by distinct boundaries that form between the segments (Kimmel 1993; Moens et al 1996). The formation of boundaries and development of the individual rhombomeres is orchestrated by the expression pattern of a plethora of genes which includes (but is not exclusive to) *pbx, meis, krox20, valentino* and most importantly *hox* genes (Amores et al 1998; Moens et al 1996; Prince et al 1998).

During development of the hindbrain a molecular ground state reminiscent of rhombomere 1 (r1) is established (Waskiewicz et al 2002). Shortly after, boundaries that separate the rhombomeres begin to form, directed by the regulation of gene expression (Waskiewicz et al 2002). The first boundary separates r3 from r4, followed by formation of the r4/r5 boundary, which completes the formation of the r4 segment (Moens et al 1998; Moens et al 1996). This is significant because the r4 segment houses the Mauthner cell and suggests an importance in sending signals to neighboring rhombomeres (Moens et al 1998; Moens et al 1996). Next the r1/r2, r2/r3 and r6/r7 boundaries are formed. The r5/r6boundary is the last to form which may be due to the formation of the r5 and r6 segments from a common precursor (Moens et al 1998; Moens et al 1996). These two segments each contain a homologue of the Mauthner cell, known as MiD2cm and MiD3cm respectively (Metcalfe et al 1986).

The hindbrain is considered the most ancient part of the vertebrate brain (Jackman et al 2000; Moens & Prince 2002) and contains the cerebellum, medulla oblongata and the pons. The cerebellum largely contributes to coordinating motor behaviors whereas the medulla oblongata and the pons control respiration, circulation and several other motor functions (Moens & Prince 2002). The hindbrain also gives rise to cranial nerves five through twelve, which contain sensory and/or motor components that are involved in controlling many behaviors including hearing and balance (Moens & Prince 2002).

In zebrafish, cranial nerves V (trigeminal) and VIII (staticoacoustic) transmit sensory stimuli to neurons of the hindbrain (Figure 1.1). These neurons

are located in the medulla and are classified as reticulospinal, vestibulospinal or reticular neurons (Kimmel et al 1982; Metcalfe et al 1986). They have axons that project down the spinal cord and synapse onto motoneurons; which terminate onto and activate muscle fibers to elicit particular motor responses (Higashijima et al 2000; Moens & Prince 2002).

Within zebrafish and goldfish the reticulospinal neurons have been classified as identifiable neurons based on the ability to find them from one fish to another with the same position, morphology and axon path (Lee et al 1993). The morphology and positioning of these neurons in the zebrafish resemble those in the goldfish and thus they have been classified as phylogenetically homologous (Lee et al 1993). The complement of reticulospinal neurons at the larval stage is retained through to the adult stage allowing for similar conclusions to be drawn between the two developmental stages and the two species (Lee & Eaton 1991; Lee et al 1993).

The reticulospinal neurons (RSN) are the first to originate in the zebrafish hindbrain. They start off as a single cluster in the midbrain and as seven separate clusters along the anterior-posterior axis of the hindbrain, with each neuromere forming around one of the clusters (Lee et al 1993; Mendelson 1986). The cluster in the midbrain forms the nucleus of the medial longitudinal fasciculus, which is an integral part of the reticulospinal system containing MeM and MeL neurons (Kimmel et al 1982; Lee et al 1993). The three anterior clusters in the hindbrain become the rostral segments, followed by the three middle segments and then one caudal segment (Lee et al 1993). The Mauthner cell develops in the most anterior

middle segment (Figure 1.1B). Arising at 7 hpf, it is one of the first cells to appear in the nervous system while the MiD2cm and MiD3cm cells appear at 9 hpf, residing in the second and third middle segments respectively (Figure 1.1B) (Mendelson 1986). In total there are 27 different types of RSNs comprising the reticulospinal system, which forms the primary descending system of zebrafish at 28 hpf (Eaton & Farley 1973; Kimmel et al 1982; Metcalfe et al 1986). Based on their location, morphological characteristics and physiological activity, the reticulospinal neurons have been categorized into groups of segmental homologues (Metcalfe et al 1986; O'Malley et al 1996). Homologues have the same number of prominent dendrites and an axon that descends down the same spinal tract (Lee & Eaton 1991; Mendelson 1986; Metcalfe et al 1986; Nakayama & Oda 2004). The most studied group of homologues contains the Mauthner, MiD2cm and MiD3cm cells, also known as the Mauthner series (Metcalfe et al 1986). They all contain 2 prominent dendrites, one of which projects laterally while the other projects ventrally (Lee & Eaton 1991; Nakayama & Oda 2004). The lateral dendrite of the Mauthner cell passes through the ventrolateral vestibular nucleus before terminating on the neuropil of the acousticolateral area (Kimmel et al 1982; Kimmel et al 1981). The ventral dendrite projects through the tegmental motor nucleus and terminates on the neuropil of the ventral tegmentum (Kimmel et al 1981). Finer dendrites project off of the two prominent dendrites as well as the soma of the Mauthner cell (Kimmel et al 1981; Nakayama & Oda 2004). The prominent dendrites of the MiD2cm and MiD3cm cells have a greater

number of thin branches that cover a much larger field than the Mauthner cell (Lee & Eaton 1991; Nakayama & Oda 2004).

The Mauthner cell receives auditory, vestibular, visual, lateral line and somatosensory inputs with each modality projecting to one of the two prominent dendrites (Chang et al 1987; Faber & Korn 1975; Faber et al 1989; Zottoli & Faber 1979). To date the homologues have been shown to only receive sensory inputs from the auditory nerve and lateral line system (Kohashi & Oda 2008; Nakayama & Oda 2004; Szabo et al 2007). The axons of these three cells cross the midline and project down the dorsal bundle of the medial longitudinal fasciculus; which becomes the ventromedial fascicle once it enters the spinal cord (Lee & Eaton 1991; Metcalfe et al 1986; Nakayama & Oda 2004). The axons extend the length of the spinal cord and send out collaterals to motoneurons (Celio et al 1979; Gahtan & O'Malley 2003).

1.4 Sensory inputs to the Mauthner series

Developmentally, the first sensory input to the Mauthner cell is from the trigeminal ganglia (CN V), the first sensory neurons to appear in the head (Kimmel et al 1990). Inputs from the ear arrive at 23 hpf while axons from the lateral line neurons arrive last at 25 hpf (Kimmel et al 1990).

The trigeminal ganglia develop between the eye and the otic vesicle and contain approximately 20 bipolar neurons by 24 hpf (Figure 1.1B) (Metcalfe et al 1990). The peripheral axon arborizes in the skin of the head while the central axon projects to the hindbrain where it synapses on the lateral dendrite of the

Mauthner cell (Kimmel et al 1990; Metcalfe et al 1990). Activation of the trigeminal ganglion leads to subthreshold responses in the Mauthner cell; however it can elicit a non-Mauthner escape response (Kohashi & Oda 2008).

Rohon Beard neurons are another group of mechanosensory neurons that are some of the earliest primary neurons to develop (Bernhardt et al 1990; Metcalfe et al 1990). They are identified by their large cell body and dorsolateral position in the spinal cord (Bernhardt et al 1990; Kuwada et al 1990; Metcalfe et al 1990). Axogenesis occurs between 15 to 17 hpf with cells containing two ipsilateral longitudinal axons that project within the dorsal longitudinal fasciculus (Bernhardt et al 1990; Kuwada et al 1990). One ascends rostrally into the hindbrain and synapses onto the Mauthner cell (Figure 1.1B) while the other descends caudally into the tail region (Bernhardt et al 1990; Kimmel et al 1990; Kuwada et al 1990; Metcalfe et al 1990). Peripheral axons project off of the longitudinal axon and terminate in the skin of the trunk (Bernhardt et al 1990; Kuwada et al 1990; Metcalfe et al 1990; Reyes et al 2004). Mechanical stimulation of the skin elicits the firing of action potentials in these cells and evokes EPSPs in the ventral dendrite of the Mauthner cell (Chang et al 1987; Svoboda et al 2001). Each trunk hemisegment contains anywhere from 1 to 4 Rohon-Beard cells, however this number slowly decreases as these cells undergo programmed cell death during the first week of development (Lewis & Eisen 2003; Reyes et al 2004; Slatter et al 2005; Svoboda et al 2001).

As the Rohon Beard cells die off, perception of somatosensory stimuli occurs via neurons of the dorsal root ganglia (DRG), which transmit the signal to

the Mauthner cell (Kohashi & Oda 2008; Lewis & Eisen 2003). These ganglia contain bipolar neurons, which begin to differentiate at 36 hpf and are present lateral to the spinal cord by 45 hpf (An et al 2002; Bernhardt et al 1990; Reyes et al 2004). Axogenesis occurs between 2 to 4 days post fertilization (dpf) with a central axon extending into the spinal cord, where it bifurcates into ascending and descending branches within the dorsal longitudinal fasciculus (Bernhardt et al 1990; Reyes et al 2004). The peripheral axon projects ventrally from the soma, arborizing in the skin of the trunk (Bernhardt et al 1990; Reyes et al 2004).

The lateral line system is comprised of the anterodorsal ganglion and the anteroventral ganglion whose nerves connect the neuromasts, contained within the head, to the central nervous system (Raible & Kruse 2000). The anterdorsal ganglion fuses with the trigeminal ganglion and the anteroventral ganglion fuses with the facial sensory ganglion (Raible & Kruse 2000). Altogether they enter into the CNS anterior to the otic vesicle (Raible & Kruse 2000). The posterior lateral line found within the trunk and tail contains sensory afferents that also project to the hindbrain. In both zebrafish and goldfish, these afferents only synapse onto the lateral dendrite of the ipsilateral Mauthner cell (Korn & Faber 1975; Metcalfe et al 1985). The lateral line and posterior lateral line systems provide minimal stimulation to the Mauthner series and are believed to modulate the Mauthner cell's response to visual and auditory inputs (Chang et al 1987; Faber & Korn 1975; Kohashi & Oda 2008).

Visual information is sent through the optic nerve to the optic tectum which sends tectobulbar tracts to the ventral dendrite of the Mauthner cell (Zottoli

et al 1987). Visual stimuli produce EPSPs in the Mauthner cell, with rostral cues enhancing the escape response more so than caudal cues (Canfield 2006; Zottoli et al 1987).

Auditory information is the primary stimulus to evoke an escape response and is detected by the otic vesicles (Eaton & Emberley 1991; Haddon & Lewis 1996; Zottoli 1977). The inner ear of the zebrafish forms on both sides of the hindbrain adjacent to rhombomeres four through six, developing from the otic placode (Haddon & Lewis 1996). The otic placode cavitates to become the otic vesicle, which contains epithelial cells that give rise to the hair cells, support cells and associated sensory neurons (Haddon & Lewis 1996; Whitfield et al 2002). At 24 hpf some of the epithelial cells begin to differentiate to form sensory patches (Haddon & Lewis 1996). Initially five sensory patches form, three cristae and two maculae, each consisting of a collection of sensory hair cells and support cells (Haddon & Lewis 1996; Whitfield et al 2002). The two maculae develop first to become the utricle and the saccule while the lagena, the third maculae, appears later on in development at 9 dpf (Haddon & Lewis 1996; Moorman 2001; Whitfield et al 2002). All three are covered by otoliths and contain a unique arrangement of sensory hair cells (Figure 1.1B) (Haddon & Lewis 1996; Hudspeth 1989; Whitfield et al 1996). These three organs are sensors for linear acceleration, gravity and sound (Haddon & Lewis 1996). The saccule predominantly transmits auditory signals, while the utricule is primarily responsible for vestibular information (Whitfield et al 2002). The three cristae

develop into the semicircular canals and form the angular acceleration system (Moorman 2001; Whitfield et al 2002).

Associated with the sensory hair cells are bipolar sensory neurons which relay information to the brain (Haddon & Lewis 1996; Sapede & Pujades 2010). Neuroblasts, epithelial cells that delaminated from the otic vesicle, differentiate to become these sensory neurons which form the staticoacoustic ($VIII^{th}$) ganglion (Figure 1.1B) (Haddon & Lewis 1996). In adult goldfish the $VIII^{th}$ nerve afferents form discrete bundles which project medially to rhombomeres 4, 5 and 6 (Nakayama & Oda 2004). The saccular, lagenar and utricular afferent fibers provide monosynaptic input onto the lateral dendrite of the Mauthner cell (Szabo et al 2007).

The saccular afferents form the greatest number of synapses with a wide variety of endings including small and large myelinated club endings (SMCE and LMCEs) and small and large vesicle boutons (SVBs and LVBs), otherwise known as endbulbs (Nakajima 1974; Szabo et al 2007). The myelinated club endings are mixed synapses, containing gap junctions and chemical synapses, whereas the vesicle boutons are predominantly chemical synpases (Kimmel et al 1981; Lin & Faber 1988; Nakajima 1974). The LVBs that are mixed synapses differ from the MCEs as they contain fewer gap junctions (Kimmel et al 1981; Nakajima 1974). The lagenar and utricular afferents project to the dorsal and ventral portion of the lateral dendrite respectively. They form very few synapses (less than 15 each) and have endbulb terminals (Nakajima 1974; Szabo et al 2007).

The auditory pathway, consisting of the hair cells, the VIIIth nerve and the Mauthner cell, is established by 27 hpf (Tanimoto et al 2009). Although this pathway is present early on in development, the Mauthner cell does not start responding to sound stimuli until 40 hpf (Tanimoto et al 2009). At 60 hpf the auditory system develops the ability to transmit sound stimuli by converting the mechanical vibration to an electrical signal (Tanimoto et al 2009). Sound stimuli or electrical stimulation of the VIIIth nerve elicits EPSPs in the Mauthner cell and its serial homologues (Nakayama & Oda 2004; Szabo 2006). The onset latency of the potentials in the Mauthner cell is significantly less than for the MiD2cm and MiD3cm cells on account of the different type of afferent fibers that synapse onto them (Furukawa & Ishii 1967; Nakayama & Oda 2004; Pereda et al 1995). The potentials are comprised of fast (electrical) and slow (chemical) components, which represent the mixed synapses between the eighth nerve and lateral dendrite (Lin & Faber 1988; Nakayama & Oda 2004; Szabo 2006). Sound and pressure waves are the primary stimuli to activate the Mauthner series which initiate muscular contractions to elicit an escape response (Casagrand et al 1999; Eaton et al 1981; Neumeister et al 2008; Zottoli 1977).

1.5 Motor outputs of the Mauthner series

To activate the body musculature, the axons of the Mauthner series project down the contralateral side of the spinal cord sending out collaterals to the spinal motoneurons (Celio et al 1979; Gahtan & O'Malley 2003). The Mauthner axon has short unbranched collaterals that form chemical synapses with primary and

secondary motoneurons and descending interneurons (Celio et al 1979; Fetcho 1992; Fetcho & O'Malley 1995; Svoboda & Fetcho 1996). The descending interneurons are electrotonically connected with two to four motoneurons (Celio et al 1979; Gahtan & O'Malley 2003). Primary collaterals from the MiD2cm axon are highly branched and project to both the ipsilateral and contralateral spinal cord. The MiD3cm axon also has extensively branched collaterals but they remain in the ipsilateral spinal cord (Gahtan & O'Malley 2003).

The axon collaterals of the Mauthner series synapse onto and contribute to the synchronous activation of the spinal motoneurons (Fetcho & O'Malley 1995; Gahtan & O'Malley 2003). The firing of the motoneurons in the contralateral spinal cord leads to the contraction of the body and tail musculature which drives the escape response of the fish (Fetcho & O'Malley 1995). This response can occur even while a fish is swimming as the Mauthner neuron is able to override the swimming circuits (Svoboda & Fetcho 1996). This override capability results from the axon collaterals of the Mauthner cell synapsing directly onto the axon hillock of the motoneurons (Celio et al 1979; Faber et al 1989; Fetcho 1992).

1.6 Escape response of zebrafish

The escape response is an evasive behavior used by animals to protect themselves from predators (Eaton et al 1977; Weihs 1973). The response in teleost fish is a two stage behavior in which the animal makes a C-bend with their body to orientate and then propel them away from danger (Figure 1.1A) (Eaton et al 1977; Kimmel et al 1980; Weihs 1973; Zottoli 1977). In zebrafish, this

behavior first occurs early on in development (21 hpf) and is very similar to that seen in adult fish (Kimmel et al 1980; Saint-Amant & Drapeau 1998). The escape response is highly variable as the escape trajectory is capable of being in any direction within a 360^{o} radius, depending on the direction from which the stimulus is perceived (Eaton et al 1988; Eaton & Emberley 1991; Foreman & Eaton 1993). The stimulus, usually a pressure wave, activates the brainstem escape network (BEN) which is comprised of approximately 82% of the neurons found within the midbrain and hindbrain of the zebrafish (Eaton & Emberley 1991; Gahtan et al 2002). The physiological function of each of these neurons and the role they play in the escape response has yet to be characterized but they are believed to contribute to either the directional control of the response or to coordinate the sequencing of events (Gahtan et al 2002). The BEN neurons have been classified into two categories A1 and A2, which produce the major side (agonist) and minor side (antagonist) contractions respectively, of the body and tail musculature (Foreman & Eaton 1993). The A1 neurons, which includes the Mauthner series, have decussating axons that activate the trunk musculature on the contralateral side of the fish (Foreman & Eaton 1993). The agonist contraction orients the fish away from the stimulus, which is known as stage 1 of the response (Eaton et al 1988; Foreman & Eaton 1993). Stage two commences when the fish begins to propel itself in the direction of the initial turn (Foreman & Eaton 1993; Weihs 1973). During this stage the fish may undergo a direction change induced by the antagonist contraction. The antagonist contraction is elicited by the A2 neurons which have axons that project down the ipsilateral spinal cord and

activate trunk musculature on the same side that the stimulus was perceived (Eaton et al 1988; Foreman & Eaton 1993). The final escape trajectory angle (ETA) of the fish is a function of the magnitudes of the agonist and antagonist contractions and the interval between when they occur (Eaton et al 1988; Eaton et al 2001; Foreman & Eaton 1993). The magnitude and timing of the agonist and antagonist contractions are controlled by which BEN neurons are activated, which is dependent on the direction that the stimulus is perceived (Eaton & Emberley 1991; Eaton et al 2001; Foreman & Eaton 1993). Rostral stimuli maximally activate the A1 neurons resulting in a large unilateral turn and ETA thus turning the fish upwards of 180^{o} away from the stimulus. Stimulation of the mid body activates both the A1 and A2 neurons such that the final trajectory is approximately 90^{o} to the right or left. Caudal stimuli minimally activate the A1 neurons and maximally activate the A2 neurons producing a small escape trajectory angle which directs the fish in a forward direction (Eaton et al 2001; Foreman & Eaton 1993).

The Mauthner series, the crucial cells of the A1 neurons, are responsible for inducing the escape response in zebrafish {Eaton, 1984; Kimmel, 1980; Prugh, 1982; Zottoli, 1977}. Specifically the Mauthner cell is required for the activation of a short latency C-start (SLC) response, a response which occurs within 5 to 6 ms of detecting the stimulus (Burgess & Granato 2007; Kimmel et al 1980; Kohashi & Oda 2008; Liu & Fetcho 1999). The SLC performance is probabilistic in that its likelihood of occurring increases with stimulus intensity but the parameters of the response remain unaffected (Burgess & Granato 2007).

Fish in which the cells of the Mauthner series have been ablated elicit a long latency C-start (LLC) response which is characterized by a significantly increased latency and turn duration and a significantly decreased angular velocity (Eaton & Kimmel 1980; Kohashi & Oda 2008; Liu & Fetcho 1999). The performance of the LLC response is graded with respect to the stimulus intensity in contrast to the probabilistic SLC performance, indicating the two are controlled by different neural mechanisms (Burgess & Granato 2007).

The short latency response produced by the Mauthner cell results from the fast conduction velocity of the signal down its large axon, having a minimum number of synapses in the circuit and the short time necessary to activate the musculature (Eaton et al 1982; Eaton et al 1988). In freely swimming zebrafish a stimulus to the head will activate the Mauthner series and elicit a fast and large escape response (Foreman & Eaton 1993; Liu & Fetcho 1999; O'Malley et al 1996). A stimulus to the tail will only activate the Mauthner cell producing a quick but smaller response (Foreman & Eaton 1993; Liu & Fetcho 1999; O'Malley et al 1996). The difference in the cell activation results from the MiD2cm and MiD3cm not receiving inputs from the caudal region as previously described (Liu & Fetcho 1999; O'Malley et al 1996).

Another difference within the Mauthner series is the firing rate of the cells (Nakayama & Oda 2004; O'Malley et al 1996). When stimulated the Mauthner cell will fire one action potential, followed by an IPSP and will then temporarily cease firing (Eaton & Kimmel 1980; Nakayama & Oda 2004; O'Malley et al 1996; Zottoli 1977). The homologues fire multiple action potentials when

stimulated, with a frequency proportional to the intensity of the stimulus (Nakayama & Oda 2004; O'Malley et al 1996). The difference in firing properties is attributed to the inhibitory inputs onto the Mauthner cell and the conductance of different types of potassium currents (Furukawa & Furshpan 1963; Nakayama & Oda 2004).

Inhibition of the Mauthner cell occurs via an extrinsic hyperpolarization potential (EHP), a distinct positive spike that follows the Mauthner spike when recording from the axon cap of the Mauthner cell, and by a recurrent collateral inhibitory network (Furukawa & Furshpan 1963; Korn & Faber 2005). The EHP is a form of nonsynaptic electrical inhibition generated by outward currents from axon collaterals located near the Mauthner cell which cause the extracellular potential to become positive resulting in the hyperpolarization of the Mauthner cell (Furukawa & Furshpan 1963; Korn & Faber 2005). The EHP coincides with the firing of passive hyperpolarizing interneurons that synapse onto the axon cap and Mauthner soma (Faber & Korn 1975; Furukawa & Furshpan 1963; Triller & Korn 1981). Passive hyperpolarizing interneurons are located adjacent to the Mauthner cell and are classified as either commissural or collateral neurons (Faber & Korn 1973; Korn & Faber 1975; Triller & Korn 1981). Commissural neurons are activated directly by the staticoacoustic nerve, firing one action potential that has the same latency as the EHP (Charpier et al 1994; Faber & Korn 1973; Korn & Faber 1975). These neurons synapse onto both Mauthner neurons and contribute to the feedforward inhibition of the Mauthner cell (Triller and Korn 1981; Charpier et al. 1994; Hatta and Korn 1999; Korn and Faber 2005).

The collateral neurons provide recurrent inhibition onto the ipsilateral Mauthner cell (Korn and Faber 1975; Charpier et al. 1994; Hatta and Korn 1999). These neurons respond to inputs from the 8th nerve by firing multiple action potentials (Charpier et al 1994; Faber & Korn 1973). These two inhibitory inputs ensure that only one Mauthner cell fires in response to an aversive stimulus and prevents the activated cell from firing multiple action potentials (Furukawa & Furshpan 1963; Nakayama & Oda 2004). Nakayama and Oda (2004) demonstrated in conjunction with the inhibitory networks, potassium currents also affected the firing activity of the Mauthner cell in adult goldfish. Pharmacologically blocking a subset of voltage gated potassium channels resulted in the Mauthner cell firing multiple action potentials (Nakayama & Oda 2004).

Figure 1.1 Escape response of the larval zebrafish and the neural circuitry involved.

(A) Schematic of a larval zebrafish undergoing the escape response. A stimulus, such as a touch to the head (triangle), results in the contraction of the tail musculature resulting in the fish making a characteristic C-bend that points the fish away from the stimulus. This is followed by a few tail flicks that propel the fish away from the stimulus. (B) A diagram of some of the sensory inputs onto the Mauthner series of the zebrafish at 48 hpf. The Mauthner cells (M) are a pair of reticulospinal neurons located in rhombomere 4 of the hindbrain. They receive sensory inputs from cranial nerve V (the trigeminal ganglion (T)), cranial nerve VIII (the staticoacoustic ganglion (S)) and from Rohon Beard (RB) neurons of the spinal cord. Two other pairs of reticulospinal neurons, MiD2cm and MiD3cm, located in rhombomeres 5 and 6 are classified as morphological homologues of the Mauthner cell. They also receive inputs from the trigeminal and staticoacoustic ganglia. All three pairs make up the Mauthner series. (O) is the otic vesicle.

A

B

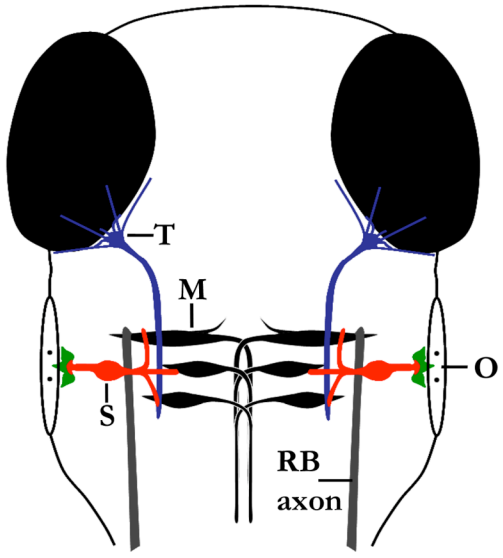

1.7 Voltage gated potassium channels

Despite only showing a single type of voltage gated potassium (Kv) channel was contributing to the firing of a single action potential in the Mauthner cell of adult goldfish (Nakayama & Oda 2004); preparations that have been studied more extensively, such as cells of the medial nucleus of the trapezoid body in mice and rats, have shown several different types of Kv channels are present and contribute to regulating the properties of neurons including their threshold potential, number of action potentials fired and the frequency at which they fire (Brew and Forsythe, 1995; Wang 98). The ability of Kv channels to regulate so many different properties is a result of the large family of proteins which comprises Kv channels (Gutman 2005). Kv channels are further diversified by heteromeric arrangements of their subunits and the association of auxiliary subunits which alter the properties of the individual channels (Coetzee et al 1999).

The Kv channel family of proteins was first characterized in *Drosophila* through the discovery of the four different gene subfamilies, Shaker, Shab, Shaw and Shal (Kamb et al 1987; Papazian et al 1987; Schwarz et al 1988). The mammalian homologues of all these genes have since been discovered and renamed Kv1, Kv2, Kv3 and Kv4 respectively (Gutman 2005; Pak et al 1991a; Pak et al 1991b; Swanson et al 1990; Wei et al 1990; Yokoyama et al 1989). These constitute the four major Kv gene subfamilies that have been studied to date although several others do exist. In humans the subsequent genes were named Kv 5 through 12, although homologues are present in other vertebrates as well as in *Drosophila* (Gutman 2005; McKeown et al 2008).

Shaker, Shab, Shaw and Shal are comprised of three different regions, a 5' end, a core region and a 3' end (Jan & Jan 1992; Schwarz et al 1988). The core region is conserved between all transcripts of a particular gene and encodes for the S1 through S6 transmembrane domains (Schwarz et al 1988). For each gene there are multiple 5' and 3' ends, which through alternative splicing, give rise to different transcripts resulting in an increased channel diversity (Kamb et al 1988; Schwarz et al 1988). In vertebrates the Kv subfamilies contain multiple genes each encoding one particular protein (Gutman 2005; McKeown et al 2008). For example the Kv1 subfamily consists of the genes Kv1.1 through 1.8. Each of these encode a protein, called the alpha subunit (Gutman 2005). These genes and the proteins they encode have been well conserved through evolution (Pak et al 1991a; Pak et al 1991b; Wei et al 1990). Orthologue genes (eg. Shaker and Kv1) have a greater similarity between one another than paralogues (eg. Shaker vs Shab) (Butler et al 1989). Within proteins, the S1 to S6 region has a greater amino acid identity between homologues of different species than between subfamilies of the same species (Pak et al 1991a; Pak et al 1991b).

Functional voltage gated potassium channels (VGKC) are tetrameric structures comprised of four alpha subunits (Coetzee et al 1999; McKeown et al 2008; Pongs 1992). Each alpha subunit contains a cytoplasmic N-terminus, six transmembrane spanning segments and a cytoplasmic C-terminus (Figure 1.2) (Coetzee et al 1999; McKeown et al 2008). Within the N-terminus, the T1 domain directs the assembly of the alpha subunits into a tetrameric structure and is the docking platform for auxiliary subunits (Li et al 1993; Sewing et al 1996). The N-

terminus may also contain an inactivation peptide which blocks the pore of the channel producing a transient A-type current (Hoshi et al 1990). An alpha subunit is divided into two primary domains a voltage sensing domain, which drives the activation of the channel and a pore domain which conducts the potassium ions (McKeown et al 2008; Pongs 1992).

1.7.1 Activation, deactivation and inactivation

The voltage sensing domain is comprised of the S1 through S4 segments, with the S4 segment considered the most critical as it is the actual voltage sensor (Figure 1.2) (Noda et al 1984; Shao & Papazian 1993; Tempel et al 1987). Every third amino acid of this alpha helix is either an arginine or a lysine residue (Bezanilla 2000; Noda et al 1984; Tempel et al 1987). The voltage sensor is held near the intracellular membrane surface due to the negative resting membrane potential (Jiang et al 2003). As the membrane becomes depolarized the voltage sensor moves through the membrane towards the extracellular surface and is recorded as a gating current (Armstrong & Bezanilla 1973; Jiang et al 2003; Spires & Begenisich 1989). The basic residues of the S4 segment contribute unequally to the gating current while the uncharged residues are responsible for stabilizing the protein (Aggarwal & MacKinnon 1996; Liman et al 1991; Logothetis et al 1993; Perozo et al 1994). The gating current is responsible for the opening of the channel, which occurs through the process of channel activation (Armstrong & Bezanilla 1973; Seoh et al 1996). During this process, the potassium channel passes through a series of transition states, the rate of which

becomes progressively faster as the channel nears the open conformation; supported by the faster kinetics of the on gating currents of Shaker channels elicited from more depolarized potentials (Bezanilla et al 1991; Taglialatela & Stefani 1993; Zagotta et al 1989; Zagotta et al 1994). Once open, the potassium channel is able to conduct potassium ions out of the cell (Papazian et al 1991; Zagotta et al 1989). Upon repolarization of the cell, the channel returns to its closed conformation through the process of deactivation (Bezanilla et al 1991; Hoshi et al 1994). The channel deactivates by transitioning through multiple closed states, with the rate increasing as the channel approaches the closed conformation (Bezanilla et al 1991; Hoshi et al 1994).

Prior to deactivation, open potassium channels may inactivate, a process which also disrupts potassium conductance but through an alternative mechanism (Iverson et al 1988; Yellen 1998). There are two different forms of inactivation in voltage gated potassium channels, N-type inactivation which is very fast and C-type inactivation which is very slow (Choi et al 1991; Hoshi et al 1991)..

N-type inactivation occurs via the occlusion of the channel pore by a 'ball and chain' (Figure 1.2) (Armstrong & Bezanilla 1977; Choi et al 1991; Hoshi et al 1990; Zagotta et al 1990). The 'ball and chain' comprises the first 80 residues within the amino terminal of Kv1.4, 3.3 and 3.4 subunits (Hoshi et al 1990; Rettig et al 1992; Zagotta et al 1990). The first 20 form the ball/ inactivation particle while the remaining 60 amino acids form the chain (Hoshi et al 1990; Zagotta et al 1990). The ball binds to the S4-S5 loop within the pore preventing ion conduction (Holmgren et al 1996; Hoshi et al 1994). Although only one ball is

necessary for inactivation, some channels may have as many as 4 inactivation particles (MacKinnon et al 1993). A greater number of particles leads to a more complete and faster rate of inactivation (Hashimoto et al 2000; MacKinnon et al 1993).

C-type inactivation results in the slow decay of current after rapid channel activation (Hoshi et al 1991; Yellen 1998). Subunits act in a cooperative manner to restrict the external mouth of the pore (Liu et al 1996; Ogielska et al 1995; Yellen et al 1994) while the selectivity filter partially collapses reducing the channels permeability to potassium (Starkus et al 1997; Yellen 1998).

Channels that undergo N-type inactivation elicit transient A-type currents while channels that undergo C-type inactivation elicit delayed rectifier currents (Dolly & Parcej 1996; Hoshi et al 1991; Storm 1988). Although Kv4 channels elicit transient A-type currents they do not undergo N- or C-type inactivation (Jerng & Covarrubias 1997; Jerng et al 1999; Pak et al 1991a). The exact mechanism has not been fully elucidated but it is known that they inactivate from a pre-open closed state (ie. closed state inactivation) (Bahring & Covarrubias 2010; Jerng et al 1999). Mammalian homomeric Kv1.1 channels elicit delayed rectifier currents with a midpoint of activation (V_{50}) of -30 mV (Grissmer et al 1994; Po et al 1993; Stuhmer et al 1989).

1.7.2 Pore domain and selectivity filter

The pore is comprised of the H5 segment, the S4-S5 loop and the S5 and S6 domains (Hartmann et al 1991; Lopez et al 1994; Slesinger et al 1993;

Taglialatela et al 1994; Yellen 2002; Yool & Schwarz 1991). The H5 segment, found within all potassium channels belonging to the six transmembrane family, forms the pore lining region as it stretches down into the membrane and loops back out (Figure 1.2) (MacKinnon & Yellen 1990; Yellen et al 1991; Yool & Schwarz 1991). The 3-D structure of the pore is highly conserved among potassium channels and is 45 Å in length (Doyle et al 1998; MacKinnon et al 1998). Starting from the intracellular side of the channel there is an internal pore that opens into a wide cavity which narrows into the selectivity filter that empties into the outer vestibule (Doyle et al 1998). The selectivity filter contains within it the signature sequence TXXTXGYG, which is highly conserved across potassium channels, and polar residues with carbonyl oxygen atoms that project into the pore (Doyle et al 1998; Heginbotham et al 1992; Heginbotham et al 1994; MacKinnon et al 1998). Several features that contribute to the selectivity include the hydrated state of the ion, the number of carbonyl ligands and the rigidity of the pore (Dudev & Lim 2009). The structure of the pore provides a low resistance, energy efficient pathway for potassium ion conduction (Doyle et al 1998). From the intracellular side, potassium ions pass through the internal pore and enter the water filled cavity, which helps stabilize the ions (Doyle et al 1998; Roux & MacKinnon 1999; Zhou et al 2001). Prior to entering the filter the potassium ions are dehydrated (Doyle et al 1998). The potassium ions pass through the selectivity filter in a single file manner. As the potassium ions move between the different sites in the selectivity filter they interact with the carbonyl oxygen atoms, which act to stabilize the ions within the pore; much like the water molecules do in the

water filled cavity (Doyle et al 1998; Hidalgo & MacKinnon 1995; Lipkind et al 1995). At the extracellular side one ion is expelled while the other two potassium ions remain within the filter (Berneche & Roux 2001; 2003; Doyle et al 1998). Under physiological conditions, the rate of conduction can reach 10^8 ions per second (Morais-Cabral et al 2001).

1.7.3 Tetramerization domain

The alpha subunits join together in homomeric or heteromeric structures (Isacoff et al 1990; Ruppersberg et al 1990). Kv1 to Kv4, Kv7, and Kv10 to Kv12 form functional channels comprised of subunits from their own subfamily (Gutman 2005). The Kv5, 6, 8 and 9 subunits are modifiers/silencers that coassemble with Kv2 channels to alter their kinetics (Gutman 2005). The T1 domain is critical for proper assembly of potassium channels to form either homo- or heterotetrameric structures within specific subfamilies (Hopkins et al 1994; Kreusch et al 1998; Li et al 1993; Shen et al 1993). The T1 domain is a highly conserved 100 residue sequence within the amino terminal which is divided into 3 regions, the N-terminal, the hydrophobic core and the C-terminal (Figure 1.2) (Kreusch et al 1998; Li et al 1992; Liu et al 2005; Sewing et al 1996; Shen et al 1993). The T1 sequences of Kv1, Kv2, Kv3 and Kv4 channels have 24 positions that are highly conserved with 7 absolute identities between them (Kreusch et al 1998). The most conserved residues are found within the hydrophobic core giving rise to highly conserved primary and secondary structures and are the sites for intersubunit interactions (Liu et al 2005). Within the Kv1 subfamily there are 13

separate interactions, comprised of hydrogen bonds and disulfide bridges, that occur between the conserved set of residues (Kreusch et al 1998; Liu et al 2005). Stabilization is further enhanced by many other intersubunit interactions that occur throughout the S1 to S6 domains (Tu et al 1996).

Homomeric channels have unique properties including activation and inactivation kinetics as well as specific sensitivities to different pharmacological agents (Isacoff et al 1990; Ruppersberg et al 1990). Heterotetrameric arrangements increase the diversity of Kv channels by altering the conductance and kinetics of the channel, its sensitivity towards a particular toxin and the expression levels of the different subunits that form the channel (Akhtar 2002; Isacoff et al 1990; Ruppersberg et al 1990; Sokolov et al 2007).

1.7.4 Expression levels of alpha subunits

Of the Kv1 subunits, total protein expression in the mammalian (bovine, human, mouse and rat) CNS from highest to lowest is 1.2 > 1.1 > 1.4, 1.6 > 1.3 > 1.5, although this can vary depending on several factors including cell type and stage of development (Coleman et al 1999; Hallows & Tempel 1998; Koch et al 1997; Shamotienko et al 1997; Utsunomiya et al 2008). However, surface expression of these proteins is quite different with Kv1.4 being the most concentrated in the plasma membrane followed by Kv1.2, while the majority of Kv1.1 is retained in the endoplasmic reticulum (Manganas & Trimmer 2000). Kv1.3 and 1.5 are also found to be expressed at the surface while 1.6 is not (Manganas & Trimmer 2000). Yet surface expression levels can be altered by the

formation of heteromeric channels (Manganas & Trimmer 2000). Kv1.4 increases the surface expression levels of 1.2 and 1.1 while Kv1.1 reduces the amount of Kv1.4 in the plasma membrane (Manganas & Trimmer 2000; Zhu et al 2001; 2003).

The regulation of channel trafficking is attributed to the ER retention signal in the outer pore and the forward trafficking signal within the C-terminus of the Kv1 channel (Li et al 2000; Manganas et al 2001; Misonou & Trimmer 2004; Zhu et al 2001). Within the Kv1.4 subunit, the pore domain contains amino acids that promote folding and exit from the ER; while those in the Kv1.1 pore induce high ER retention and reduce protein stability (Zhu et al 2005; Zhu et al 2001; 2003). The VXXSL motif, found within the C-terminus of the Kv1.4 subunit, further promotes channel trafficking and surface expression (Li et al 2000). Changing a single amino acid in this motif can reduce its trafficking ability significantly. This is observed with the Kv1.2 subunit which has a reduced surface expression on account of having an asparagine in place of the leucine (Li et al 2000). Although these two different regions regulate surface expression, the dominant signal is the ER retention signal within the pore of the channel (Misonou & Trimmer 2004).

1.7.5 Heteromultimeric arrangement of voltage gated potassium channel subfamily 1

Depending on the organism and region of the nervous system heterotetrameric Kv channels have been found in several different combinations (Coleman et al 1999; Shamotienko et al 1997; Wang et al 1999). In rat brain

channels may be comprised of Kv1.1 and 1.2 or 1.1 and 1.4 subunits, although Kv1.6 subunits have also been found to be associated with either of these heteromers (Wang et al 1999). Furthermore channels containing four different subunits (1.1/1.2/1.4/1.6 or 1.2/1.3/1.4/1.6) have been isolated in bovine brain (Shamotienko et al 1997).

The combination of multiple subunits produces functional channels with unique properties, although determining which subunits are present and their stoichiometry has proven difficult *in vivo* (Akhtar 2002; Sokolov et al 2007). Thus concatemers, in which Kv1.1 and 1.2 or Kv1.2 and 1.6 subunits are linked together, have been developed to deduce these properties (Akhtar 2002; Sokolov et al 2007). These channels elicit similar delayed rectifier currents to the homomeric Kv1.1, 1.2 and 1.6 channels, but they have distinct properties that are intermediate between the two parent homomeric channels (Akhtar 2002; Sokolov et al 2007). In the case of the 1.1-1.2 concatemer, the channel had a V_{50} = -26.5 ± 1.67 mV, a value skewed towards the midpoint of activation of the homomeric Kv1.1 channel (V_{50} = -30.8 ± 1.59 mV) (Akhtar 2002).

1.7.6 Auxiliary subunits of voltage gated potassium channels

Kv channels may have auxiliary subunits associated with them that can affect their inactivation properties and expression levels (Coleman et al 1999; Hanlon & Wallace 2002). Beta subunits associate with the Kv1 family, while Kv5, 6, 8 and 9 associate with the Kv2 family (Gutman 2005). Kv3 has no known auxiliary subunits while several have been shown to associate with the Kv4

subfamily including KChIP and DPPX (Gutman 2005). Kv10 and 11 have auxiliary subunits while none have been discovered for Kv12 (Gutman 2005).

The beta (β) subunits are divided into 3 distinct classes, β1, 2 and 3, with classes 1 and 3 also containing subfamilies of splice variants (Hanlon & Wallace 2002; Heinemann et al 1995; Morales et al 1995; Rettig et al 1994). The beta subunits are approximately 400 amino acids in length and contain an N-terminus and a C-terminus. The amino terminal structure and sequence is quite variable between classes and within subfamilies, having an amino acid identity that is less than 10% (England et al 1995; Heinemann et al 1995; McCormack et al 1995). Whereas the carboxy terminus has a very high amino acid identity between the different classes of beta subunits which is also retained between different species (bovine, ferret, human and rat) (Rettig et al. 1994; England et al. 1995; Heinemann et al. 1995; Majumder et al. 1995; McCormack et al. 1995; Morales et al. 1995).

The amino terminals of β1, 2 and 3 contain 72, 38 and 79 amino acids respectively and share few if any common identities (England et al 1995; Morales et al 1995). The longer amino terminals within β1 and 3 are due to the presence of an inactivation domain similar to that found in the Kv1.4 alpha subunit (Accili et al 1997; Heinemann et al 1995; Morales et al 1995; Rettig et al 1994). Yet only the β1 subunit, when coexpressed with functional Kv1 channels, is able to introduce N-type inactivation; the β3 subunit does not (Heinemann et al 1996; Majumder et al 1995; Morales et al 1995). The degree of inactivation is dependent on the β1 subfamily member that is expressed and the alpha subunit it associates

with (Heinemann, Rettig et al. 1995; Morales, Castellino et al. 1995; Heinemann, Rettig et al. 1996; Wang, Kiehn et al. 1996). When β1 is co-expressed with Kv1.5 the current completely inactivates, whereas co-expression with Kv1.6 has no effect on the current (Heinemann et al 1996). The Kv1.1 channel when co-expressed with the β1.1 subunit causes the current to switch from a delayed rectifier current to a fast inactivating current composed of fast and slow time courses of inactivation (Heinemann et al 1996; Jow et al 2004; Rettig et al 1994). However, the presence of intracellular calcium has been shown to eliminate this effect and currents return to having only a slow inactivation component (Jow et al 2004).

In contrast to the N-terminal, the C-terminus is highly conserved between classes and is responsible for binding to the alpha subunit (Accili et al 1997; Heinemann et al 1995; Parcej et al 1992; Rhodes et al 1995; Sewing et al 1996; Shi et al 1996). The beta subunits are peripheral membrane proteins, which bind to the amino terminus of the alpha subunit in a region that overlaps with the T1 domain (Gulbis et al 2000; Scott et al 1994; Sewing et al 1996). The extent to which beta subunits associate with alpha subunits is quite variable and some may not associate together at all (Nakahira et al 1996; Rhodes et al 1995). Alpha and beta subunits combine early on while the proteins are still present in the endoplasmic reticulum (ER) (Shi et al 1996). The β1 subunit binds independently to alpha subunits with a stoichiometry of $\alpha_4\beta_n$, where n = 0 through 4 (Xu et al 1998). The β2 subunits are self associating, forming their own tetramer before assembling with the alpha subunits in an $\alpha_4\beta_4$ stoichiometry (Xu et al 1998).

Beta subunits promote stabilization of the Kv channels and can increase their surface expression resulting in increased current amplitudes (Accili et al 1997; Shi et al 1996; Xu et al 1998). The β2 subunit is predominantly responsible for these actions due to its high avidity for the alpha subunit (Xu et al 1998). The coexpression of Kv1.1 with β2 in COS-1 cells was observed to increase the surface expression of the Kv1.1 subunit (Shi et al 1996).

1.7.7 Pharmacological agents of voltage gated potassium channels

A channel's sensitivity to different toxins can be altered by the composition of subunits (Akhtar 2002; Sokolov et al 2007). The toxins tetraethylammonium (TEA) and 4-aminopyridine (4-AP) are pore blockers of voltage gated potassium channels that can act both extra- and intracellularly (Mathie et al 1998; Stanfield 1983; Stephens et al 1994). TEA is a quaternary ammonium ion that has the same diameter as a hydrated potassium ion (Stanfield 1983). It binds to all subunits of a potassium channel, characteristic of the energy additivity model (Hopkins 1998; Kavanaugh et al 1992). 4-AP is a monoamine derivative of pyridine (Glover 1982). It is more potent than TEA and is known to block both A-type and delayed rectifier currents (Glover 1982; Mathie et al 1998). Although commonly used to block Kv channels, these toxins are not useful for classifying the presence of specific alpha subunits (Mathie et al 1998).

Dendrotoxins (DTX), a group of peptides isolated from the venom of Mamba snakes of the Elapid family, have a much higher potency and selectivity for voltage gated potassium channels, particularly the Kv1 subfamily (Benishin et

al 1988; Berndt et al 1993; Foray et al 1993; Harvey 2001; Harvey & Karlsson 1980). There are six different dendrotoxin peptides: alpha, beta, gamma, delta, K and I, each containing 57 to 60 residues with their own unique amino acid compositions (Benishin et al 1988; Harvey & Karlsson 1980). The C-terminals are highly conserved while the first 30 residues contain more variability (Benishin et al 1988). Structurally they all contain a 3_{10} helix, a hairpin beta sheet and an alpha helix which are connected through disulfide bridges (Berndt et al 1993; Foray et al 1993; Harvey & Karlsson 1980; Lancelin et al 1994). It is these structural motifs that are essential for their ability to bind extracellularly and block the pore of voltage gated potassium channels (Hollecker et al 1993; Hurst et al 1991; Smith et al 1997). Within the H5 segment of the Kv alpha subunit, the three residues critical for binding DTX are alanine 352, glutamate 353 and tyrosine 379 which are conserved between rat, mouse and human (Hurst et al 1991).

Dendrotoxins block in a dose dependent fashion with altered affinities for particular alpha subunits (Hall et al 1994). DTXα can bind to channels containing Kv1.1, 1.2 and 1.6; however it has the greatest affinity for the 1.2 subunit (Wang et al 1999). Meanwhile DTX_K acts specifically on channels containing Kv1.1, only requiring the presence of one subunit to produce maximum inhibition of the current (Robertson, Owen et al. 1996; Akhtar 2002; Sokolov, Shamotienko et al. 2007). DTX_K has a very high affinity for the Kv1.1 subunit, blocking rat Kv1.1 channels expressed in oocytes with an IC_{50} = 2.5nM (Robertson et al 1996).

1.7.8 Regulation of cellular activity by voltage gated potassium channels

The diversity of Kv channels including their different patterns of expression, the arrangement of different heterotetramers and the association of auxiliary subunits enables them to play a diverse number of roles to regulate neuronal activity (Johnston et al 2010).

Kv4 channels are responsible for preventing the back propagation of action potentials into the soma and dendrites of neurons by regulating the membrane excitability in these regions (Pongs 2008). They are able to do so because they conduct transient currents and are found at a higher density in the distal dendrites compared to the proximal dendrites and soma (Hoffman et al 1997). During the repolarization phase of an action potential these channels activate and inactivate very quickly. When the cell is hyperpolarized these channels are removed from their inactive state and are available to respond to the next wave of depolarization via EPSPs. During this depolarization, the Kv4 channels are activated, thus reducing the amplitude of the EPSP and preventing the dendrites from reaching threshold and eliciting a second action potential (Hoffman et al 1997; Magee & Carruth 1999).

Kv3 channels enable neurons to sustain a high frequency firing rate (Nakamura & Takahashi 2007; Pongs 2008). Kv3 channels activate at more depolarized potentials however they have rapid activation and deactivation kinetics (Hernandez-Pineda et al 1999). Furthermore they conduct a larger amount of current compared to other Kv channels (Nakamura and Takahashi, 2007). Thus Kv3 currents mediate a high frequency firing rate by facilitating the

rapid repolarization of the neuron and removing sodium channels from their inactive state (Hernandez-Pineda et al 1999).

Kv2 channels also affect the action potential duration and assist in high frequency firing by contributing to the interspike interval (Johnston et al 2008; Malin & Nerbonne 2002).

Kv1 currents regulate the membrane potential and establish the action potential threshold (Dodson et al 2002; Goldberg et al 2008), and as such, they help to establish cellular excitability (Chi & Nicol 2007). They also affect the waveform of the action potential and the size of the afterhyperpolarization (Kole et al 2007). Furthermore, Kv1 channels prevent neurons from firing irregularly, thus enabling high fidelity transmission (Ishikawa et al 2003; Nakamura & Takahashi 2007). Kv1.1 channels have been shown to regulate the firing rate and stabilize the onset latency of action potentials (Barnes-Davies et al 2004; Chi & Nicol 2007; Kopp-Scheinpflug et al 2003). The significance of Kv1.1 in regulating cellular excitability is evidenced by specific mutations of the Kv1.1 subunit which causes episodic ataxia-1, while kcna1 (the gene encoding Kv1.1) knockout mice experience epileptic seizures early on in development (Brunt & van Weerden 1990; D'Adamo et al 1999; Smart et al 1998).

Figure 1.2. Alpha subunit of a voltage gated potassium channel.

A functional Kv channel is comprised of four alpha subunits. Each alpha subunit contains an amino (N) terminus, six transmembrane domains (TMDs I – VI) and a carboxy (C) terminus. In Kv channels the N-terminus contains a tetramerization (T1) domain which is where the alpha subunits interact and it also distinguishes the alpha subunits of the different subfamilies. The N-terminus of Kv1.4, 3.3 and 3.4 subunits contain an inactivation ball and chain (ID) which occludes the pore causing the channel to undergo N-type inactivation. The H5 segment, TMDs V and VI and the S4-S5 linker forms the pore of the channel. Within the H5 segment is the selectivity filter which restricts the channel to only conduct potassium ions.

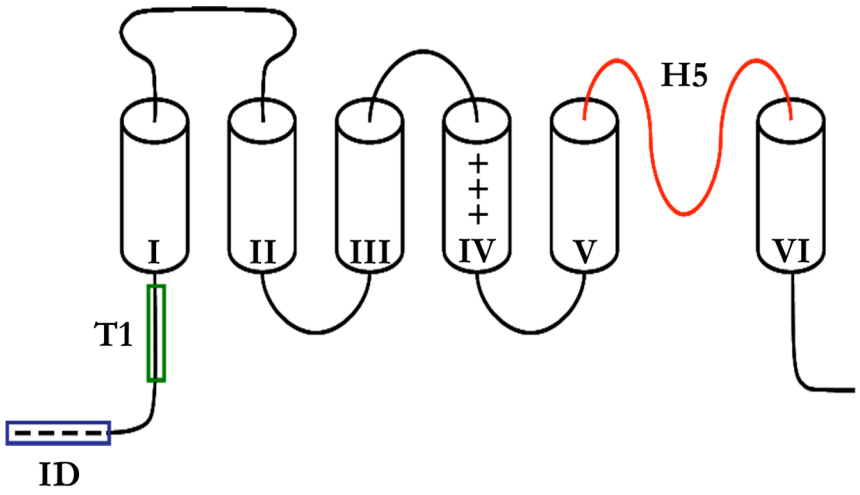
H5
I
II
III
IV
V
VI
T1
ID

1.8 Research objectives and hypotheses

In adult goldfish the Mauthner cell will only fire a single action potential in response to a stimulus, even if that stimulus is maintained for an extended period of time (Nakayama & Oda 2004). This characteristic property of the Mauthner cell has been in part attributed to the currents produced by Kv1 channels which repolarize the cell and prevent further action potentials from being initiated during the sustained stimulus (Nakayama & Oda 2004). In general, little has been done to record potassium currents from teleost fish and no work has been done to record potassium currents of the Mauthner cell or its homologues in larval (48 hpf) zebrafish. Preliminary work in the lab determined Kv1.1 to be expressed in different populations of neurons of larval zebrafish and a review of the literature had shown these channels to be important in regulating neuronal firing rate (Barnes-Davies et al 2004; Chi & Nicol 2007) Therefore, the focus of my thesis was to establish the presence of Kv1.1 containing channels in the Mauthner and MiD2cm cells of zebrafish at 48 hpf and how they contributed to regulating the excitability of these cells.

My objectives for this thesis were:

- to identify the expression of Kv1.1 in larval zebrafish at 48 hpf
- to record potassium currents from the Mauthner and MiD2cm cells and determine what fraction of the current was being conducted by channels containing Kv1.1.

- to record action potentials from these cells and identify how Kv1.1 channels were regulating their firing behavior through pharmacological means.
- to inject zebrafish Kv1.1 into *Xenopus* oocytes and use two electrode voltage clamp to characterize the current.

I hypothesized that Kv1.1 would be associated with the Mauthner cell at the time of hatching (48 hpf). Based on mammalian type channels, I hypothesized that zebrafish Kv1.1 channels would elicit delayed rectifier currents. In addition, I examined the firing properties of these cells to determine if they behaved in the same manner as that seen in larval zebrafish and adult goldfish, where the Mauthner cell fires one action potential and the MiD2cm cell fires multiple action potentials (Nakayama & Oda 2004; O'Malley et al 1996). I hypothesized that the two cells would have the same firing properties at 48 hpf as they do in the adult fish, on account of the Kv1.1 channels ensuring the Mauthner cell fired a single action potential.

My results suggest that the Mauthner cell and its homologue, MiD2cm, express different populations of potassium channels, one of which contains the Kv1.1 subunit. Although the Mauthner and MiD2cm cells contain the same types of Kv currents, both an A-type and a delayed rectifier, the current density of each and how they contribute to the total Kv current appears to be different. As for the firing behavior, preliminary recordings confirmed the firing patterns of the two cells at 48 hpf were similar to those observed in adult zebrafish, although the properties of the action potentials were different.

2. Materials and Methods

2.1 Zebrafish

The AB line of zebrafish was obtained from Oregon and cared for based on established protocols (Westerfield, 1995). Adult fish were kept in holding tanks at 28.5°C in a room with 14 hours of light and 10 hours of dark. Groups of five fish were placed in mating tanks overnight and eggs were collected between 8 AM and noon the following morning. Eggs were placed in a petri dish filled with egg water and kept at 28.5° C until experimented upon.

2.2 Immunohistochemistry

At 24 hpf embryos were placed in 0.003% phenylthiourea (PTU) to block pigment formation. PTU was prepared by adding 0.003 g of PTU to 100 ml of egg water. At 48 hpf, fish were dechorionated and fixed with 2% paraformaldehyde (PFA) for 2 hours. The larvae were washed for 2 hours in 1x PBS at 15 minute intervals and then permeabilized using 4% Triton X-100 (containing 2% bovine serum albumin (BSA) and 10% goat serum) for 30 minutes. Immediately after permeabilization, they were placed in primary antibody at 4^{o}C for 48 hours. The antibody was diluted (to the appropriate concentration) in 0.4% Triton X-100 containing 2% BSA and 10% goat serum. Following incubation in primary antibody, larvae were washed in 1x PBS at 30 minute intervals for 2.5 hours at room temperature, then placed in secondary antibody overnight at 4^{o}C. The secondary antibody was diluted in 10% normal goat serum and 1x PBS. Larvae were washed at room temperature with 1x PBS at 30 minute intervals for 7 hours

and then mounted on glass slides and cleared using glycerol. Mounting consisted of removing the yolk sac and separating the head from the tail. The head was placed on its ventral side and the tail on its right side. A plastic coverslip was placed overtop and sealed to the slide with nail polish.

To detect Kv1.1 two different rabbit polyclonal antibodies, anti-Kv1.1 (1:200, Alamone Labs) and anti-Kv1.1 (1:200, Sigma), were used. A mouse monoclonal antibody, anti-3A10 (1:250, Developmental Studies Hybridoma Bank, University of Iowa) was used to identify the Mauthner neuron. The secondary antibodies used were goat anti-rabbit IgG coupled to Alexa-Fluor 568 (1:2000, Molecular probes) and goat anti-mouse IgG coupled to Alexa Fluor 488 (1:1000, Molecular Probes).

Larvae were viewed on a Zeiss LSM confocal microscope using a 20x objective lens and images were compiled using Zeiss LSM Image Browser software.

2.3 Molecular biology

2.3.1 Reverse Transcription- Polymerase Chain Reaction

Primers were designed to produce ~1000 base pair PCR products and to ensure the product included as much of the 3' UTR as possible. The primer pair for LOC795942 was f62942/ r62942 with sequences Fwd 5'-CATCGGGGGCAAGATTGTGGGTTC -3' and Rev 5'-GCTCCTCCTTCGGCATTGTGCTGTC -3'. The primer pair for LOC571208 was f17108/ r17108 with sequences:

Fwd 5'- AAGCTTTCCAGACACTCCAAGGGC -3' and
Rev 5'- TTGTTATGGCAGTGTCGTATCTCATCAG -3'. Primers were reconstituted in 500 µl of TE buffer, vortexed and spun down to produce primer stock solutions. To make a 20 µM working solution, 10 µl of primer stock solution was added to molecular grade water. The volume, in µl, of molecular grade water to be added was determined by taking the nmol value from the IDT tube that the primer came in and subtracting 10 µl. The PCR ½ reaction conditions were as follows (in µl): 20.25 molecular grade water, 2.5 10x PCR buffer, 0.5 10 mM dNTPs, 0.5 cDNA, 0.5 Fwd primer, 0.5 Rev primer and 0.25 Taq 20a polymerase. For the f17108/ r17108 primer pair all the conditions were the same except the magnesium concentration was increased to 3 mM. The following PCR program (DKVPCRG) was run in the thermocycler: 1. 2 min at 94^{o}C, 2. 30 s at 94^{o}C, 3. 20 s at 60 ± 8^{o}C, 4. 90 s at 72^{o}C, 5. Go to step 2, repeat 35 times, 6. 7 min at 72^{o}C, 7. Hold at 4^{o}C.

RNA was isolated from whole 48 hpf larvae or adult brain using the Trizol extraction protocol as per Invitrogen. To convert the RNA to cDNA the Maxima first strand cDNA synthesis kit (Fermentas) was used.

PCR products were run on a 1% agarose gel (length of 6.4 cm from top to bottom) for 24 minutes at 125 V. The gel was post-stained in ethidium bromide for 10 minutes, destained for 10 minutes in water then imaged using the Alpha Imager. Bands were cut out and extracted using the QIAquick Gel Extraction Kit (Qiagen).

To sequence the 62942 PCR product it was cloned into pCR 2.1 TOPO vector which was then transfected into One shot Chemically competent *E. coli* cells. Cells were plated on LB+AMP plates and grown overnight at 37^{o}C. Isolated colonies were chosen to run a colony PCR. The colony PCR reaction was (in µl): 263.25 molecular grade water, 32.5 10x PCR buffer, 6.5 10 mM dNTPs, 6.5 M13 Fwd primer, 6.5 M13 Rev primer, 3.25 Taq 20(a) polymerase then aliquoted into 23 tubes at 12.5 µl each. Colonies were removed from the plate using a yellow pipette tip and dipped into one tube. The colony PCR program was: 1. 10 min at 94^{o}C, 2. 30 s at 94^{o}C, 3. 20 s at 50^{o}C, 4. 90 s at 72^{o}C, 5. Go to step 2 repeat 25 times, 6. 7 min at 72^{o}C, 7. Hold at 4^{o}C. The products were run on a gel, stained and then imaged as previously mentioned.

Those colonies containing a plasmid with an insert were grown up in 2ml of LB+AMP medium overnight in a 37°C shaker at 240 rpm. The plasmid was isolated from the colonies using a Plasmid Mini Kit (Qiagen) in preparation for a sequencing reaction. The sequencing reaction was (in µl): 2 ET terminator cycle sequencing dye, 4 Sequencing buffer, 1.8 molecular grade water, 0.2 primer, 2 plasmid. For each plasmid two reactions were set up; one contained the M13 Fwd primer while the second contained the M13 Rev primer. The sequencing program was: 1. 20 s at 94^{o}C, 2. 20 s at 50^{o}C, 3. 90 s at 60^{o}C, 4. Go to step 1 repeat 25 times, 5. Hold at 4^{o}C. The 17108 PCR product was directly sequenced without cloning into a vector using Big Dye v3.1. The sequencing reaction was (in µl): 2 Premix, 3 5x buffer, 10 PCR product, 0.25 primer, 4.75 molecular grade water. Two reactions were set up, one using the f17108 primer and the second using the

r17108 primer. The sequencing program was: 1. 30 s at 96°C, 2. 15 s at 63°C, 3. 1 min 30 s at 60°C, 4. Go to step 1 repeat 25 times, 5. Hold at 4°C. Sequencing reactions were cleaned by the following steps. To each PCR product 45 µl of ice cold 95% ethanol (stored at -20°C) was added. To a clean 1.5 ml eppendorf tube, 1µl of sodium-acetate EDTA was added. The PCR product and ethanol were mixed by pipetting then transferred to the tube containing the sodium-acetate EDTA. The tube was vortexed then centrifuged at max speed for 10 minutes. The supernatant was aspirated off followed by the addition of 750 µl of 75% ethanol. The tube was vortexed and then centrigued for 5 minutes at max speed. The ethanol was aspirated off and then taken to the Molecular Biology Service Unit (MBSU) in the department of Biological Sciences to be sequenced.

2.3.2 In situ hybridization

For *in situ* hybridization experiments, embryos were placed in 0.003% PTU at 24 hpf to reduce pigmentation. At 48 hpf larvae were dechorionated and fixed using 4% PFA overnight at 4°C. They were washed using PBS-T (1x PBS with 0.1% Tween 20) at room temperature at 5-minute intervals for 25 minutes. Larvae were permeabilized with proteinase K (10 µg/ml) in PBS-T for 5 minutes. They were fixed again in 4% PFA for 20 minutes and then rinsed in PBS-T for 25 minutes. The larvae were placed in hybridization mix overnight at 65°C followed by probe overnight at 65°C. The probe was diluted in hybridization mix at 1:200. Probe synthesis is described later on. Three 5 minute washes using 2:1 Hyb mix to 2x SSC, 1:2 Hyb mix to 2x SSC and 2x SSC at 65°C preceded the stringency

washes. Stringency wash 1 (0.2x SSC and 0.1% Tween 20) for 20 minutes at 65^{o}C was followed by two high stringency washes (0.1x SSC and 0.1% Tween 20) each 20 minutes at 65^{o}C. The stringency washes were followed by three 5 minute washes at room temperature using 2:1 0.2x SSC to PBS-T, 1:2 0.2x SSC to PBS-T and PBS-T. Blocking solution (PBS-T, 2% sheep serum and 2 mg/ml BSA) was applied for 1 hour at room temperature before the larvae were placed in antibody overnight at 4^{o}C. Anti-digoxigenin-AP antibody (1:5000, Roche Applied Science) was diluted in blocking solution. Larvae were washed 5 times at 15 minute intervals using PBS-T then rinsed in coloration buffer at 5 minute intervals for 20 minutes. In 10 ml of coloration buffer, 45 µl of NBT (Roche Applied Sciences) and 35 µl of BCIP (Roche Applied Sciences) were added. 500 µl of this mixture was added to the embryos for the coloration reaction. Larvae were incubated in the dark at room temperature until a blue/purple reaction product was visible, which was approximately 3 hours for this set of experiments. The reaction was stopped using 100% MeOH + 0.1% Tween 20, in which two quick washes were followed by two fifteen minute washes. The fish were mounted in the same manner as described for the immunohistochemistry experiments and then imaged using a Zeiss Axio Imager Z1 compound microscope with an Axiocam HR digital camera.

Sense and antisense probes were made to detect the transcript of LOC795942. The pCR 2.1 TOPO vector containing the 62942 product was linearized by incubating the following reaction at 37^{o}C for 2 hours. The reaction was (in µl): 20 plasmid DNA, 4 10x buffer, 2.5 Enzyme (hindIII), 13.5 molecular

grade water. A phenol/chloroform extraction and ethanol precipitation was used to isolate the DNA. The linearized DNA was resuspended in 15 µl of DEPC water. 1 µl of DNA was run out on the gel to verify it was linearized.

Probes were synthesized using the following reaction (in µl): 2 µg linearized DNA, 2 10x transcription buffer, 2 10x DIG labeling mix, 1 T7 polymerase, 1 RNase inhibitor and DEPC water to 20 µl which was incubated at 37 ^{o}C for 2 hours. After one hour, 1 µl of the T7 polymerase was added to the reaction mix. After the 2 hours 1 µl of RNase free DNase was added to the reaction and incubated for 5 minutes at 37^{o}C. To stop the reaction 2 µl of 0.25 M EDTA pH 8 was added after which the probe was run through a Sigma Post Reaction Purification Column. 5 µl of the probe was diluted in hybridization solution (hybridization mix containing tRNA) at a 1:200 concentration and stored at -20^{o}C. 25 µl of DEPC water was added to the remainder of the probe and stored at -80^{o}C.

2.4 Electrophysiology

2.4.1 Larval dissection

At 48 hpf fish were placed in a recording dish and anaesthetized using 0.02% tricaine (MS-222; Sigma Chemical, St. Louis, MO) in physiological saline. The fish was pinned through the notochord onto a sylgard platform. A dissection of the head exposed the ventral surface of the brain while keeping it intact with the spinal cord. The Mauthner cell and MiD2cm were viewed under Nomarski

Differential Interference Contrast (DIC) and were identified based on their morphology and position in the hindbrain.

2.4.2 Whole cell voltage clamp

Two different extracellular solutions were used to record potassium currents: a nominally Ca-free solution and another that contained calcium. Normal ECS contained (in mM): 137 NaCl, 2.9 KCl, 2.1 $CaCl_2$, 1.2 $MgCl_2$, 10 HEPES and 10 Glucose. The K^+ isolating extracellular solution contained (in mM): 137 NaCl, 2.9 KCl, 0.7 $CdCl_2$, 1.2 MgCl, 10 HEPES and 10 Glucose. Both solutions were adjusted to pH 7.8 using NaOH and an osmolarity of 290 ± 2 mOsm. D-tubocurarine (curare, 10 μM, Sigma) was used to block acetylcholine receptors and TTX (1 μM, Alamone Labs) was used to block voltage gated sodium channels. The flow rate of the extracellular solution was adjusted between 1 and 1.5 ml/min. Pipettes were pulled to approximately 4 MΩ and were filled with a K^+-gluconate solution (in mM): 115 K-gluconate, 15 KCl, 2 NaCl, 10 HEPES, 10 EGTA, 4 Mg-ATP and 0.4 Li-GTP. It was adjusted to pH 7.2 using KOH and an osmolarity between 290 ± 2 mOsm. For Mauthner cell recordings, the input resistance (R_{input}) ranged between 40 and 55 MΩ, while access resistance (Ra) was between 5 and 7 MΩ (Table 3.1). Recordings were compensated by 75%. For MiD2cm recordings, R_{input} was greater than 100 MΩ while Ra ranged between 5 and 11 MΩ (Table 3.1). All of these recordings were compensated by 80%. Recordings were aborted if the access resistance changed by more than 20%.

To run current-voltage protocols, the cell was initially held at -60 mV before being stepped down to -90 mV for 25 ms. For the Mauthner neuron the cell was stepped from -90 mV to 40 mV at 10 mV intervals lasting 220 ms before being stepped down to -90 mV. The MiD2cm cell was run through the same protocol with the exception that it was only depolarized to 30 mV. For comparative analysis, to account for the difference in the size of the cells, the current density was calculated by dividing the current amplitude by the membrane capacitance (Cm) (Table 3.1). Of the currents recorded in the Mauthner cell, two different values were measured; the first at the highest amplitude (peak current) of each trace and the second at time 198 ms of the trace (sustained current). The peak value was measured to investigate the total current, while the second value at 198 ms was measured to investigate the remaining current that did not undergo N-type inactivation. For the MiD2cm cell the current values were measured at 198 ms of the trace (sustained current). The time 198 ms was an arbitrarily chosen time point near the end of the current trace so the sustained currents were consistently measured between traces and cells.

Conductance is normally calculated by plotting the tail current against the voltage step. However recording tail currents in the Mauthner cell proved difficult due to the presence of multiple potassium currents. Instead the conductance was calculated using two different normalization procedures. The GHK normalization proposed by John Clay (2000) uses the equation:

$$g_K = I_K * 25/Vm * [((e^{(Vm/25)})-1) / ((e^{((Vm-E_K)/25)}-1)]$$

where g_K is the potassium conductance, I_K is the potassium current, Vm is the membrane potential at each step and E_K is the Nernst potential for potassium. The second procedure used to measure the conductance was by normalizing the current to the driving force (Driving force (DF) normalization) using the equation:

$$g_K = I_K / (Vm - E_K).$$

The current values measured from the current recordings were substituted into the equations to calculate the conductance. The conductance values were plotted against the holding potentials of the cell and the curves were fit with a Boltzmann function:

$$f = a / (1+\exp(-(X-X_0)/b)$$

to obtain the midpoint of activation ($X_0 = V_{50}$) and slope factor ($b = V_S$).

In the MiD2cm cell tail currents were recorded and used to plot the channel conductance, which was then fit with a Boltzmann function. Channel conductance was also determined using the GHK and DF normalization methods. The steady state activation data, obtained using the different methods, were compared for both the Mauthner and MiD2cm cells (see Appendix).

Decay kinetics of the current in the Mauthner cell was measured by fitting the current trace with a standard exponential function, using the Chebyshev fitting method (Clampfit v. 9). To determine which exponential component best fit the current, a single, double and triple exponential were run on currents elicited at steps from -10mV to 40mV. The values of the sum of squared errors were recorded and plotted in bar graphs and compared statistically using a One-Way ANOVA (see Appendix III).

2.4.3 Pharmacology

TEA was applied to the Mauthner and MiD2cm cells to block the delayed rectifier current (Coetzee et al 1999; Glover 1982; Stanfield 1983), while 4-AP was used to block the A-type current in the Mauthner cell (Coetzee et al 1999; Coutts et al 2009; Glover 1982), as it was previously shown to do in the white muscle fibers of zebrafish (Coutts et al 2009). Recordings were performed using normal ECS with the addition of D-tubocurarine (10 μM), TTX (1 μM) and TEA-Cl (5 mM) or 4-AP (5 mM). For applying drugs, a whole cell patch was first achieved and series resistance and capacitance were compensated for. Initially, the preparation was perfused with normal ECS (containing curare and TTX) and voltage gated potassium currents were recorded using the aforementioned current voltage protocol (section 2.4.2). Following the recording, TEA was washed on for 7 minutes and then the current voltage protocol was run. The same procedure was followed when applying 4-aminopyridine (4-AP), although only 4 minutes was required to wash on the drug. The time interval for applying each drug was the minimal amount of time required to produce a maximal inhibition of the current.

2.4.4 Whole cell current clamp

To record action potentials, normal ECS (with 10 μM D-tubocurarine) was perfused over the dissected larvae. Pipettes had a resistance of 3 to 4 MΩ and were filled with intracellular solution containing (in mM): 130 KCl, 2 NaCl, 10 EGTA, 10 HEPES, 4 Mg-ATP and 0.4 Li-GTP. A whole cell patch was achieved in voltage clamp mode and the series resistance and capacitance were

compensated for before switching into current clamp mode. The cell was held at -65 mV before proceeding with the recordings. Currents were injected for 50 ms. To calculate the input resistance of the cell, a single pulse of current (-0.1 nA for the Mauthner cell and -0.2 nA for the MiD2cm cell) was injected into the cell and the membrane potential of the cell was recorded (Table 3.2). To record action potentials the cell was stimulated with a series of positive current injections. The pulses of current ranged from 0.16 nA to 0.46 nA for the Mauthner cell and from 0.06 to 0.26 nA for the MiD2cm cell.

2.5 Statistical analysis

All statistics were computed using the Sigmaplot 11 Systat program. For the majority of data a Student's t-test was used. During instances where the data failed the normality or equal variance test a Mann Whitney Rank Sum test was run instead. For the pharmacological data a paired t-test was run. In the appendix when analyzing the conductance of the Kv channels in the MiD2cm cell a One-way ANOVA test was run. If the normality test failed a Kruskal-Wallis Analysis of Variance test was run in its place. All values were reported as mean ± SEM. When statistics were performed the type of test was indicated followed by the p-value.

3. Results

3.1 Expression of voltage gated potassium channel 1.1 in zebrafish larvae at 48 and 72 hours post fertilization

Our interest in identifying and understanding the role of Kv1.1 channels in the Mauthner and MiD2cm cells stemmed from preliminary data in the lab in which immunohistochemical experiments demonstrated the appearance of Kv1.1 in reticulospinal neurons of the hindbrain. The significance of Kv1.1 has been demonstrated in its role of regulating neuronal excitability (Barnes-Davies et al 2004; Chi & Nicol 2007; Dodson et al 2002; Goldberg et al 2008). Conveniently, the firing rates of the Mauthner cell and MiD2cm cell are known to be very different and therefore I hypothesized that the Mauthner cell expressed potassium channels that contain Kv1.1 while the MiD2cm cell would not. This was extrapolated from work done in adult goldfish where it was suggested that the presence of Kv1.2 in the Mauthner cell but not in the morphological homologues, was partly responsible for ensuring the Mauthner cell only fired one action potential in response to a depolarizing stimulus (Nakayama & Oda 2004). My first objective was to perform immunohistochemistry experiments to determine if the Kv1.1 subunit was expressed in the Mauthner cell and MiD2cm cell.

Two separate Kv1.1 antibodies were acquired, one from Sigma Aldrich and the other from Alamone labs. Both antibodies were independently generated against a fusion peptide that was 80 amino acids long, equivalent to residues 416 to 495 of the C-terminus of the mouse Kv1.1 channel. To determine if anti-Kv1.1 might bind to the zebrafish Kv1.1 due to sequence similarity, I performed an alignment of the zebrafish and mouse Kv1.1 with respect to the 80 amino acid

sequence (Figure 3.1). The program, Ensembl, was used to blast the protein sequence for zebrafish Kv1.1, which turned up two different proteins, ENSDARP00000085980 and ENSDARP00000011986. They will be referred to as P85980 and P11986 for convenience. P85980 was 79% identical to the mouse sequence, while P11986 was 75% identical. With respect to each other, the two zebrafish sequences were 87.5% identical for the 80 amino acids.

A full sequence alignment was also performed between the zebrafish, mouse, rat and human Kv1.1 sequences (Figure 3.1). P85980 is 492 amino acids, P11986 is 493 amino acids, while the mammalian proteins are 495 amino acids. Comparing the two zebrafish sequences showed they were 89% identical with a similarity at 94% of their amino acids. The P85980 sequence was 86% identical with a 93% similarity to the amino acids present in human, mouse or rat sequences. The P11986 sequence had an 82% identity and was 89% similar when aligned against any of the same three mammalian sequences. The regions of greatest variation occurred within the N-terminus, the S1-S2 loop and the C-terminus while the transmembrane segments and pore domain all showed high similarity (Figure 3.1) (Pak et al 1991a; Pak et al 1991b).

Immunohistochemical experiments were performed on larvae at 48 hpf (Figures 3.2 and 3.3, n = 61 larvae and 4 experiments) and 72 hpf (Figures 3.4 and 3.5, n = 62 larvae and 3 experiments). Both primary antibodies showed the exact same staining pattern within the soma of a limited number of cell populations. Staining occurred in the region behind the eye that corresponded to the location of the trigeminal neurons (Figure 3.2A and 3.4A) (Kimmel et al

1995). Antibody staining was also detected in three distinct locations of the hindbrain of the larvae and appeared to be associated with at least three different pairs of reticulospinal neurons (Figure 3.2A and 3.4A). One pair was believed to be the Mauthner cells while another may correspond to the MiD2cm cells. Staining was detected in a group of cells in the dorsal spinal cord, which, based on their location and shape, are believed to be Rohon Beard neurons (Figure 3.3A-C and 3.5A-C) (Bernhardt et al 1990; Kuwada et al 1990; Metcalfe et al 1990; Slatter et al 2005).

The 72 hpf larvae exhibited similar staining patterns for anti-Kv1.1 but with greater intensities; as well, an additional population of neurons was also stained. They were located adjacent and ventral to the spinal cord and were spaced equally distant from one another (Figure 3.5A, n = 52 larvae). Based on their position these neurons are likely dorsal root ganglion (DRG) cells (Figure 3.5A-C) (Bernhardt et al 1990).

To confirm the presence of the Kv1.1 alpha subunit in the Mauthner cell, preparations were double labeled with anti-Kv1.1 and anti-3A10 (1:250) (Figure 3.2A-C, n = 61 larve and 4 experiments and 3.4A-C, n = 62 larve and 3 experiments). Anti-3A10 is a mouse monoclonal antibody that recognizes a neurofilament that is expressed in several cells (eg. CoPa interneurons, trigeminal ganglion neurons), but of the reticulospinal neurons it distinctly stains the Mauthner cell (Figure 3.2B and 3.4B) (Hatta 1992). Z-stacked images of the larvae were taken using a confocal microscope. An average of 16 image slices of the hindbrain was obtained from each larva. Upon stacking the images, the

staining appeared white from the overlapping of the yellow (anti-Kv1.1) and blue (anti-3A10) (Figures 3.2C and 3.4C).

To confirm the specificity of the antibodies I performed several controls whereby either the primary (n = 29 larve) or secondary (n = 38 larve) antibody was omitted from the procedure, or by using a blocking peptide (n = 34) to pre-absorb the anti-Kv1.1 antibody. For the pre-absorption control, 1µl of anti-Kv1.1 was pre-incubated with 5 µl antigenic peptide (Alamone Labs), against which it was developed. When run in conjunction with the anti-3A10 antibody, the yellow anti-Kv1.1 staining was absent but blue staining appeared, suggesting the anti-Kv1.1 was unable to bind the Kv1.1 in zebrafish due to being preabsorbed by the antigenic peptide.

Imaris software (Bitplane Scientific Software, South Windsor, CT, USA) was utilized to convert a set of confocal images of the reticulospinal neurons at 72 hpf into a 3D image. The image clearly shows the Kv1.1 (red) present within the Mauthner cell (green) (Figure 3.6B). Additional cells in the hindbrain, with morphologies similar to Mauthner cell were also stained with the anti-Kv1.1 (Figure 3.6A). Based on their location and morphology, I believe these to be the Mauthner homologues, MiD2cm and MiD3cm, but this has not been confirmed experimentally (Figure 3.6A) (Metcalfe et al 1986).

The results from these experiments suggest that the zebrafish Kv1.1 subunit may be expressed in trigeminal ganglion cells, a few reticulospinal neurons, including the Mauthner cell, Rohon Beard neurons and DRG neurons.

3.2 Gene expression of voltage gated potassium channel 1.1 in zebrafish larvae at 48 hours post fertilization

My immunohistochemical data suggested that zebrafish Kv1.1 was expressed in a few different groups of neurons including the Mauthner cells and its homologue MiD2cm. I attempted to verify the specificity of the antibodies via Western blot experiments but was unsuccessful. Therefore, in order to support the findings of the immunohistochemistry experiments, I performed RT-PCR to identify the genes encoding for zebrafish Kv1.1 and *in situ* hybridization experiments to verify the cellular expression of this gene.

When performing a blast search in Ensembl two different genes emerged, ENSDARG00000062942 and ENSDARG00000017108, which will be referred to as G62942 and G17108, respectively. G62942 encoded P85980 and G17108 encoded P11986. Both genes are comprised of a 5' untranslated region (UTR), one exon and a 3' UTR. The exons were aligned and found to be 78% identical. At 48 hpf both genes were shown to be expressed however G62942 appeared to be of greater quantity (Figure 3.7A, n = 3 experiments). Beta actin was used as a positive control and as a means of qualitatively comparing the expression levels of the two different genes. Interestingly, the brain of adult zebrafish was only found to express G62942 but not G17108 (Figure 3.7B, n = 3 experiments). The PCR products were sequenced to confirm the primers were isolating the appropriate sequences of DNA (n=1).

Results from the RT-PCR experiments showed the two genes encoding the Kv1.1 proteins in zebrafish are expressed at 48 hpf, with only G62942 expression being retained in the adult.

In situ hybridizations were performed on 48 hpf larvae to determine which cells were expressing G62942 and to confirm the antibody staining (Figure 3.8, n = 2 experiments). Probes were made against the G62942 PCR product as it encodes P85980 which has a greater sequence identity with its mammalian homologues and appeared to be expressed at greater levels than G17108. The pattern and location of the *in situ* staining was the same as that observed with the anti-Kv1.1 antibody (Figure 3.8, n = 20 larvae). In the head, staining was located just caudal and lateral to the eyes which is believed to be the trigeminal neuron (Figure 3.8A) (Kimmel et al 1995). In the hindbrain three distinct cellular locations were stained; which are thought to be the Mauthner cell and two other reticulospinal neurons based on the location of the staining in comparison with the immunohistochemistry data (Figure 3.8A). Staining was also observed in cell bodies located along the dorsal edge of the trunk in distinct spots that matched the location of the anti-Kv1.1 immunohistochemistry (Figure 3.8B). This group of cells in the dorsal spinal cord is believed to be the Rohon Beard neurons based on their location, size and shape (Bernhardt et al 1990; Kuwada et al 1990; Metcalfe et al 1990).

This data, in conjunction with the immunohistochemistry, suggested that zebrafish Kv1.1 is expressed in Mauthner cell and its homologue, Mid2cm. Therefore, I proceeded to investigate the type of Kv currents present in these two cells using electrophysiology.

3.3 Recording potassium currents in the Mauthner and MiD2cm cells at 48 hours post fertilization

My initial objective was to determine the types of Kv currents present in the Mauthner and MiD2cm cells at 48 hpf, as this has yet to be examined. I then wanted to determine what proportion of the total current Kv1.1 channels were conducting in the Mauthner and the Mid2cm cells. My final goal was to establish how Kv1.1 currents regulated the firing behavior of these two cells.

To isolate the currents conducted by voltage gated potassium channels I used a K^+ isolating ECS and a K^+ gluconate ICS. The K^+ isolating ECS was modified from the normal ECS by replacing the $CaCl_2$ with $CdCl_2$, to block voltage gated calcium channels, and by adding 1 μM TTX to block voltage gated sodium channels. This solution permitted the recording of potassium currents from the Mauthner and MiD2cm cell but the patch could not be maintained for periods long enough to permit the application of pharmacological agents.

My ability to maintain the patch for longer periods was improved when recording the potassium currents in the normal ECS. The normal ECS still contained 1 μM TTX but the presence of calcium meant that the solution was no longer a truly K^+ isolating solution. To the normal ECS I added 4-AP and TEA to block the A-type and delayed rectifier currents respectively (Coetzee et al 1999; Coutts et al 2009), but my results would have to be interpreted with the caveat that calcium currents would be present and may perhaps interfere with the Kv currents. Upon analyzing the Kv currents recorded using the normal ECS, it became apparent that there were in fact multiple ionic currents and the use of K^+ isolating ECS was necessary to properly characterize the Kv currents.

Despite these complications, the Kv currents were able to be recorded from both cells using the K^+-isolating solution and will be discussed in section 3.3.1. Meanwhile the application of TEA and 4-AP in the normal ECS has provided insight into the types of Kv subunits that may be present and contributing to currents in the two different cells (section 3.3.2). Finally, comparing the results from the two solutions led us to tentatively suggest the presence of a calcium activated potassium current in the Mauthner cell.

3.3.1 Voltage gated potassium currents in the Mauthner and MiD2cm cells at 48 hours post fertilization

The Mauthner cell contained a potassium current that could be interpreted in one of two ways. It could either have been a single A-type current that did not completely inactivate or two different Kv currents, an A-type fast inactivating current and a delayed rectifier current (Figure 3.9A, n = 8). Therefore currents were measured from two different points on the trace. The first at the initial peak amplitude referred to as the peak current, and the second at the end of the trace (time = 198 ms), referred to as the sustained current. When the Mauthner cell was stepped to 40 mV, the peak current had a density of 646 ± 19 pA/pF while the sustained current had a density of 385 ± 15 pA/pF (Figure 3.9B, n = 8). In the MiD2cm only a delayed rectifier current was present (Figure 3.11A, n = 15). In these recordings, current values were measured at 198 ms of the trace and are referred to as sustained current. The current density was 1810 ± 55 pA/pF when the cell was depolarized to 30 mV (Figure 3.11B, n = 15).

Steady state activation of the potassium channels was calculated as described in the materials and methods. For the Mauthner cell, both the GHK and DF normalization methods were used to calculate the conductance of the peak and sustained currents. These curves were fit with a Boltzmann function to determine the V_{50} and V_S (Figure 3.9C, n = 8). From the GHK normalization, the midpoint of activation for the peak and sustained currents were -1.8 ± 1.5 mV and 0.0 ± 1.1 mV respectively and were not significantly different (t-test, P = 0.34, n = 8). The slope factor was 9.7 ± 0.1 mV for the peak current and 10.8 ± 0.3 mV for the sustained current, which were significantly different from one another (Mann-Whitney Rank Sum test, P = 0.005, n =8). The DF normalization method produced a curve that was shifted to the right of the GHK curve (Figure 3.9C). The peak current had a V_{50} = 8.5 ± 1.1 mV and a V_S = 12.1 ± 0.2 mV, while the sustained current had a V_{50} = 10.5 ± 0.9 mV and a V_S = 12.4 ± 0.2 mV. For the DF method, neither the V_{50} values (t-test, P = 0.17, n =8) nor the V_S values (t-test, P = 0.33, n =8) were significantly different when comparing the peak and sustained currents. Analysis comparing the two different methods is discussed in appendix I.

To determine the steady state activation of the potassium channels in the MiD2cm cell, the conductance was calculated from tail currents and using the GHK and DF normalization methods. The GHK curve was shifted left compared to the DF and tail curves, as was observed in the Mauthner cell. The tail and DF curves nearly overlapped one another, but the DF normalization produced a steeper curve. From the GHK normalization method, the sustained current had a

V_{50} = -8.2 ± 1.0 mV and a V_S = 8.8 ± 0.5 mV. The DF normalization produced a curve with a V_{50} = 0.0 ± 1.0 mV and a V_S = 10.3 ± 0.4 mV. The tail current produced a conductance curve with a V_{50} = -1.0 ± 3.1 and V_S = 14.5 ± 1.7 mV. Further analysis comparing these three methods is discussed in appendix I.

Both cells contained channels that conducted sustained currents however the steady state activation of these channels was significantly different. The midpoints of activation values for the sustained currents in the Mauthner cell were significantly depolarized compared to the values for the MiD2cm cell whether comparisons were made using the GHK or DF normalization methods (t-test, $P < 0.001$). As for the slope factors, the values pertaining to the MiD2cm sustained currents, were significantly less compared to the values of the Mauthner cell (Mann-Whitney Rank Sum test, $P < 0.01$).

For the potassium currents in the Mauthner cell, the time course of inactivation was measured, with traces best fit with a double exponential (Figure 3.10A). The fast (τ_{fast}) and slow (τ_{slow}) inactivation time constants at 10 mV were 18.5 ± 2.1 ms and 170 ± 49 ms respectively (Figure 3.10B, n = 8). The time constants at 40 mV were τ_{fast} = 14.4 ± 1.4 ms and τ_{slow} = 227 ± 38 ms respectively (Figure 3.10B, n = 8). As the cell was brought to more depolarized potentials there were no changes in the time constant of inactivation for τ_{fast} (t-test, $P > 0.1$, n = 8) or τ_{slow} (t-test, $P > 0.1$, n = 8).

3.3.2 Potassium current recordings with normal extracellular solution

As previously described, normal ECS was utilized to record potassium currents as it increased the success rate of obtaining recordings and enabled the patch to be maintained for a longer period of time. Despite the presence of the calcium impairing my ability to properly isolate the Kv currents, it allowed me to tentatively identify a third potassium current in the Mauthner cell.

The current traces obtained from the Mauthner or the MiD2cm cells appeared the same whether calcium was present or not. However, a comparison of the current densities indicated that the presence of the calcium significantly altered the amplitudes of the currents, in both the Mauthner and MiD2cm cell (Figure 3.12).

When recording from the Mauthner cell in normal ECS, the peak current had a greater current density at all voltage potentials from -50 to 30 mV (Figure 3.12A, t-test, $P < 0.05$, $n = 17$). For the sustained current of the Mauthner cell the presence of the calcium did not affect the current to the same extent. Instead the current density was only significantly increased at voltages from -50 to 0 mV (Figure 3.12B, t-test, $P < 0.05$, $n = 17$). For the sustained current of the MiD2cm cell, the opposite effect was observed. The presence of calcium significantly decreased the current density at all voltage potentials ranging from -20 to 30 mV (Figure 3.12C, t-test, $P < 0.01$, $n = 10$). The change in current densities to both the Mauthner and MiD2cm cells confirmed the presence of calcium interfered with the current recordings. However, the increase in the amplitude of the outward current in the Mauthner cell in the presence of calcium led us to hypothesize that

a calcium activated potassium channel was present and responsible for conducting the additional potassium current.

My ability to record for a longer period of time in the presence of calcium allowed me to use pharmacological blockers of Kv channels to dissect out which channel subfamilies may be associated with these cells. Two general Kv channel blockers, 4-AP (5 mM) and TEA (5 mM), were applied to understand the different components that the peak current was comprised of in the Mauthner cell. Application of 4-AP to the Mauthner cell completely blocked the peak current and exposed an inward current with a density of -196 ± 14 pA/pF (at 50 mV) (Figure 3.13, paired t-test, $P < 0.001$, $n = 8$). 4-AP also reduced the sustained current to less than half its original value from 463 ± 13 pA/pF to 189 ± 21 pA/pF at 50 mV (Figure 3.13B and 3.13D, paired t-test, $P < 0.001$ $n = 8$).

The application of TEA significantly reduced the amplitude of the peak current at more depolarized voltages (20, 30 and 40 mV, paired t-test, $P < 0.001$, $n = 6$) and the sustained current at potentials greater than -20 mV (Figure 3.14B, C and D, paired t-test, $P < 0.001$, $n = 6$). The sustained current density was reduced from 419 ± 27 pA/pF to 144 ± 12 pA/pF (at 50 mV) (Figure 3.14D, $n = 6$). Compared to the Mauthner cell, the application of TEA had a more profound effect on the potassium current of the MiD2cm cell (Figure 3.15A and B, $n = 4$). It significantly reduced the sustained current of the MiD2cm cell and revealed a transient A-type current (Figure 3.15B, paired t-test, $P < 0.001$, $n = 4$). In controls, the sustained current density was 1516 ± 49 pA/pF when held at a potential of 30 mV (Figure 3.15C, $n = 4$). Following application of TEA, the sustained current

density was reduced to 170 ± 10 pA/pF (at 30 mV), while the transient A-type current had a density of 459 ± 55 pA/pF (at 30 mV) (Figure 3.15C, n = 4).

The results of the electrophysiology showed the Mauthner and MiD2cm cells to contain both an A-type transient current and a delayed rectifier current that contribute in different proportions to their total Kv currents. Since Kv1.1 channels contribute to sustained outward currents (Po et al 1993; Stuhmer et al 1989), I hypothesized that it was contributing to the sustained currents of the Mauthner and MiD2cm cells. In addition, I hypothesized that the Mauthner cell expresses a calcium activated potassium channel (K_{Ca}) while the MiD2cm may not.

I attempted to apply DTX_K, a blocker that binds specifically to the Kv1.1 subunit (Robertson et al 1996), but could not maintain the patch long enough to wash on the drug and record an affect. Therefore, to determine the properties of the zebrafish Kv1.1 channel I attempted to express it in *Xenopus* oocytes and record the current using two electrode voltage clamp. Due to low expression, only small amplitude currents were recorded from the oocytes which were insufficient for proper analysis to be performed and thus experiments were stopped. See appendix II for details of the experiments.

3.4 Action potentials in the Mauthner and MiD2cm cells at 48 hours post fertilization

My final aim of this thesis was to establish if and how Kv1.1 channels affect the firing behavior of the Mauthner and MiD2cm cells. It has been shown in adult zebrafish and goldfish that inhibitory inputs onto the Mauthner cell

ensures it fires only one action potential in response to a stimulus (Furukawa & Furshpan 1963). Recent work in adult goldfish has suggested that the differential expression of Kv1 subunits further contributes to the altered firing behavior (Nakayama & Oda 2004). My objectives were to record action potentials from the Mauthner and MiD2cm cells at 48 hpf and then apply DTX_K to determine how blocking the Kv1.1 channels affected their firing pattern. In spite of the lack of success with applying pharmacological agents while recording potassium currents with the K^+ isolating solution, because the action potentials were being recorded with solutions closest to the physiological saline I suspected I may be able to hold the cell for a longer period of time.

Preliminary data coincides with what is already known about the firing pattern of these cells. When just stimulated to threshold the Mauthner cell generally fired one action potential (Figure 3.16A2, n = 3). Significantly greater stimuli sometimes caused the cell to fire 2 or 3 times at the onset of the stimulus (Figure 3.16A2, n = 3). The MiD2cm cell often fired multiple action potentials; however when stimulated to threshold it only fired once or twice at the onset of current injection (Figure 3.16B1 and B2, n = 6). Although increased current injection resulted in both cells eliciting multiple action potentials, their pattern of firing was very different. In the Mauthner cell the action potentials occurred at irregular intervals near the onset of the stimulus (Figure 3.16A1) while the MiD2cm cell fired action potentials at regularly spaced intervals for the duration of the stimulus (Figure 3.16B1). The number of action potentials evoked in the MiD2cm cell increased with the amount of current injected while in the Mauthner

cell the number of action potentials remained relatively constant (Figure 3.17A1 and A2). The increase in firing frequency of the MiD2cm was relatively linear with respect to the increase in current, with a slope of 1268 ± 268 Hz/nA (Figure 3.17B).

The threshold potential of the Mauthner and MiD2cm cells were not significantly different (Table 3.2, t-test, $P = 0.29$); but because the Mauthner cell had an input resistance approximately one third that of the MiD2cm cell, it meant that the Mauthner cell required three times the current to bring it to threshold. The amplitudes of the action potentials elicited by the Mauthner cell and MiD2cm were not significantly different (t-test, $P = 0.56$), but the half width of the Mauthner cell was significantly greater than that of the MiD2cm cell (Table 3.2, Mann-Whitney test, $P = 0.017$, $n = 3$ (Mauthner), $n = 6$ (MiD2cm)). Finally the amplitude of the afterhyperpolarization phase was significantly greater in the MiD2cm cell, -35.7 ± 1.1 mV ($n = 6$), compared with that in the Mauthner cell, -11.2 ± 0.8 mV ($n = 3$) (Figure 3.16A2 and B2, Table 2, t-test, $P < 0.001$).

The pharmacology using DTX_K has yet to be completed due to complications of being unable to hold the cell long enough. Therefore we cannot definitively state how Kv1.1 channels regulate the firing rate of the Mauthner and MiD2cm cells. However, based on how different the Kv currents are in the two cells, it is likely that the differential expression of multiple Kv subunits is responsible for establishing the two firing behaviors, and not just Kv1 subunits as previously proposed by Nakayama and Oda (2004).

Figure 3.1. Amino acid sequence alignment of zebrafish, human, mouse and rat voltage gated potassium channel 1.1

Sequences were blasted and retrieved using the Ensembl database. Two sequences were obtained for zebrafish whereas human, mouse and rat each only had a single sequence. Sequences were aligned using the COBALT multiple sequence alignment tool in NCBI. The top sequence is zebrafish Kv1.1 labeled Ensdarp00000085980 (P85980) and was the standard sequence against which the other four were compared. (-) denotes an identical amino acid to the P85980 sequence. X denotes a changed amino acid in the zebrafish protein P11986 that differs from all other sequences. X denotes an amino acid that differs from the P85980 sequence but is found in the human sequence. X denotes an amino acid in the mouse and/or rat sequence that is different from the zebrafish and human sequences. Blue lines signify where the T1 and transmembrane domains (Sx) of the Kv1.1 alpha subunits lie within the sequence. Red line denotes the antigenic site recognized by the Kv1.1 antibody.

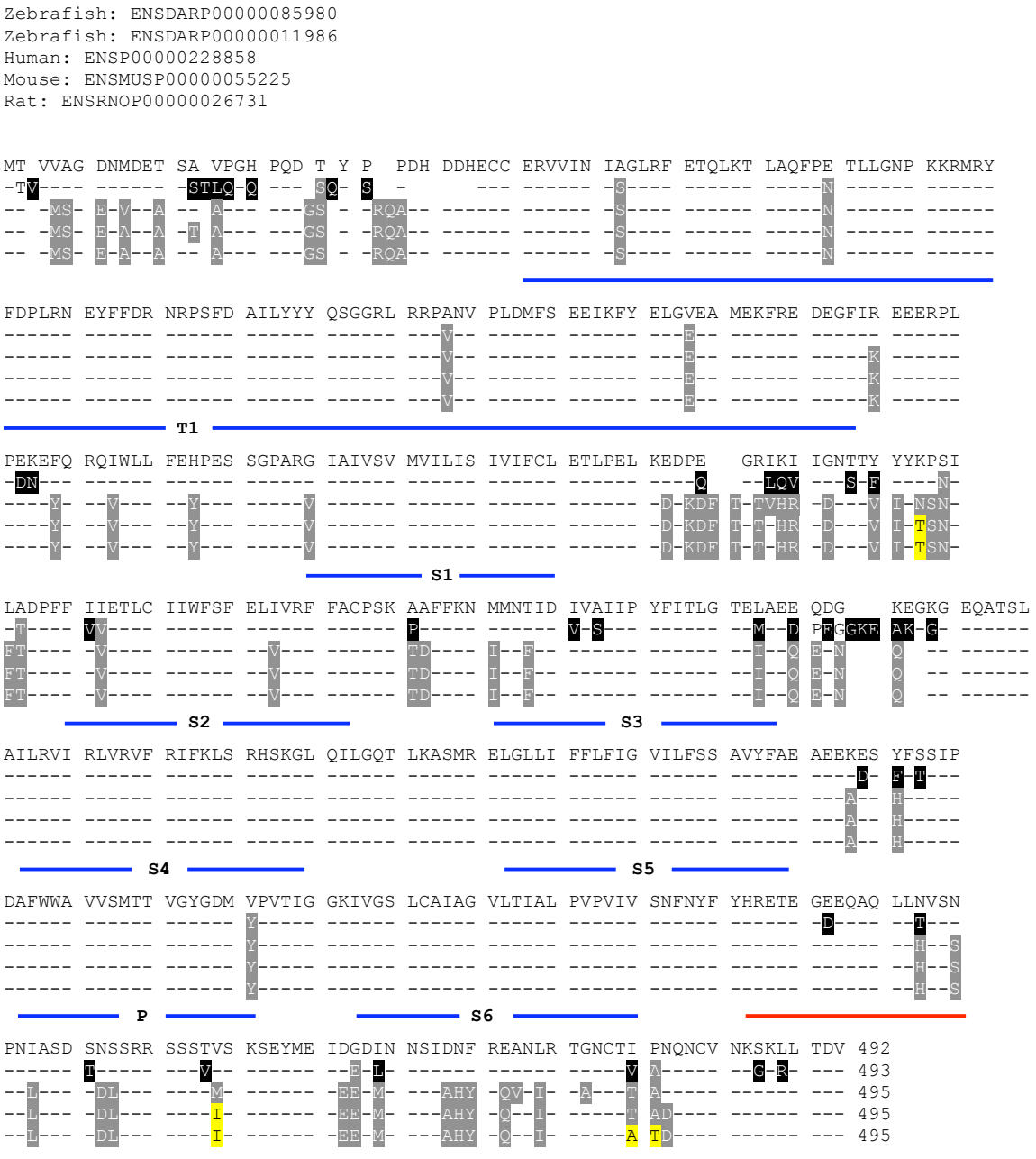
Zebrafish: ENSDARP00000085980
Zebrafish: ENSDARP00000011986
Human: ENSP00000228858
Mouse: ENSMUSP00000055225
Rat: ENSRNOP00000026731
T1
S1
S2
S3
S4
S5
P
S6

Figure 3.2. Presence of the voltage gated potassium channel 1.1 in the head of zebrafish larvae at 48 hours post fertilization

(A) Kv1.1 protein expression was detected using anti-Kv1.1. Positive staining was located behind the eye (arrow) and in the hindbrain (arrowhead). (B) The Mauthner cell (arrowhead) and neurons of the Trigeminal ganglia (arrow) were labeled with anti-3A10. (C) Merged images of A and B confirm the presence of Kv1.1 in the Mauthner cell and the Trigeminal ganglia of 48 hpf larvae (white staining). These images are a dorsal view of the fish with rostral up and caudal down. Four separate experiments were run with 10 larvae per experiment. Scale bar, 50 μm.

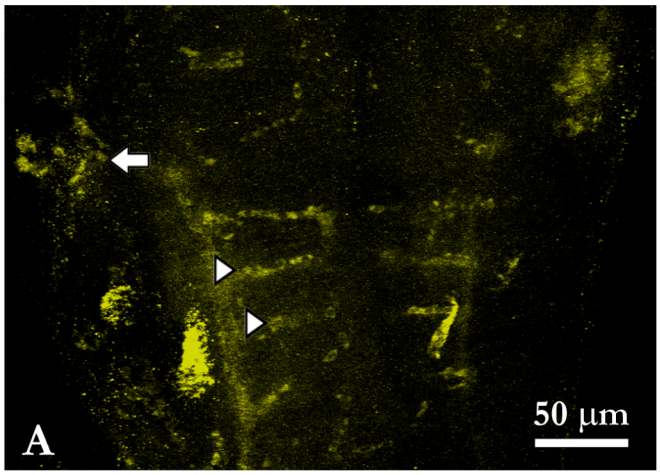

Kv1.1

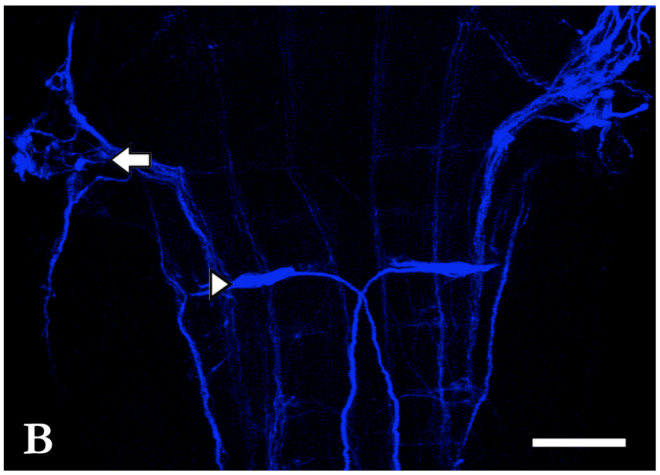

3A10

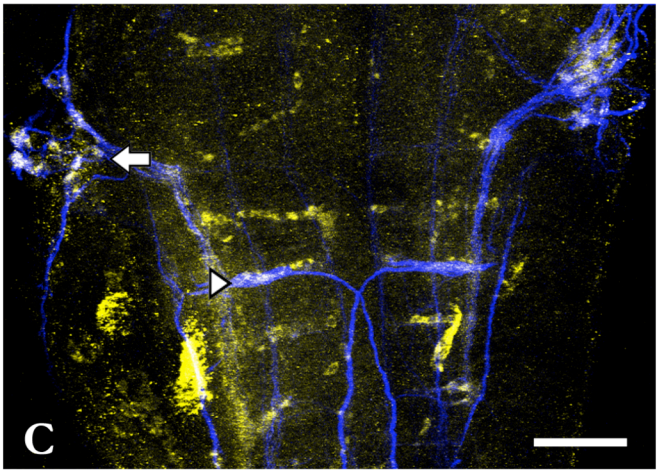

Merge

Figure 3.3. Presence of the voltage gated potassium channel 1.1 in the trunk of zebrafish larvae at 48 hours post fertilization

(A) Kv1.1 staining was detected in the soma of neurons (arrowheads) located dorsally along the trunk. (B) Axons of the spinal cord (arrows) were labeled with anti-3A10. (C) Merged images of A and B which suggest, based on location and morphology that the Kv1.1 staining is within the Rohon Beard cells of the dorsal spinal cord. In these images the head is to the right and dorsal is up. Four separate experiments were run, with 10 fish per trial. Scale bar, 50 μm.

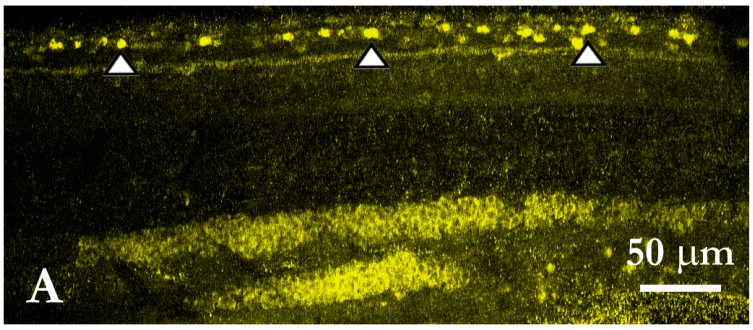

Kv1.1

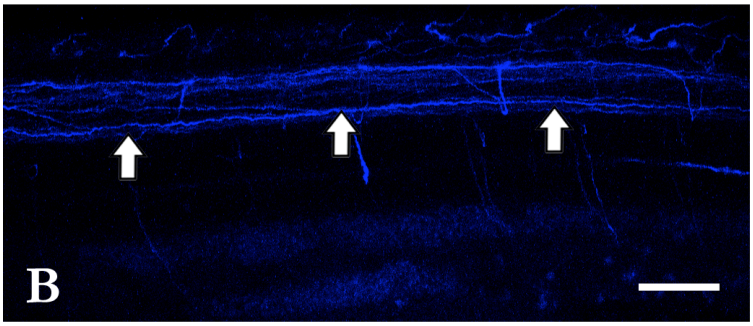

3A10

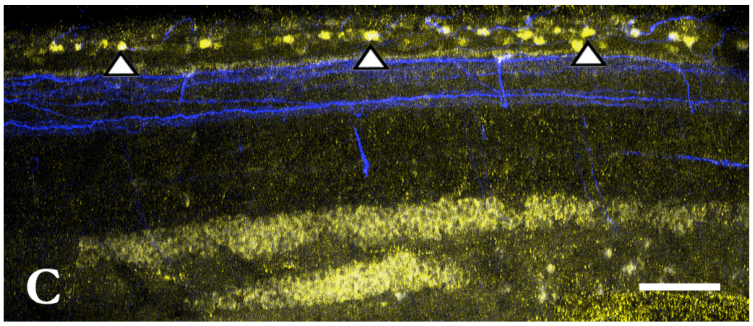

Merge

Figure 3.4. Presence of the voltage gated potassium channel 1.1 in the head of zebrafish larvae at 72 hours post fertilization

(A) Kv1.1 protein expression was detected using anti-Kv1.1. Positive staining was located behind the eye (arrow) and in the hindbrain (arrowheads). (B) The Mauthner cell (arrowhead) and neurons of the Trigeminal ganglia (arrow) were labeled with anti-3A10. (C) Merged images of A and B confirming the presence of Kv1.1 in the Mauthner cell and the Trigeminal ganglia of 48 hpf larvae. These images are a dorsal view of the fish with rostral up and caudal down. Three separate experiments were run with 10 larvae per experiment. Scale bar, 50 μm.

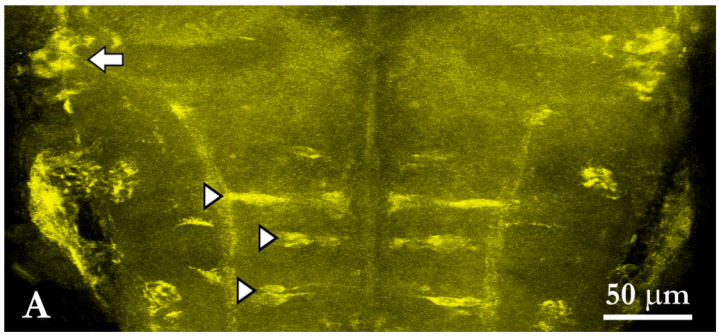

Kv1.1

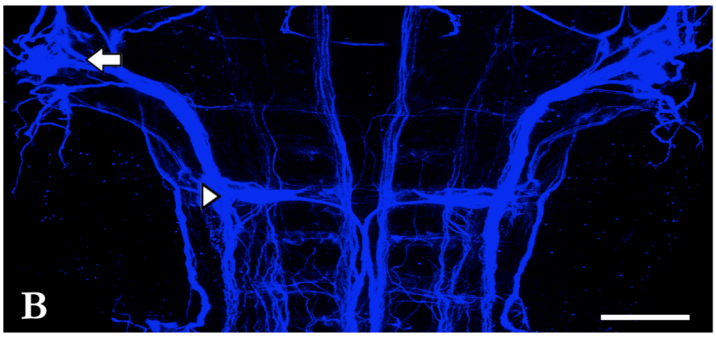

3A10

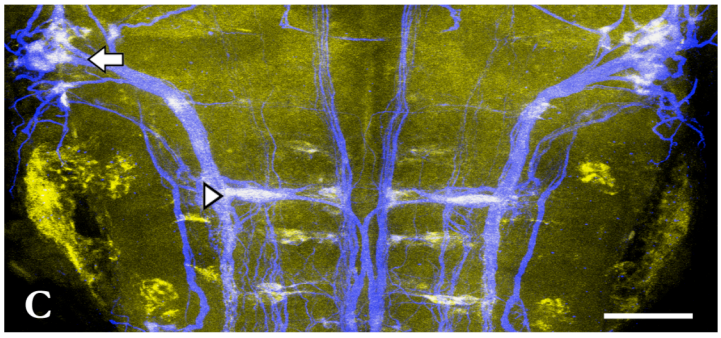

Merge

Figure 3.5. Presence of the voltage gated potassium channel 1.1 in the trunk of zebrafish larvae at 72 hours post fertilization

(A) Kv1.1 staining was detected in the soma of neurons located dorsally (arrowheads) within the trunk and along the midline (arrows). (B) Axons of the spinal cord were labeled with anti-3A10 (arrows). (C) Merged images of A and B which suggest, based on location and morphology, Kv1.1 staining is within the Rohon Beard cells of the dorsal spinal cord and in neurons of the dorsal root ganglia. In these images dorsal is up and the head is to the right. Three separate experiments were run, with 10 fish per trial. Scale bar, 50 μm.

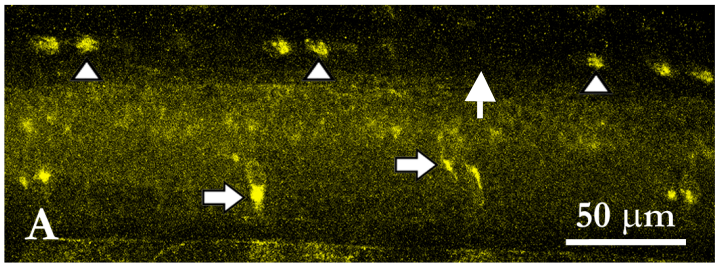

Kv1.1

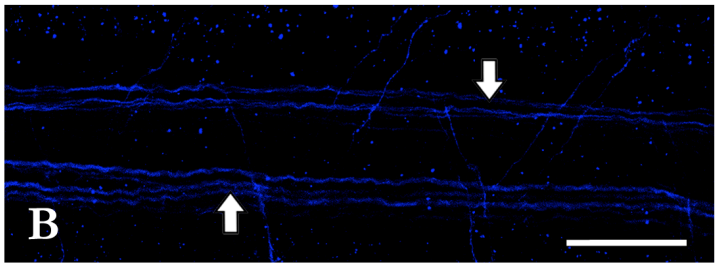

3A10

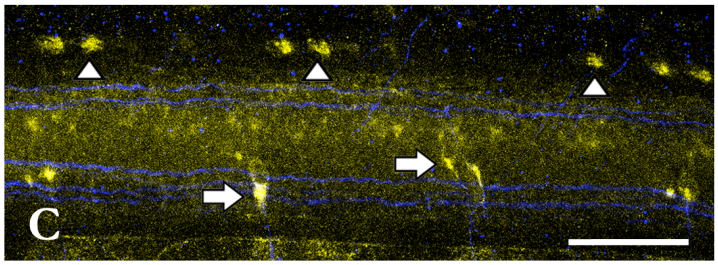

Merge

Figure 3.6. Expression of the voltage gated potassium channel 1.1 in the Mauthner cell of zebrafish larvae at 72 hours post fertilization

Confocal images were loaded into Imaris software to produce 3D images of the staining pattern in the hindbrain of 72 hpf zebrafish larvae. (A) Dorsal images of the hindbrain pertaining to the region where the Mauthner cell (in green, labeled with anti-3A10) and its two homologues lie. Kv1.1 (in red, labeled with anti-Kv1.1) is present within the soma of the Mauthner cell (arrowhead). Positive staining for Kv1.1 also appears in other cells of the hindbrain, one of which, based on its location, is proposed to be the MiD2cm cell (arrow). These images are a dorsal view of the fish with rostral up and caudal down. (B) The soma of the Mauthner cell (green) containing Kv1.1 (red), the majority of which appears to be retained within the cell. Dorsal is up, ventral down and the otic vesicle to the right. Scale bars, 20 μm.

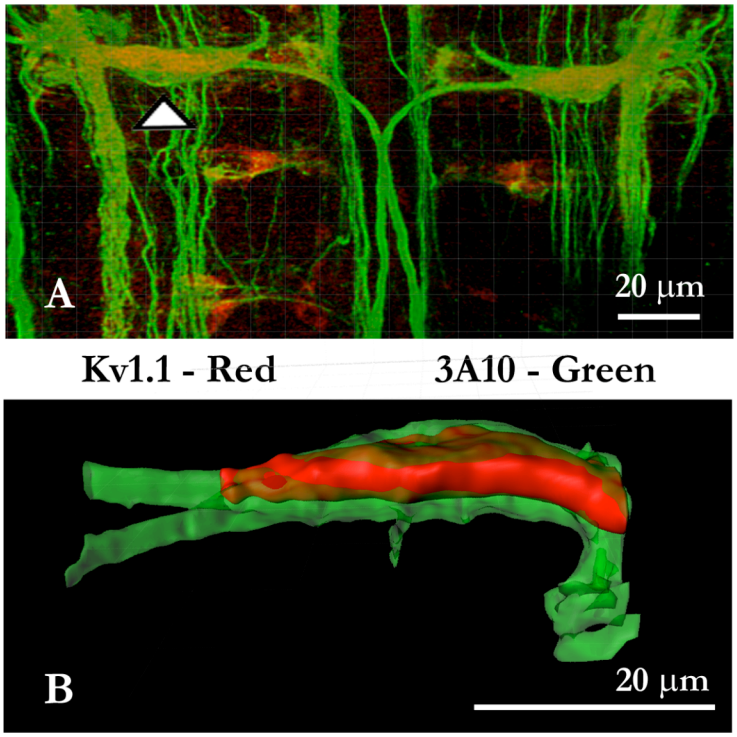
A
20 μm
Kv1.1 - Red
3A10 - Green
B
20 μm

Figure 3.7. Presence of mRNA encoding the voltage gated potassium channel 1.1 in 48 hour post fertilization zebrafish larvae and brain of adult zebrafish

RT-PCR was utilized to determine which two genes encoding the zebrafish Kv1.1 protein were being expressed at the 48 hpf larval stage and in adult brain. The two genes that encode the protein are G62942 and G17108. The PCR products were designed to be 914 bp for G62942 and 1072 bp for G17108. The lane designations for images A and B are: the far left lane is a 1kb DNA ladder (Fermentas), the 2nd lane is zebrafish β-actin, the 3rd lane is G62942 and the last lane on the right is G17108. (A) At 48 hpf both genes were expressed (n = 3 experiments). (B) In brain of adult zebrafish only a PCR product for G62942 was detected (n = 3 experiments).

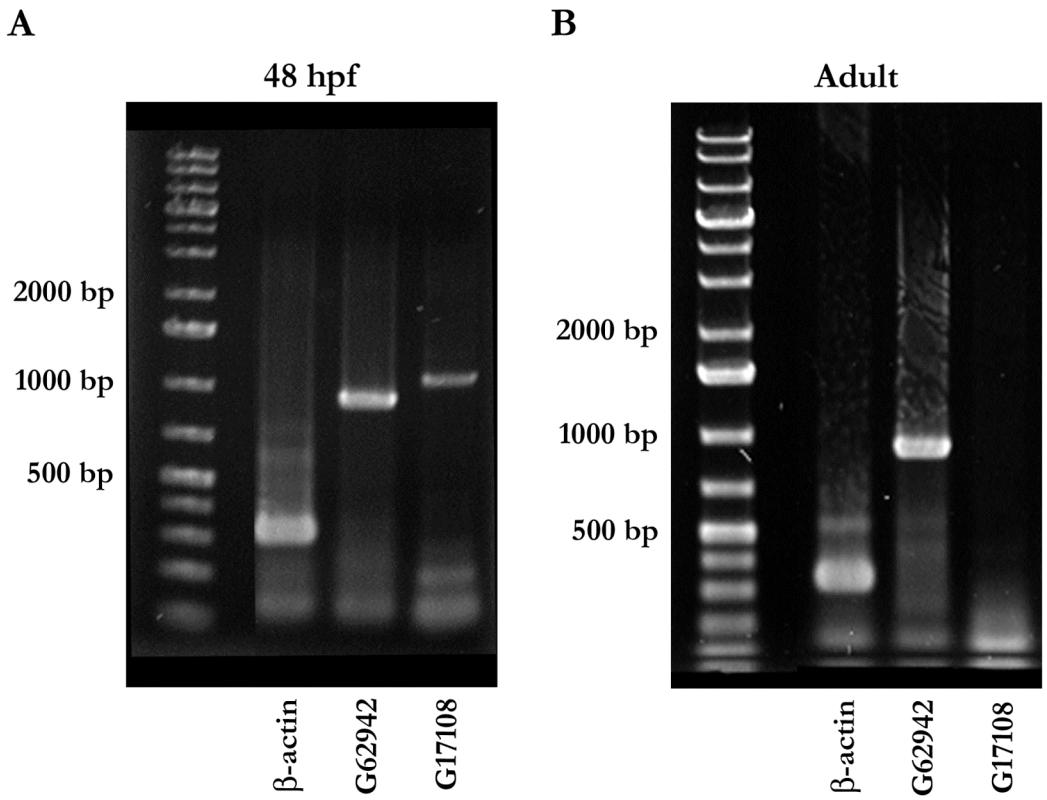
A
48 hpf
2000 bp
1000 bp
500 bp
β-actin
G62942
G17108
B
Adult
2000 bp
1000 bp
500 bp
β-actin
G62942
G17108

Figure 3.8. mRNA expression of the voltage gated potassium channel 1.1 in the head and trunk of zebrafish larvae at 48 hours post fertilization

In situ hybridizations were performed on 48 hpf larvae to determine the cellular expression pattern of Kv1.1 mRNA and confirm the staining pattern observed with the antibodies. DIG labeled RNA probes were produced against the G62942 sequence. (A) Staining in the head was located behind the eyes (arrow), believed to be the trigeminal ganglia and within the hindbrain, suspected of being the reticulospinal neurons (arrowheads), the most rostral being the Mauthner cell. The image is a dorsal view of the head, rostral up and caudal down. (B) Staining in the trunk was located along the dorsal edge (arrowhead) believed to be the Rohon Beard cells. Dorsal side is up and rostral is to the left. (n = 3 experiments, 10 fish per experiment). Scale bar, 50 μm.

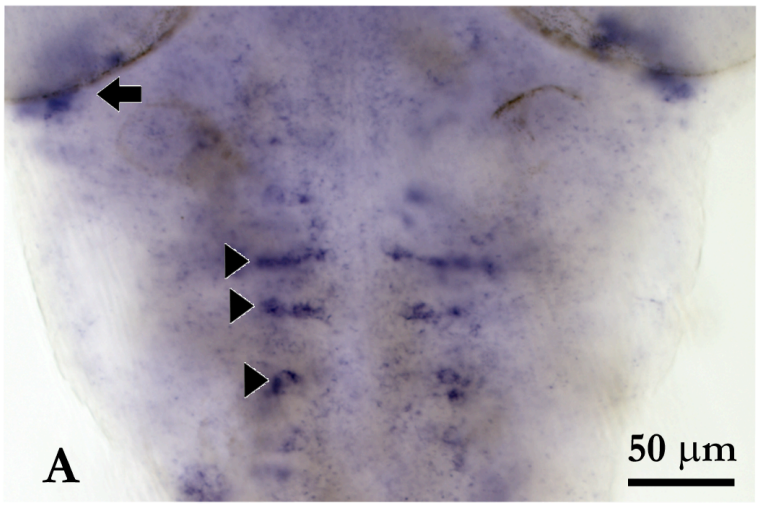
A
50 μm

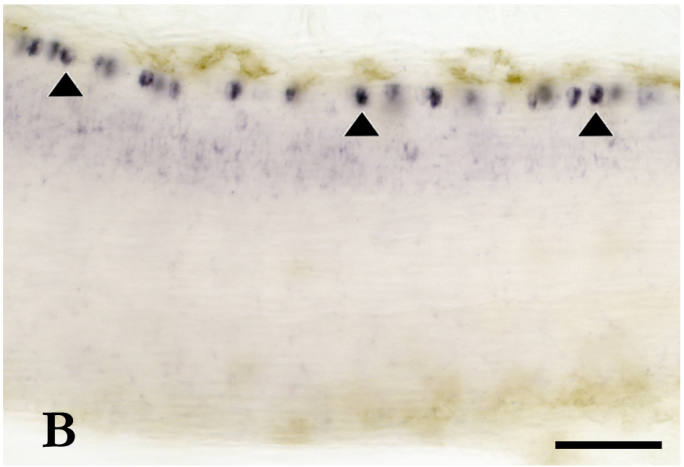
B

Figure 3.9. Voltage gated potassium channel currents in the Mauthner cell at 48 hours post fertilization

(A) Kv currents in the Mauthner cell were recorded using K^+ isolating ECS (calcium replaced with cadmium). Currents were evoked from the Mauthner cell by 220ms voltage steps ranging from -80 to +40 mV in 10 mV intervals. (B) Current voltage relationship of the peak (Δ) and sustained (□) currents in the Mauthner cell (n = 8). The peak current density was greater, comprised of the transient and delayed rectifier currents. The sustained current density, largely comprised of the delayed rectifier current, was smaller in amplitude. (C) Conductance-voltage plots of the peak (Δ) and sustained (□) currents calculated using the GHK normalization (white symbols) and DF normalization (grey symbols) methods, that were fit with a Boltzmann function.

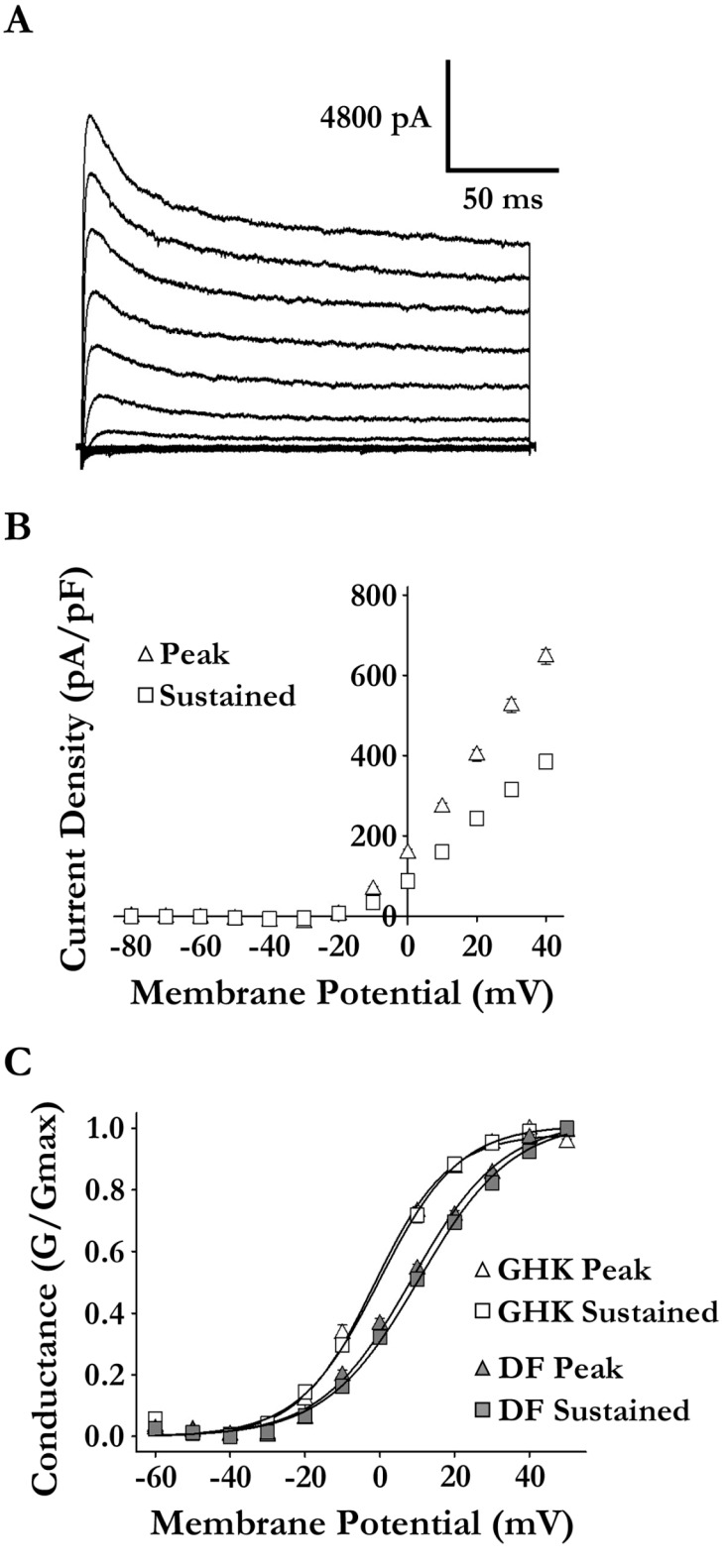
A
4800 pA
50 ms
B
Current Density (pA/pF)
Peak
Sustained
800
600
400
200
0
-80 -60 -40 -20 0 20 40
Membrane Potential (mV)
C
Conductance (G/Gmax)
1.0
0.8
0.6
0.4
0.2
0.0
GHK Peak
GHK Sustained
DF Peak
DF Sustained
-60 -40 -20 0 20 40
Membrane Potential (mV)

Figure 3.10. Decay kinetics of the A-type current in the Mauthner cell at 48 hours post fertilization

(A) Kv currents elicited using stepwise depolarizations were best fit with a double exponential function (dashed red line) as opposed to a single exponential (dashed blue line) for steps ranging from 10 to 40 mV. Example trace shown is exponential functions fit to current elicited at 40 mV. (B) Fast (Δ) and slow (■) inactivation time constants (τ, ms) of the double exponential function (n = 8). At the potentials, which the decay kinetics were measured there was no significant difference in the fast or slow time constants of inactivation.

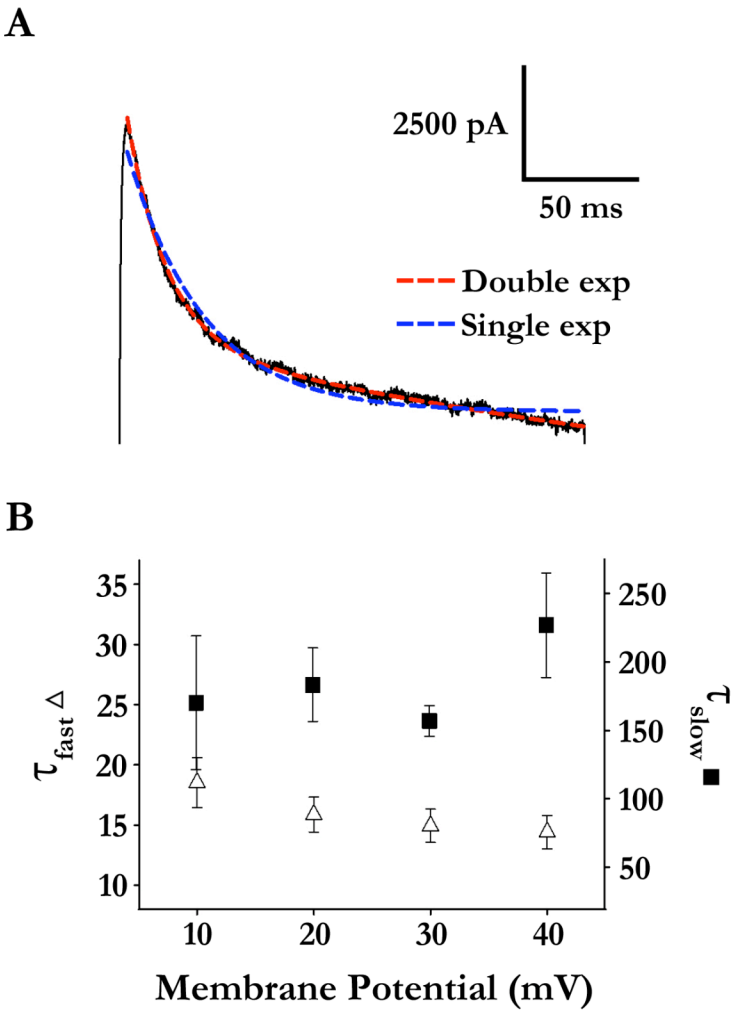
A
2500 pA
50 ms
Double exp
Single exp
B
35
30
25
20
15
10
250
200
150
100
50
10
20
30
40
Membrane Potential (mV)

Figure 3.11. Voltage gated potassium channel currents in the MiD2cm cell at 48 hours post fertilization

(A) Kv currents in the MiD2cm cell were recorded using K^+ isolating ECS (calcium replaced with cadmium). Currents were evoked from the cell using 220ms voltage steps ranging from -80 to +30 mV at 10 mV intervals. (B) Current voltage relationship of the sustained (○) current density in the MiD2cm cell (n = 15). (C) Conductance-voltage plots of the potassium current derived from tail currents (●) or calculated using the GHK (○) or DF (●) normalization methods and fit with a Boltzmann function.

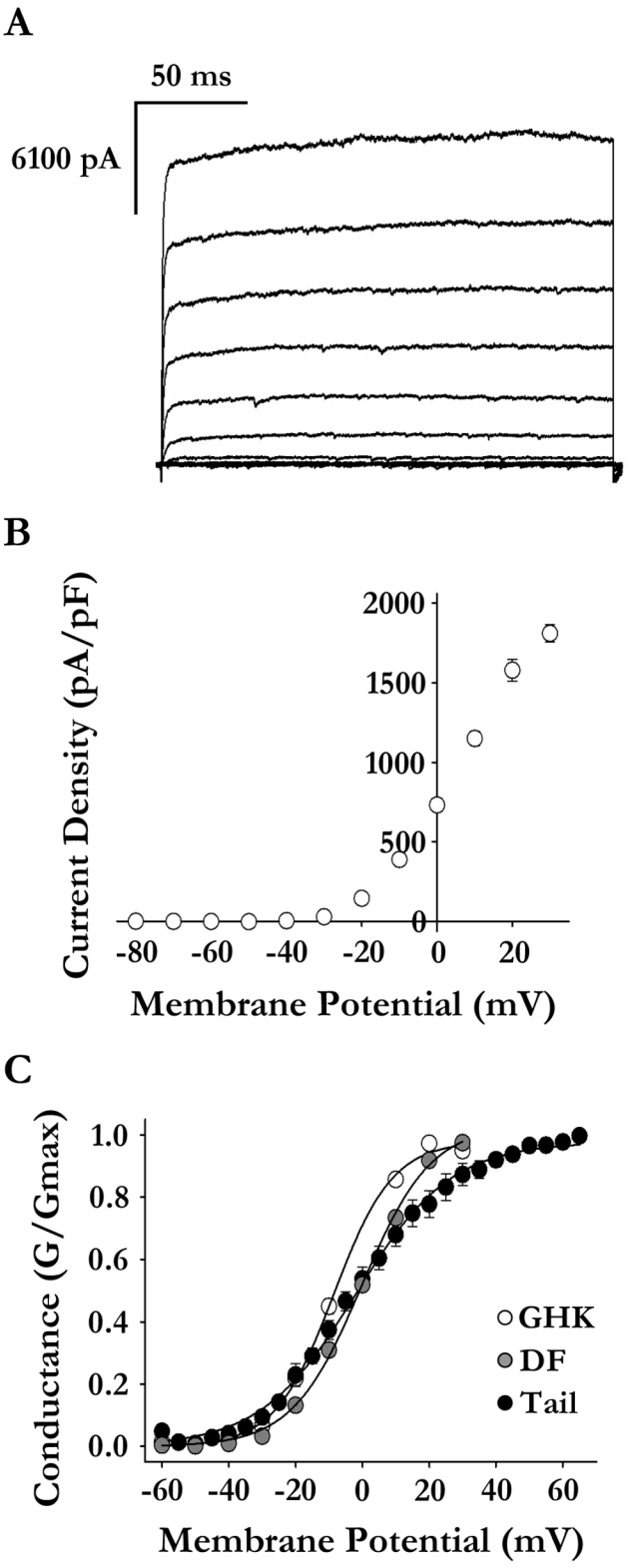
A
50 ms
6100 pA
B
Current Density (pA/pF)
2000
1500
1000
500
0
-80
-60
-40
-20
0
20
Membrane Potential (mV)
C
Conductance (G/Gmax)
1.0
0.8
0.6
0.4
0.2
0.0
-60
-40
-20
0
20
40
60
Membrane Potential (mV)
GHK
DF
Tail

Figure 3.12. Effect of calcium on isolating voltage gated potassium channel currents in the Mauthner and MiD2cm cells at 48 hours post fertilization

Currents were measured using two different extracellular solutions (ECS), normal ECS (white symbol) containing calcium and K^+ isolating ECS (black symbol) in which the calcium was replaced with cadmium. (A) Amplitude of the peak current density in the Mauthner cell was significantly reduced after replacing calcium with cadmium (t-test, $P < 0.05$, n = 17 normal ECS, n = 8, K^+ isolating ECS). (B) Amplitude of the sustained current density in the Mauthner cell was significantly reduced at potentials ranging from -50 to 0 mV when calcium was replaced with cadmium (Mann Whitney test, $P < 0.05$). (C) Amplitude of the sustained current density in the MiD2cm cell was significantly increased with the removal of calcium (t-test, $P < 0.01$, n = 10, normal ECS, n = 15, K^+ isolating ECS).

A

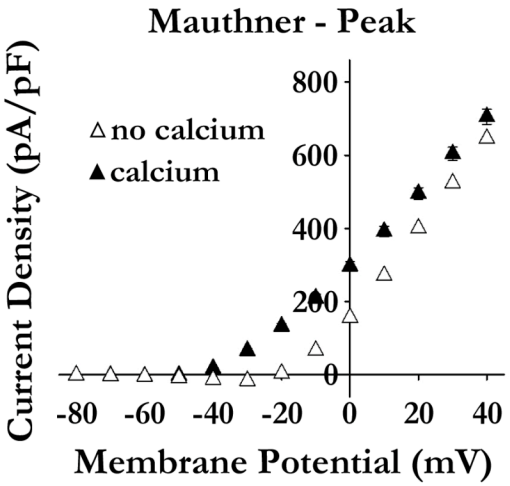
Mauthner - Peak
Current Density (pA/pF)
no calcium
calcium
800
600
400
200
0
-80 -60 -40 -20 0 20 40
Membrane Potential (mV)

B

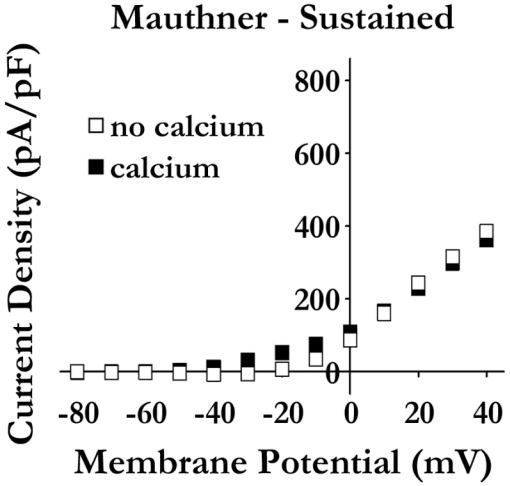
Mauthner - Sustained
Current Density (pA/pF)
no calcium
calcium
800
600
400
200
0
-80 -60 -40 -20 0 20 40
Membrane Potential (mV)

C

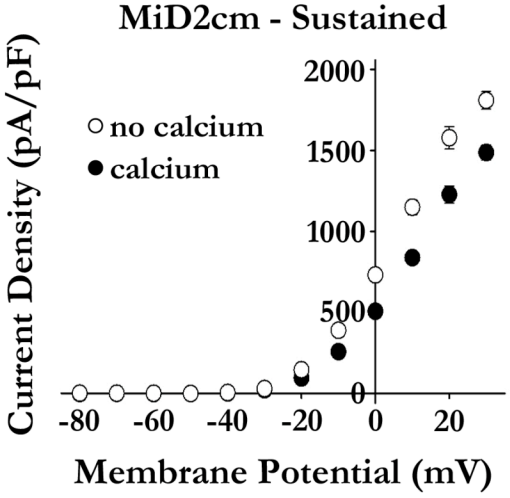
MiD2cm - Sustained
Current Density (pA/pF)
no calcium
calcium
2000
1500
1000
500
0
-80 -60 -40 -20 0 20
Membrane Potential (mV)

Figure 3.13. Effect of 4-aminopyridine on potassium currents in the Mauthner cell at 48 hours post fertilization

(A) Potassium currents recorded in normal ECS (contains calcium) were evoked by 220 ms depolarization steps ranging from -80 to 50 mV at 10 mV increments. (B) Potassium currents evoked using the same voltage protocol as in (A) after the application of 5 mM 4-AP. (C) Current voltage relation showing a complete inhibition of the peak current (▲) which exposed an inward current (♦) (paired t-test, $P < 0.05$, $n = 8$). (D) Current voltage relation showing 4-AP inhibited the sustained current (■) (paired t-test, $P < 0.05$, $n = 8$). Black symbols denote current amplitude before 4-AP and grey symbols current amplitude after 4-AP.

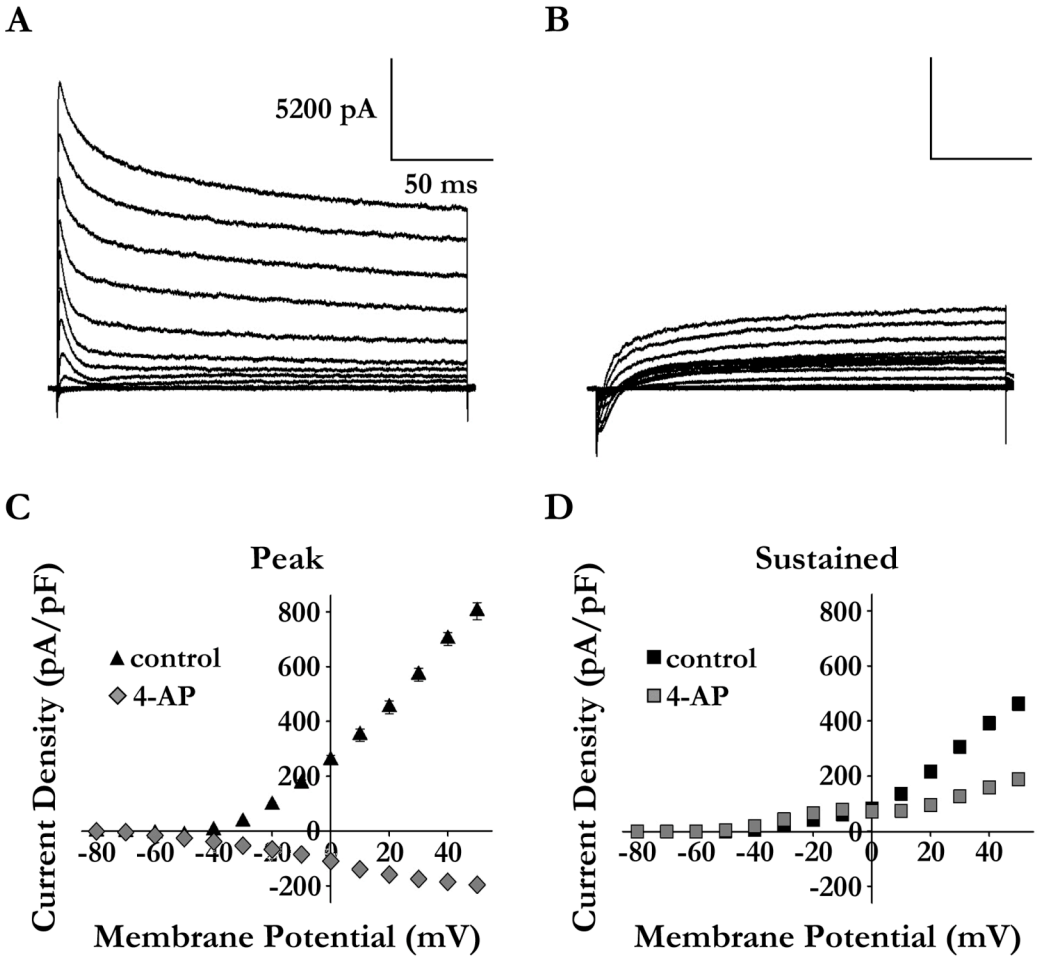
A
B
5200 pA
50 ms
C
D
Peak
Sustained
control
4-AP
Current Density (pA/pF)
Membrane Potential (mV)
800
600
400
200
0
-200
-80
-60
-40
-20
20
40

Figure 3.14. Effect of tetraethylammonium on potassium currents in the Mauthner cell at 48 hours post fertilization

(A) Potassium currents recorded in normal ECS (contains calcium) were evoked by 220 ms depolarization steps ranging from -80 to 50 mV at 10 mV increments. (B) Potassium currents evoked using the same voltage protocol as in (A) after the application of 5 mM TEA. (C) Current voltage relation showing TEA only affected the peak current at voltages ≥ 20 mV (▲) (paired t-test, $P < 0.01$, $n = 6$). (D) Current voltage relation showing partial inhibition of the sustained current by TEA (■) (paired t –test, $P < 0.05$, $n = 6$). Black symbols denote current amplitude before TEA and grey symbols denote current amplitude after TEA.

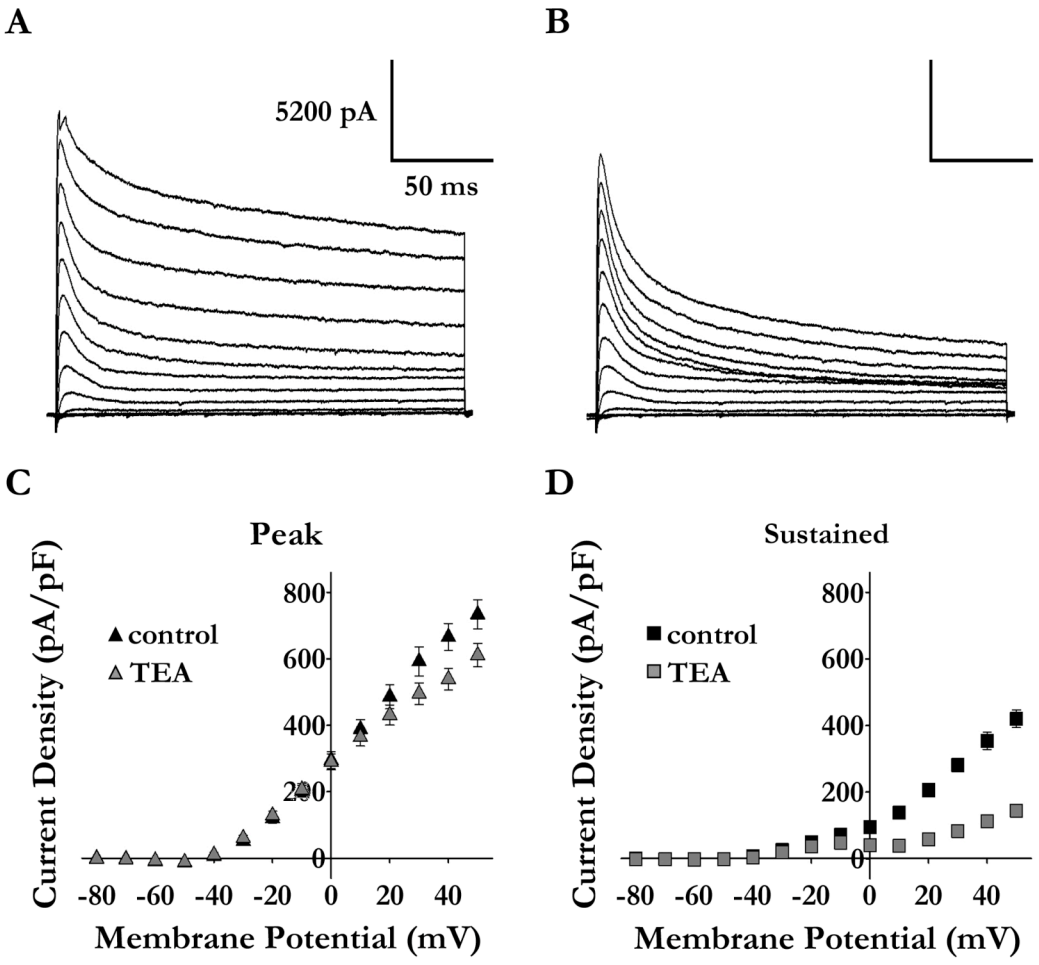
A
B
5200 pA
50 ms
C
D
Peak
Sustained
Current Density (pA/pF)
control
TEA
800
600
400
200
0
-80 -60 -40 -20 0 20 40
Membrane Potential (mV)

Figure 3.15. Effect of tetraethylammonium on potassium currents in the MiD2cm cell at 48 hours post fertilization

(A) Potassium currents evoked in normal ECS (contains calcium) with 220 ms depolarization steps ranging from -80 to 30 mV at 10 mV increments. (B) Potassium currents evoked using the same voltage protocol as in (A) after application of 5 mM TEA exposed a second A-type current. (C) Current voltage relations of the exposed A-type current (▲) and the much reduced sustained current density (●) in the presence of TEA (paired t-test, $P < 0.001$, $n = 4$). (●) is the sustained current density prior to application of TEA.

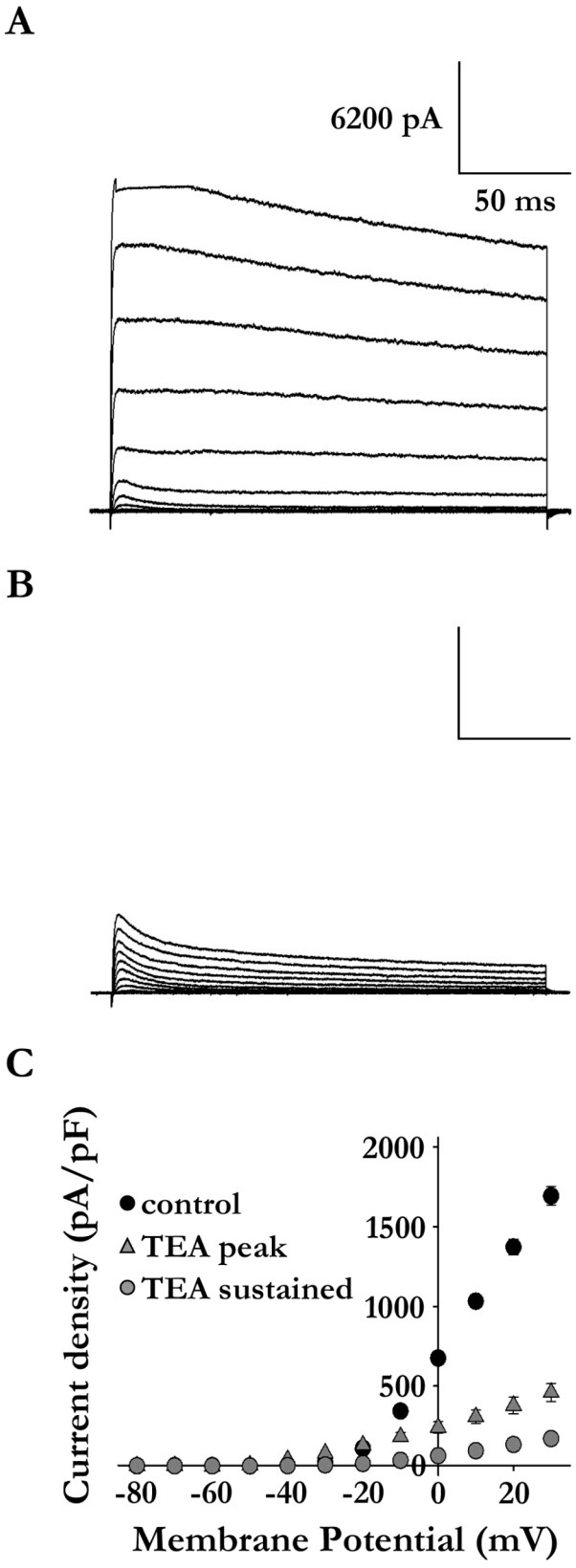
A
6200 pA
50 ms
B
C
Current density (pA/pF)
control
TEA peak
TEA sustained
2000
1500
1000
500
0
-80
-60
-40
-20
0
20
Membrane Potential (mV)

Figure 3.16. Firing activity of the Mauthner and MiD2cm cells at 48 hours post fertilization

(A1 and A2) Representative traces of the Mauthner cell firing action potentials when injected with different amounts of current. (A3) Current pulse protocol, 50 ms in duration, used to evoke action potentials from the Mauthner cell. For this particular cell, 0.36 nA of current was required to cause the cell to fire a single action potential (A2). Injecting 0.48 nA of current into the Mauthner cell caused it to fire multiple action potentials (A1). (B1 and B2) Representative traces of the MiD2cm cell firing action potentials when injected with different amounts of current. (B3) Current pulse protocol, 50 ms in duration, used to evoke action potentials from the MiD2cm cell. (B2) For this particular cell, stimulating it with 0.10 nA of current caused it to fire a single action potential. (B1) The MiD2cm cell fired multiple action potentials when stimulated with 0.14 nA of current. The trends observed in A1, A2, B1 and B2 were similar from cell to cell, however the amount of injected current varied by a few hundredths of a nanoampere. Three recordings were made from the Mauthner cell and seven from the MiD2cm cell. Scale bar dimensions for A1 are the same as in A2 and for B1 the same as in B2.

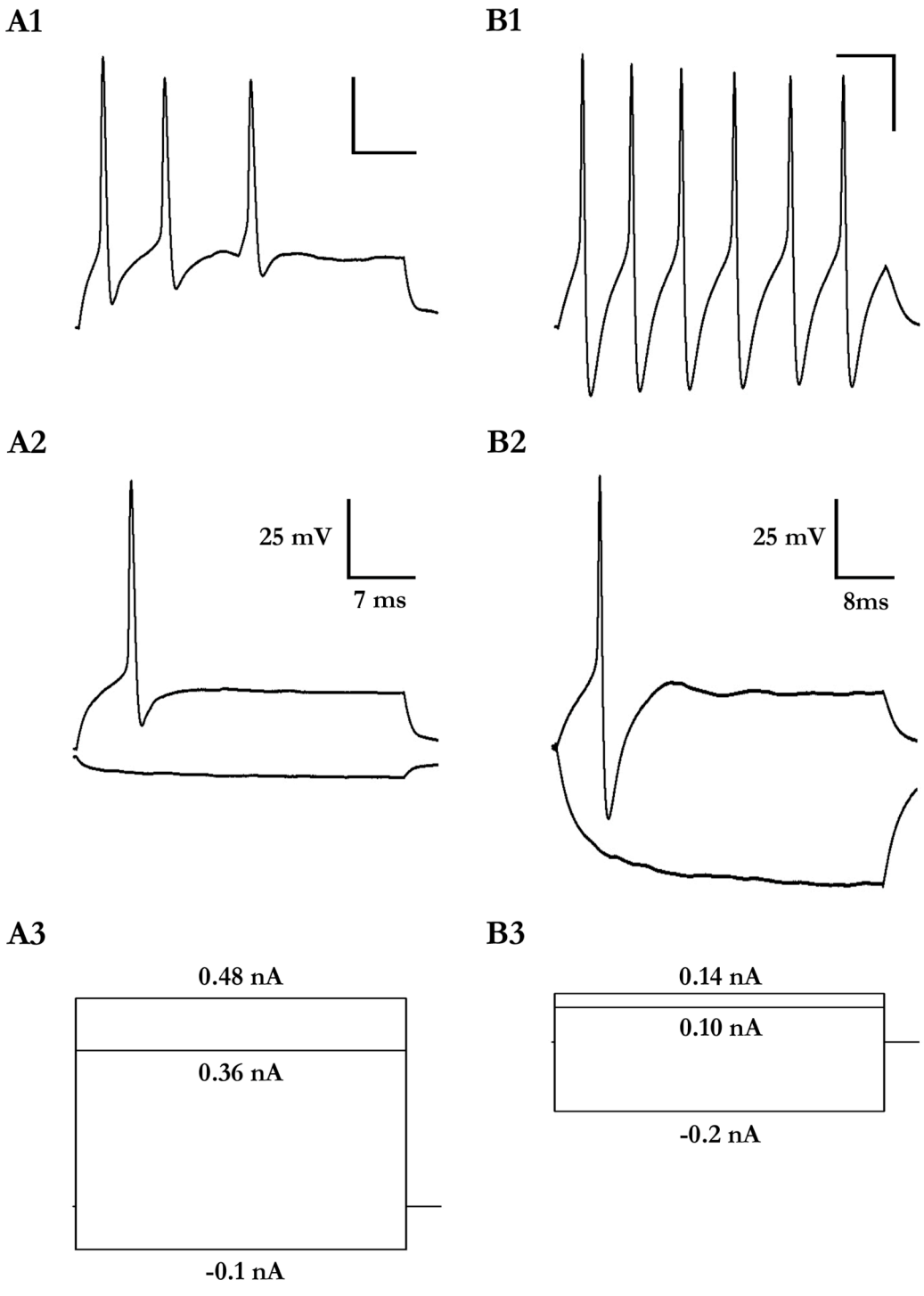
A1
B1
A2
25 mV
7 ms
B2
25 mV
8ms
A3
0.48 nA
0.36 nA
-0.1 nA
B3
0.14 nA
0.10 nA
-0.2 nA

Figure 3.17. Firing frequency of the Mauthner and MiD2cm cells at 48 hours post fertilization

The numbers of action potentials evoked from the Mauthner and MiD2cm cells in response to different amounts of injected current were counted. (A1) The Mauthner cell fired anywhere from 1 to 4 action potentials (n = 3). (A2) The number of action potentials evoked in the MiD2cm cell appeared to increase every time the amount of injected current was increased (n = 5). (B) The relationship between the firing frequency and input current for the MiD2cm cell (n = 5).

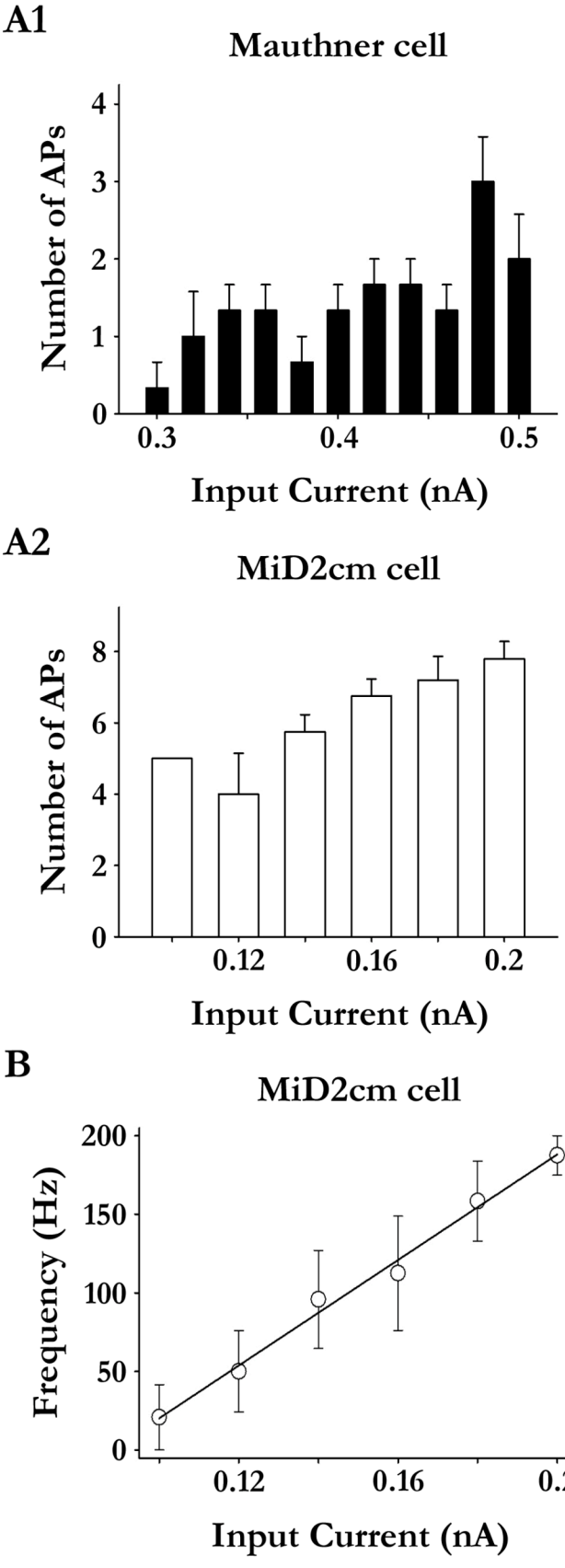
A1
Mauthner cell
Number of APs
0
1
2
3
4
0.3
0.4
0.5
Input Current (nA)
A2
MiD2cm cell
Number of APs
0
2
4
6
8
0.12
0.16
0.2
Input Current (nA)
B
MiD2cm cell
Frequency (Hz)
0
50
100
150
200
0.12
0.16
0.2
Input Current (nA)

Table 3.1. Passive membrane properties of the Mauthner and MiD2cm cells at 48 hours post fertilization

Cell type	Cm (pF)	R_{input} (MΩ)	Rm (MΩ)	Ra (MΩ)
Mauthner	22.7 ± 0.4 (8)	48.4 ± 1.9 (3)	41.5 ± 2.2 (8)	6.0 ± 0.2 (8)
MiD2cm	10.1 ± 0.3 (15)	289 ± 25 (7)	280 ± 24 (15)	7.8 ± 0.6 (15)

All values were recorded immediately after obtaining a whole cell patch in voltage clamp mode. All values are given as Mean ± SE (n). Cm is membrane capacitance, R_{input} is input resistance, R_m is membrane resistance and R_a is access resistance.

Figure 3.18. Diagram of action potential measurements

The threshold potential was recorded at the inflection point of the trace where the slow depolarization turned upwards into the depolarization phase of the action potential (1). The amplitude was measured from the threshold potential to the peak of the action potential (2). The half width was measured where the action potential had reached half its amplitude (3). The afterhyperpolarization was measured from the valley of the hyperpolarization phase to the resting potential the cell returned to (4).

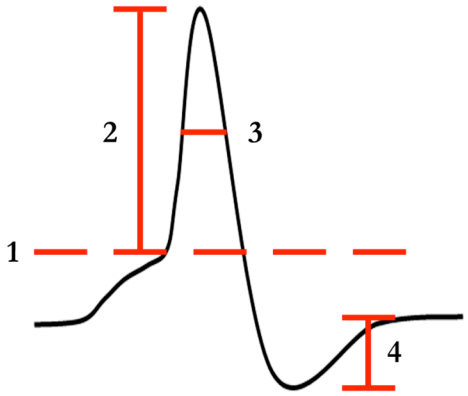

Table 3.2. Action potential parameters of the Mauthner and MiD2cm cells at 48 hours post fertilization

Cell type	R_{input} (MΩ)	Threshold[1] (mV)	Amplitude[2] (mV)	1/2 width[3] (ms)	AHP[4] (mV)
Mauthner	65.8 ± 4.5 (3)	-37.3 ± 0.4 (3)	55.6 ± 1.5 (3)	0.60 ± 0.04 (3)	-11.2 ± 0.8 (3)
MiD2cm	206 ± 12 (6)	-34.2 ± 1.8 (6)	54.2 ± 1.4 (6)	0.38 ± 0.01[a] (6)	-35.8 ± 1.1[b] (6)

Input resistance (R_{input}) was calculated using Ohm's Law. A pulse of negative current was injected into the cell for 50 ms and the membrane potential of the cell was recorded. The input resistance was calculated by dividing the recorded membrane potential by the injected current. The remaining parameters were measured when a cell fired a single action potential. Values are Mean ± SE (n). [a] Significantly different from Mauthner cell, Mann-Whitney test, $P = 0.017$. [b] Significantly different from Mauthner cell, t-test, $P < 0.001$.

4. Discussion

The Mauthner and MiD2cm cells have significantly different activities when stimulated, the Mauthner cell fires a single action potential while the MiD2cm cell fires multiple action potentials (O'Malley et al 1996; Zottoli 1977). One of the major factors underlying this difference in activity is likely to be the expression of different Kv1 channel subunits which conduct different types of currents (Nakayama & Oda 2004).

The focus of this thesis was to understand if and how the zebrafish Kv1.1 channel regulated the firing behavior of the Mauthner and MiD2cm cells at 48 hpf. My initial aim was to determine which cells were expressing the zebrafish Kv1.1 subunit. This was followed by determining the types of Kv currents present in the two different cells through the use of whole cell voltage clamp recording and the application of pharmacological agents. Upon concluding that Kv1.1 was associated with the M-series I sought to express the Kv1.1 subunit in Xenopus oocytes to determine the properties of the current conducted by homomeric Kv1.1 channels and infer its contribution to the total Kv current in the Mauthner and MiD2cm cells. Finally, I wanted to assess if inhibiting Kv1.1 channels by pharmacological means altered the firing patterns of the Mauthner and MiD2cm cells. My ultimate goal was to understand the role of Kv1.1 in regulating the behavior of the Mauthner and MiD2cm cells and hypothesize how this might contribute to eliciting an escape response.

I was successful in reaching some of my objectives including determining the expression pattern of Kv1.1 in 48 hpf zebrafish, recording Kv currents and

beginning to record action potentials. Immunohistochemistry and in situ hybridization experiments indicate zebrafish Kv1.1 is expressed in the Mauthner and MiD2cm cells at 48 hpf. Yet the total Kv current in these two cells is significantly different, suggesting a differential expression of Kv subunits beyond the Kv1 subfamily, as previously suggested (Nakayama & Oda 2004). My data shows the Mauthner cell contains an inactivating A-type current, a delayed rectifier current and possibly a calcium activated potassium current. The MiD2cm cell also contains a delayed rectifier current, but with a much greater current density than that in the Mauthner cell, and a transient A-type current, which was only revealed after the application of TEA. Meanwhile, preliminary results show the Mauthner cell fires a single action potential when brought to threshold while the MiD2cm cell fires multiple action potentials.

4.1 Contribution of the voltage gate potassium channel 1.1 to the sustained current in Mauthner and MiD2cm cells

The sustained current in the Mauthner and MiD2cm cells is a delayed rectifier current as it has a threshold of activation between -40 and -30 mV and inactivates very slowly (Dolly & Parcej 1996). Human, mouse and rat Kv1.1 elicit delayed rectifier currents and thus I hypothesize that the zebrafish Kv1.1 conducts this type of current as well (Grissmer et al 1994; Po et al 1993; Stuhmer et al 1989). A sequence alignment of the two zebrafish Kv1.1 and mammalian homologues shows a relatively high similarity between them with a similar length of the amino terminal. There are only 33 amino acids upstream of the T1 domain suggesting the zebrafish Kv1.1 does not have an inactivation domain in its amino

terminal to produce A-type currents (Hoshi et al 1990; Zagotta et al 1990). Therefore I suspect that the zebrafish Kv1.1 is only contributing to the sustained current in the Mauthner and MiD2cm cells and not the fast inactivating A-type current.

Delayed rectifier currents and ion channels containing Kv1.1 are blocked by TEA (Hopkins 1998; Stanfield 1983). In my experiments, the application of TEA inhibited the sustained currents of the Mauthner and MiD2cm cells by 65% and 85% respectively, when held at 50 and 30 mV. The two residues that greatly contribute to the sensitivity of TEA are D431 and T449 of the Shaker subunit, which reside on either end of the H5 segment (MacKinnon & Yellen 1990). Both of the Kv1.1 proteins in zebrafish contain aspartate at residue 358, which is the equivalent position to Shaker 431 (MacKinnon & Yellen 1990). However P85980 has a valine at residue 376, which has been shown to render the potassium subunit less sensitive to TEA (MacKinnon & Yellen 1990). The second protein, P11986, has a tyrosine at residue 376 which is identical to the mammalian homologues in the alignment. A T449Y mutation in the Shaker subunit actually rendered the channels more sensitive to TEA, suggesting the P11986 subunit may be more sensitive to TEA than P85980 (MacKinnon & Yellen 1990). That both subunits contain residues in the pore region that are bound by TEA suggests these channels are capable of being blocked by TEA. Thus the Kv1.1 channels are likely contributing to the sustained current in both the Mauthner and MiD2cm cells.

Finally, the presence of Kv1.1 in the Mauthner and MiD2cm cells is supported by both the immunohistochemical and in situ staining. The mRNA

expression only represents the expression of G62942, whereas the antibody could be binding to the C-terminus of either of the two zebrafish Kv1.1 proteins. There is a high probability both proteins are being expressed at 48 hpf, as the RT-PCR results showed both genes were being expressed at this stage of development. It would be interesting to determine their functional significance; especially since only G62942 was found to be expressed in the adult brain.

The purpose of expressing zebrafish Kv1.1 in oocytes was to examine its properties in isolation from the other currents and to confirm that it conducted a delayed rectifier current. However, I was unable to express the channel in the oocytes. It is known that the majority of Kv1.1 protein is retained in the ER with little being expressed at the surface (Manganas & Trimmer 2000). Therefore low surface expression of the channel may be responsible for observing only small currents (Chouinard et al 1995). However several experiments, in which human, mouse and rat Kv1.1 was expressed in oocytes, have shown the presence of a delayed rectifier current (Hopkins et al 1994; Ruppersberg et al 1990). Furthermore, zebrafish channels have also been successfully expressed in *Xenopus* oocytes, therefore it is unlikely to be a problem of the zebrafish protein being incompatible with the oocyte expression system (Nakamura & Coetzee 2008).

If the problem of the oocyte experiments is resolved then recording the currents will allow for the zebrafish Kv1.1 currents to be properly characterized. Expressing the second protein, P11986 in oocytes, and comparing its current and

pharmacological sensitivity with that of P85980 would establish the function of each of these proteins in the 48 hpf zebrafish.

4.2 Heteromeric arrangements of the voltage gated potassium channel subfamily 1 in the Mauthner and MiD2cm cells

To better understand the characteristics of the sustained current in the Mauthner and MiD2cm cells, steady state activation of the currents were calculated and compared. The conductance parameters of the sustained currents were considerably different from values obtained for mammalian homomeric channels expressed in HEK-293 cells (Sokolov et al 2007) suggesting the presence of heteromeric potassium channels in the Mauthner and MiD2cm cells. Furthermore, the V_{50} and V_S of the sustained currents obtained from the two cells were significantly different suggesting a difference in the types of subunits comprising the VGKCs in the Mauthner and MiD2cm cells. Similar observations have been made by expressing concatamers of channels containing two different types of Kv1 subunits (Akhtar 2002; Sokolov et al 2007). A Kv1.1-1.2 concatamer expressed in HEK293 cells had a $V_{50} = -0.7 \pm 1.6$ mV, a value similar to that of the sustained current in the Mauthner cell (Sokolov et al 2007). From our studies it is clear that Kv1.1 is present in the Mauthner cell, while work on adult goldfish established the expression of Kv1.2 in the Mauthner cell but not in its morphological homologues (Nakayama & Oda 2004). As the cells of the goldfish and zebrafish are phylogenetically homologous with similar firing patterns, it is possible that they may express the same types of Kv channels (Eaton & Farley 1975; Lee et al 1993; Zottoli 1977). Therefore, Kv1.1-1.2 heteromers

may be conducting the sustained potassium current in the Mauthner cell of 48 hpf zebrafish.

The MiD2cm cell of 48 hpf zebrafish, appears to express the Kv1.1 subunit (present work) but not Kv1.2 (Nakayama & Oda 2004). Therefore, the sustained currents in the MiD2cm cell may be conducted by Kv1.1 homomers or a heteromer comprised of Kv1.1 and other Kv1 subunits. Homomeric Kv1.1 channels expressed in oocytes or other cell lines have a $V_{50} \sim -30$ mV (Akhtar 2002; Stuhmer et al 1989). In the MiD2cm cell the half activation was much more depolarized with a value of -8.19 ± 1.02 mV. This suggests that the current is not being conducted by homomeric channels but rather a heteromeric arrangement that contains Kv1.1 (Akhtar 2002; Sokolov et al 2007). One possibility is a Kv1.1-1.6 heteromer, as Kv1.6 is highly expressed in vertebrate (Scott et al 1994; Sokolov et al 2007). In making these comparisons and conclusions one must consider the previous data is derived from studies done on mammalian channels and may not be an accurate representation of the zebrafish Kv1 channel subfamily. Furthermore the activation parameters of the zebrafish currents are derived from total Kv currents and thus are likely a summation of more than one Kv channel, see appendix I for more details.

The altered sensitivity of Kv1 alpha subunits to TEA also supports the possibility of channels with different heteromeric arrangements in the Mauthner and MiD2cm cells (Sokolov et al 2007). All subunits of a Kv1 channel contribute to the binding of TEA, however the sensitivity of the alpha subunits to TEA is 1.1 > 1.6 > 1.2 (Kavanaugh et al 1992; Sokolov et al 2007). Since the Kv1.2 subunit

is relatively insensitive to TEA, the hypothetical 1.1-1.2 heteromer in the Mauthner cell would be inhibited to a lesser extent than the hypothetical 1.1-1.6 heteromer of the MiD2cm cell as both of these subunits are more sensitive to TEA (Hopkins 1998; Sokolov et al 2007). The TEA inhibition of a smaller proportion of the sustained current in the Mauthner cell compared to the MiD2cm cell is consistent with the hypothesis that two different heteromeric channels are being expressed (Al-Sabi et al 2010; Sokolov et al 2007).

The conclusions from the pharmacology experiments are loosely drawn inferences that must be taken with caution as proper dose responses for 4-AP and TEA were not determined. In addition, the Kv currents were contaminated with voltage gated calcium and calcium activated potassium currents which left residual currents that could not be properly accounted for.

4.3 Firing behavior of the Mauthner and MiD2cm cells

Depolarizing both the Mauthner and MiD2cm cells to just above threshold elicited the firing of a single action potential. Larger suprathreshold stimuli induced the Mauthner cell to fire a few action potentials at the onset of the current injection before becoming inactive for the remainder of the stimulus. In young larval zebrafish (2-4 dpf) it has been suggested that the cell firing a burst of action potentials is due to the immature inhibitory synapses at this stage of development, because in older larvae (7-14 dpf), which contain fully functioning inhibitory networks, the Mauthner cells were observed to fire a single action potential (Chong & Drapeau 2007; Koyama et al 2011; O'Malley et al 1996; Takahashi et

al 2002). In addition, a short bursting of action potentials at the beginning of the current pulse also occurred in the Mauthner cell of adult goldfish when inhibitory inputs were blocked with strychnine and bicuculline (Nakayama & Oda 2004). Therefore in 48 hpf zebrafish larvae, the ability of the Mauthner cell to fire multiple action potentials in response to a large input of positive current is likely due to an immature inhibitory network (Chong & Drapeau 2007).

In the MiD2cm cell, action potentials fired at regular intervals for the duration of the stimulus. A tonic repetitive firing pattern was also observed in the morphological homologues of adult goldfish with the frequency of action potentials increasing proportionally with the current stimulus (Nakayama & Oda 2004). The frequency and firing pattern of action potentials in the soma of a neuron provides information about the stimulus it has received (Bean 2007). Thus the firing pattern of the MiD2cm may be correlated with the direction of the stimulus and strength of the sensory input, ultimately affecting its contribution to the stage 1 bend of the escape response (Canfield 2006; Eaton & Emberley 1991; Foreman & Eaton 1993; O'Malley et al 1996).

The direction that the zebrafish perceives a stimulus dictates the degree of activation of the Mauthner series which determines the trajectory angle of the escape response (Eaton & Emberley 1991; Foreman & Eaton 1993). Rostral stimuli maximally activate the Mauthner series leading to a large turn of the fish while caudal stimuli only activate the Mauthner cell resulting in a smaller turn (Canfield 2006; Eaton et al 2001; Foreman & Eaton 1993). Since the Mauthner cell always responds in the same manner when stimulated, it has been proposed

that the homologues provide the extra input necessary to increase the escape trajectory angle (Casagrand et al 1999; Foreman & Eaton 1993; O'Malley et al 1996).

If stimuli to the front of the head provide the greatest sensory input to the homologues, it would cause them to fire at a maximum frequency. This would result in the activation of a large amount of trunk musculature producing a large body bend and escape trajectory angle. As the stimulus moved towards the side of the fish, the homologues would be stimulated to a lesser degree. Therefore they would fire at a lower frequency, activate less musculature and the escape trajectory angle would be smaller. Finally as caudal stimuli do not activate the homologues they would not fire at all and thus would not contribute to the escape response (Foreman & Eaton 1993; Liu & Fetcho 1999; O'Malley et al 1996).

The difference in the firing behavior of the Mauthner and MiD2cm cells is important and necessary for initiating a proper escape response for survival purposes (Foreman & Eaton 1993; Nakayama & Oda 2004; O'Malley et al 1996) and appears to be established early on in development (Saint-Amant & Drapeau 1998). Although the inhibitory circuits onto the Mauthner cell may still be immature at 48 hpf, the suites of potassium channels expressed likely underlie and may compensate to attain the Mauthner cell's distinct firing behavior (Chong & Drapeau 2007; Nakayama & Oda 2004). My data coincides with this hypothesis as the firing behavior of the two cells is different, as are the Kv currents.

4.4 Sustained voltage gated potassium currents regulate the firing activity of the Mauthner and MiD2cm cells

My findings suggest the sustained potassium currents in the Mauthner and MiD2cm cells are being conducted in part by channels that contain the Kv1.1 subunit. However, that the sustained current density in the MiD2cm cell is of greater amplitude and the current is more sensitive to TEA suggests different populations of channels are present. I suspect these differences account for the sustained currents of the Mauthner and MiD2cm cells affecting their firing behaviors in different manners.

In the Mauthner cell of 48 hpf larval zebrafish the Kv1 channels likely contain the Kv1.1 subunit and are suspected to regulate the firing of the Mauthner cell. This regulation was clearly demonstrated in the Mauthner cell of adult goldfish with the application of DTX-I, a blocker of Kv1.1, 1.2 and 1.6 subunits, which caused the Mauthner cell to fire multiple action potentials (Nakayama & Oda 2004). Similar observations have also been made in several other preparations. For example, the application of DTX-I to neurons of the MNTB caused them to fire a train of action potentials (Brew & Forsythe 1995). It was later revealed that Kv1.1 containing channels limit them to firing a single action potential by returning the membrane potential to below threshold (Dodson et al 2002). The Kv1.1 subunit plays a similar role in rat DRG neurons as application of DTX_K resulted in the firing of multiple action potentials (Chi & Nicol 2007). The general consensus for how mammalian Kv1.1 channels facilitate the firing of a single action potential has been attributed to their threshold of activation being near the threshold potential of the cell as well as their slower deactivation kinetics

(Glazebrook et al 2002; Goldberg et al 2008; Guan et al 2007). It is postulated that activating near the threshold potential permits the channels to limit the depolarization phase and accelerate the repolarization phase (Glazebrook et al 2002). A reduction in the depolarization phase is also believed to be due to the strong conductance that these channels can have (Brew et al 2003). Finally the slower deactivation kinetics of Kv1 channels are also suspected of contributing to a prolonged repolarization phase preventing the cell from reaching threshold again after the first action potential, thus limiting their ability to fire multiple action potentials (Glazebrook et al 2002; Guan et al 2007).

To understand the role of Kv1.1 containing channels in the Mauthner cell of 48 hpf larvae the intention was to apply DTX_K and record action potentials. As this has yet to be completed, I hypothesize that the application of DTX_K will cause the Mauthner cell to fire action potentials through the duration of the current stimulus, as seen in the adult goldfish (Nakayama & Oda 2004). As previously mentioned, there is a possibility that the Kv1 channels are heteromers comprised of Kv1.1 and 1.2 subunits if not others. However, only a single Kv1.1 subunit is necessary for the DTX_K to bind and effectively block the channel (Harvey 1997; Tytgat et al 1995). Therefore all Kv1.1 containing channels should be blocked, allowing for its role to be determined.

The MiD2cm cell fires action potentials of similar amplitudes at a high frequency, which suggests that the sustained potassium current is functionally different than in the Mauthner cell, which does not fire at a high frequency.

Additionally, the tonic firing suggests that there is at least a second population of Kv channels present that enable the repetitive firing.

Beyond regulating cell excitability, Kv1 currents control several other properties associated with action potentials. Kv1 currents increase the current and voltage threshold for the generation of action potentials in GABAergic interneurons of the neocortex (Goldberg et al 2008). Within the axon initial segment of pyramidal cells, Kv1 currents shorten the duration of action potentials and increase the amplitude of the afterhyperpolarization, which increases the fidelity of action potential propagation during periods of high frequency firing (Kole et al 2007). The reduced duration and larger afterhyperpolarization were two features that distinguished the action potentials elicited by the MiD2cm cell from those of the Mauthner cell. I suspect these distinguished features of the MiD2cm cell are attributed to a population of heteromeric Kv1 channels that differ from those present in the Mauthner cell. Inhibition of the Kv1.1 containing channels with the application of DTX_K would demonstrate the role of these channels in the MiD2cm cell.

Regarding the greater sustained current density in the MiD2cm cell, one possible explanation is the presence of a large conductance potassium channel (Brew & Forsythe 1995; Hernandez-Pineda et al 1999). The likely candidate is Kv3 channels as they are sensitive to TEA and allow for the firing of a train of action potentials (Baranauskas et al 2003; Brew & Forsythe 1995; Ding et al 2010; Ishikawa et al 2003). Kv3 channels activate at more depolarized potentials (Vm > -40 mV) and conduct delayed rectifier currents with fast activation and

deactivation kinetics (Hernandez-Pineda et al 1999; Martina et al 1998; Rudy & McBain 2001). This current contributes to shortening the duration of the action potential, accelerating the repolarization phase of an action potential and producing a large fast afterhyperpolarization (Baranauskas et al 2003; Ding et al 2010; Martina et al 1998). The rapid repolarization and fast afterhyperpolarization facilitates the removal of sodium channels from inactivation and the deactivation of Kv3 channels to mediate the high frequency firing of the neuron (Ding et al 2010; Rudy & McBain 2001). The channel properties of zebrafish Kv3.3 expressed in Xenopus oocytes are similar to its mammalian counterpart which suggests it would play a role in permitting neurons to fire at high frequencies (Mock et al 2010). The MiD2cm cell fires action potentials, which have a shorter duration and larger afterhyperpolarization, at a higher frequency compared to the Mauthner cell. I propose that this behavior is due to Kv1 and Kv3 channels acting in a cooperative manner to enable the MiD2cm cell to fire action potentials at a high frequency with sustained amplitude (Ding et al 2010; Ishikawa et al 2003; Martina et al 1998).

4.5 Transient A-type current in the Mauthner and MiD2cm cells

Transient A-type currents are conducted by channels that contain Kv1.4, Kv3.3, Kv3.4 or Kv4 subunits (Baldwin et al 1991; Coetzee et al 1999; Schroter et al 1991; Stuhmer et al 1989). Kv3 channels form high voltage activated channels with a $V_{50} \sim 15$ mV (Baranauskas et al 2003; Hernandez-Pineda et al 1999) and are sensitive to TEA with an $IC_{50} = 0.3$ mM (Rettig et al 1992; Schroter

et al 1991). In my experiments, 5 mM TEA did not block the transient A-type current in the Mauthner cell and the activation threshold of the peak current was -40 mV. This eliminated the possibility that a zebrafish Kv3.3 or Kv3.4 homologue is contributing to the A-type current in the Mauthner cell.

The application of 5 mM 4-AP inhibited the transient current, but Kv1.4 and Kv4 subunits are all sensitive to 4-AP and insensitive to TEA (Coetzee et al 1999). They are classified as low voltage activated channels as they have activation thresholds more negative than -50 mV (Baldwin et al 1991; Coetzee et al 1999; Nakamura & Coetzee 2008; Serodio et al 1994). A distinguishing feature between the two channels is that the decay kinetics of Kv1.4 channels is best fit with a single exponential while the decay kinetics of the Kv4 currents have been fit with either a double or triple exponential (Hashimoto et al 2000; Pak et al 1991a; Po et al 1993; Serodio et al 1996). I found that the inactivating component of the transient current in the Mauthner cell was best fit with a double exponential function. These characteristics of the current all point towards the A-type current being conducted by the presence of a Kv4 subunit (Song et al 1998) rather than a Kv1.4 subunit. Furthermore, evidence negating the presence of a Kv1.4 subunit, discussed below, further supports the presence of a Kv4 subunit.

The zebrafish Kv1.1 subunit is present in the Mauthner cell and it has been shown that when Kv1.1 and 1.4 are expressed in the same cell, a proportion of channels are Kv1.1-1.4 heteromers (Isacoff et al 1990; Ruppersberg et al 1990). The Kv1.1-1.4 heteromeric arrangement when expressed in oocytes produces a transient A-type current that has an inactivation time constant (τ) of 228 ms. This

is much slower than that of the Kv1.4 homomeric channels expressed in oocytes where τ = 109 ms, which is still much slower than the value obtained in the Mauthner cell (τ_{fast} = 30 ms) (Imbrici et al 2011; Ruppersberg et al 1990). Also to note, Kv1.4 homomers are insensitive to TEA, while the application of TEA to Kv1.4-1.1 heteromers reduced the amplitude of the transient component by 50% (Ruppersberg et al 1990). In the Mauthner cell, TEA did not produce this same effect on the transient component. Finally, preliminary immunohistochemical experiments using antibodies against Kv1.4 and Kv3.4 showed no positive staining in zebrafish larvae (data not shown). Although technical issues may have contributed to a lack of staining, I tentatively conclude that Kv1.4 channels may not be associated with zebrafish Mauthner cells and instead it is Kv4 channels that conduct the transient A-type current in the Mauthner cell.

Kv4 channels are generally found in the soma and dendrites of neurons where they regulate local membrane depolarizations and modulate back propagating action potentials (Birnbaum et al 2004; Hoffman et al 1997). In hippocampal pyramidal cells the transient current present in the soma and dendrites reduces the amplitude of action potentials and limits their back propagation (Hoffman et al 1997). Therefore in the Mauthner cell, the transient current may be contributing to ensuring the Mauthner cell only fires a single action potential when stimulated (Zottoli 1977). By modulating the back propagation of action potentials, the transient current may be functioning with the inhibitory networks to prevent the firing of a burst of action potentials at the onset

of the stimulus (Hoffman et al 1997; Magee & Carruth 1999; Nakayama & Oda 2004).

In the MiD2cm, the application of 5 mM TEA blocked 85% of the current and appeared to reveal an A-type current. This remaining current inactivated and was best fit with a double exponential function. The conductance was calculated using the GHK normalization which produced an activation curve that could be fit with a Boltzmann function. This curve resembled the activation curve of the peak current in the Mauthner cell but was slightly shifted in the hyperpolarized direction. Because the application of TEA was performed in normal ECS, the calcium currents likely interfered with the A-type potassium current as was shown to occur with the sustained current of the MiD2cm cell (Figure 3.12). Therefore the current density of the A-type current is probably greater than what was recorded. Application of TEA in the K^+ isolating solution would eliminate the calcium current, allowing for the transient current to be properly characterized and compared with the A-type current in the Mauthner cell.

4.6 Use of the Goldman Hodgkin Katz normalization to calculate channel conductance

The ideal means of determining the conductance of voltage gated potassium channels is from tail currents as they are all measured from a single membrane potential and driving force. Unfortunately, measuring tail currents produced by I_A channels can be unreliable due to their small amplitude (Clay 2009). Traditionally, in steady state activation analysis, the current voltage (I-V) relation was thought to be linearly proportional to the driving force ($V-E_K$) in

physiological saline and ion conductance was calculated by dividing the peak current by the driving force (Clay 1998; Hodgkin & Huxley 1952b). In the last few decades, research has shown that Hodgkin and Huxley's models may not be an accurate representation of channel properties (Clay 1998). Instead, it has been argued that the I-V relation is a nonlinear function of the driving force which is best described by the Goldman Hodgkin Katz (GHK) equation (Clay 1984; 1991). Determining steady state activation using the GHK normalization produces a curve with a steeper voltage dependence that reaches saturation at depolarized potentials (Clay 1998; 2000). Several studies have used this new methodology to analyze the activation of A-type potassium channels (Johnston et al 2008; Nakamura & Takahashi 2007; Persson et al 2005). Due to the inability to measure reliable tail currents from the Mauthner cell I normalized the current using two normalization methods, GHK and DF, to determine the conductance of the peak and sustained currents (Clay 2000) (see Appendix I). For consistency the same methods were used to calculate the conductance of the potassium currents in the MiD2cm cell. Yet, because the MiD2cm cell predominantly contained a delayed rectifier current, I was able to successfully record tail currents from which I derived a conductance voltage plot. Thus for the MiD2cm cell, the steady state activation attained using the three different methods were compared and analyzed (see Appendix I).

The final confounding challenge that I have encountered throughout my electrophysiology experiments is the inability to maintain the patch for an extended period of time in potassium isolating solution, to apply Kv channel

blockers. Groups that have used the GHK normalization to determine ion conductance, either expressed individual subunits in an expression system (Persson et al 2005) or were able to separate individual currents (fast-inactivating from slow-inactivating) using pharmacology (Johnston et al 2008; Nakamura & Takahashi 2007). In the Mauthner cell, the total Kv current consists of both fast inactivating and delayed rectifier currents which likely contribute to both the peak and sustained currents. Thus the calculated conductance of the peak and sustained currents using the GHK normalization is probably a hybrid of the steady states of activation of the different Kv channels. Therefore isolation of the transient and sustained currents using a voltage protocol or pharmacology is necessary to properly characterize the steady state activation of the individual channels (Johnston et al 2008). As for the MiD2cm cell, if my hypothesis that Kv1 and Kv3 channels are conducting the current is true, then separation of these currents through pharmacology would also be required to calculate the conductance of the individual channels.

4.7 Voltage gated calcium and calcium activated potassium channels

To block the individual components of the potassium currents while recording from the Mauthner and MiD2cm cells using a K^+ isolating solution was quite challenging as I could not maintain the patch long enough to apply the different pharmacological agents. Therefore, I used normal ECS, which contained calcium, and added 4-AP and TEA to isolate and identify the different components of the potassium currents. However, with the Mauthner and MiD2cm

cells containing voltage gated calcium channels (VGCCs) (O'Malley et al 1996), the calcium affected my ability to isolate the potassium currents and was suspected of interfering with the current recordings. The application of 4-AP to the Mauthner cell inhibited the peak current and revealed an inward current that was likely due to the influx of calcium.

Therefore, to determine if the suspected calcium currents in the Mauthner and MiD2cm cells were interfering with the potassium currents recorded using normal ECS, I compared the peak and sustained current densities in the presence and absence of calcium (Figure 3.12). As expected, in the absence of calcium, the potassium current density was significantly increased in the MiD2cm cell, indicative of the inward calcium current interfering with the ability to record the total outward potassium current.

In the Mauthner cell the opposite effect was observed. The presence of cadmium resulted in a significant decrease in the potassium current density. This suggested that accompanying the activation of the voltage gated calcium channels was a calcium activated potassium channel (K_{Ca}) that also contributed to the outward potassium current during recordings in which calcium was present (Ishikawa et al 2003). By blocking the VGCCs with cadmium, calcium was unable to enter the cell and contribute to the activation of the K_{Ca} channel (Ishikawa et al 2003). Therefore in the Mauthner cell, the decrease in potassium current density was believed to be attributed to the K_{Ca} channel being unable to conduct outward potassium current. Application of K_{Ca} channel blockers such as apamin (small conductance K_{Ca} blocker) or IbTX (large conductance K_{Ca} blocker)

should block the channel and reduce the current density (Ishikawa et al 2003; Jin et al 2000), thereby confirming the presence of a calcium activated potassium current in the Mauthner cell.

4.8 Role of the voltage gated potassium channel 1.1 in Trigeminal, Rohon Beard, and Dorsal Root Ganglion neurons

My findings indicated that Kv1.1 channels are expressed in the soma of three different populations of sensory neurons. One population of cells staining for zebrafish Kv1.1 was located behind the eyes, believed to be trigeminal ganglia based on its location (Metcalfe et al 1990). A second population of neurons was located in the dorsal part of the spinal cord that stretched the length of the tail. Based on their dorsolateral positioning and size of the soma I believe these to be the Rohon Beard sensory neurons (Bernhardt et al 1990; Metcalfe et al 1990). Similar staining was shown in stage 40 *Xenopus* embryos against XSha1, the Xenopus gene encoding Kv1.1 (Ribera & Nguyen 1993). Finally positive staining for zebrafish Kv1.1 was located in cell bodies along the midline of the trunk of 72 hpf larvae, which I believe to be neurons of the dorsal root ganglia (An et al 2002; Reyes et al 2004). These three populations of neurons perceive somatosensory stimuli and then transmit the signal to the Mauthner cell (Clarke et al 1984; Kohashi & Oda 2008; Lewis & Eisen 2003; Metcalfe et al 1990; Svoboda et al 2001). Because the Mauthner cell is a high threshold neuron, stimulation by the Trigeminal, Rohan Beard or DRG neurons evoke EPSPs but do not bring the cell to threshold (Chang et al 1987; Kohashi & Oda 2008; Svoboda et al 2001). Therefore, it has been proposed that these weaker excitatory inputs act in

conjunction with signals from the auditory nerve, the primary stimulus that brings the Mauthner cell to threshold, to modulate the response of the Mauthner cell and ensure it reaches threshold (Chang et al 1987; Kohashi & Oda 2008). I hypothesize that, to ensure the Mauthner cell only elicits an escape response to threatening stimuli and is not hyper-stimulated, the activity of these sensory neurons is regulated through voltage gated potassium channels raising their firing threshold and limiting the number of action potentials they fire.

As Kv1.1 channels are known to regulate the excitability of neurons (Barnes-Davies et al 2004; Chi & Nicol 2007; England et al 1995; Glazebrook et al 2002; Kopp-Scheinpflug et al 2003; Smart et al 1998), they may be performing this very role in the Trigeminal, Rohan Beard and DRG neurons of zebrafish. Kv1.1 containing channels limit rat DRGs to firing a single action potential (Chi & Nicol 2007). In addition sustained potassium currents have been recorded from the Rohan Beard neurons of larval zebrafish and embryonic *Xenopus* and shown to regulate their firing properties (Nakano et al 2010; O'Dowd et al 1988; Winlove & Roberts 2011). Based on these studies, I suspect that the Kv1.1 channels are responsible for regulating the activity of the Rohon Beard, Trigeminal and Dorsal root neurons as well. This would enable the proper transmission of sensory information to the Mauthner cell which would contribute to its activation so it could elicit an escape response in the presence of an aversive stimulus.

4.9 Future directions

The focus of my thesis was to determine how Kv1.1 channels regulated the firing properties of the Mauthner and MiD2cm cells. Through my investigation I was able to conclude that Kv1.1 is being expressed in both the Mauthner and MiD2cm cells, yet the total Kv currents are very different. The Kv current in the Mauthner cell is composed of a transient current and a delayed rectifier current, while the current in the MiD2cm cell is predominantly a delayed rectifier current with an underlying transient current.

For the Mauthner cell I have hypothesized that the delayed rectifier current is conducted by heteromeric Kv1 channels, which includes Kv1.1, and that its role is to ensure the Mauthner cell fires a single action potential. I have proposed the transient current is conducted by Kv4 channels, which regulates the membrane potential of the dendrites and soma further contributing to the reduced excitability. In the MiD2cm cell I have postulated Kv1 and Kv3 channels are present, producing currents that enable the high frequency firing of action potentials. These hypotheses are all areas to direct future studies to better characterize the Kv currents and how they contribute to regulating to the differential firing behaviors of the Mauthner and MiD2cm cells.

The characterization of the zebrafish Kv1.1 current has yet to be elucidated, but there are still options available to do so. One option includes reattempting to apply DTX_K while recording in K^+ isolating solution. If the presence of cadmium does not permit functional recordings, then calcium may have to be reintroduced to the system along with the addition of calcium channel

blockers. If DTX_K can successfully block some of the current, then through current subtraction the Kv1.1 current may be isolated. Further attempts can also be made in trying to express the zebrafish channel in an expression system. It may mean cloning out the open reading frame of P11986 and trying to express it in the oocytes. If not an additional expression system, such as HEK-293 or CHO cells, may be required. Finally, using morpholinos to knock down the zebrafish Kv1.1 genes and then recording Kv currents from the two different cells may provide insight into the role of these channels and their current. Upon characterizing the current, the next objective would be in understanding the role of Kv1.1 in regulating the firing behavior. This would involve recording action potentials in the presence of DTX_K or after knocking out the Kv1.1 gene(s) with morpholinos. If morpholinos were used, behavioral studies could be performed by partially embedding the larvae in agarose (Sylvain et al 2010) to observe changes in the escape response and correlate them to the altered firing activity.

A characterization of the other Kv subunits that may be present and how they affect the behavior of the Mauthner and MiD2cm cells would develop a greater understanding of the role of the different Kv channels in regulating neuronal activity and how this contributes to their functioning as a neuronal network. The suite of Kv subunits in the two different cells could be identified through single cell RT-PCR and/or in situ hybridization (Song et al 1998). Based on the subunits identified, currents could be isolated by voltage protocols (Johnston et al 2008), to separate the transient current from the sustained current in the Mauthner cell, or using specific pharmacological agents to determine if the

sustained current of the MiD2cm cell is conducted by Kv1 and/or Kv3 channels (Nakamura & Takahashi 2007). Ideally the same experiments should be performed in the MiD3cm cell because although it is a homologue with similar features of the MiD2cm cell, some studies have shown there to be discrepancies between the activity of the MiD2cm and MiD3cm cells (Kohashi & Oda 2008; Nakayama & Oda 2004). Upon completing the full characterization of all the Kv channels expressed in the Mauthner series, the data could be incorporated into a computer program, for example "Neuron", to run simulations to model how they contribute to regulating the escape response of the zebrafish.

A profile of the Kv currents and expression of the Kv subunits developmentally may provide insight into any functional changes the neurons may be undergoing and whether this correlates to changes in the escape response. In the muscle fibers of zebrafish, Kv currents were observed to increase in current density and alter their activation kinetics from 1 dpf to 6 dpf (Coutts et al 2006). Unfortunately, recording currents from the Mauthner cell at 72 hpf and beyond becomes difficult, however recordings could be performed at earlier stages of development, ie 33, 36 and 42 hpf, to determine if the properties of the Kv currents change. Furthermore, expression studies of the different subunits could be performed over longer periods of development (1 dpf to 7 dpf) using RT-PCR to observe if and when gene expression is being turned on and off.

The work of this thesis has provided insight that the behavior of the Mauthner series of neurons appears to be regulated by more than one type of potassium channel. Only after identifying each of the subunits and characterizing

them on an individual basis can the sum of the parts be joined together to understand how they function as a whole to regulate the activity of the Mauthner series.

5. Literature Cited

Accili EA, Kiehn J, Yang Q, Wang Z, Brown AM, Wible BA. 1997. Separable Kvβ subunit domains alter expression and gating of potassium channels. *The Journal of Biological Chemistry* 272:25824-31

Aggarwal SK, MacKinnon R. 1996. Contribution of the S4 segment to gating charge in the *Shaker* K^+ channel. *Neuron* 16:1169-77

Akhtar S. 2002. Characteristics of Brain Kv1 Channels Tailored to Mimic Native Counterparts by Tandem Linkage of alpha Subunits. IMPLICATIONS FOR K+ CHANNELOPATHIES. *Journal of Biological Chemistry* 277:16376-82

Al-Sabi A, Shamotienko O, Dhochartaigh SN, Muniyappa N, Le Berre M, et al. 2010. Arrangement of Kv1 subunits dictates sensitivity to tetraethylammonium. *The Journal of General Physiology* 136:273-82

Amores A, Force AG, Yan Y-L, Joly L, Amemiya C, et al. 1998. Zebrafish *hox* clusters and vertebrate genome evolution *Science* 282:1711-4

An M, Luo R, Henion PD. 2002. Differentiation and maturation of zebrafish dorsal root and sympathetic ganglion neurons. *The Journal of Comparative Neurology* 446:267-75

Armstrong CM, Bezanilla F. 1973. Currents related to movement of the gating particles of the sodium channels. *Nature* 242:459-61

Armstrong CM, Bezanilla F. 1977. Inactivation of the sodium channel II. Gating current experiments. *Journal of General Physiology* 70:567-90

Bahring R, Covarrubias M. 2010. Mechanisms of closed-state inactivation in voltage-gated ion channels. *The Journal of Physiology* 589:461-79

Baldwin TJ, Tsaur M-L, Lopez GA, Jan YN, Jan LY. 1991. Characterization of a mammalian cDNA for an inactivating voltage-sensitive K^+ channel. *Neuron* 7:471-83

Baranauskas G, Tkatch T, Nagata K, Yeh JZ, Surmeier DJ. 2003. Kv3.4 subunits enhance the repolarizing efficiency of Kv3.1 channels in fast-spiking neurons. *Nature Neuroscience* 6:258-66

Barnes-Davies M, Barker MC, Osmani F, Forsythe ID. 2004. Kv1 currents mediate a gradient of principal neuron excitability across the tonotopic axis in the rat lateral superior olive. *European Journal of Neuroscience* 19:325-33

Bean BP. 2007. The action potential in mammalian central neurons. *Nature Reviews Neuroscience* 8:451-65

Benishin CG, Sorensen RG, Brown WE, Krueger BK, Blaustein MP. 1988. Four polypeptide components of green mamba venom selectively block certain potassium channels in rat brain synaptosomes. *Molecular Pharmacology* 34:152-9

Berndt KD, Guntert P, Wuthrich K. 1993. Nuclear magnetic resonance solution structure of dendrotoxin K from the venom of dendroaspis polylepis polylepis. *Journal of Molecular Biology* 234:735-50

Berneche S, Roux B. 2001. Energetics of ion conduction through the K^+ channel. *Nature* 414:73-7

Berneche S, Roux B. 2003. A microscopic view of ion conduction through the K+ channel. *Proceedings of the National Academy of Sciences* 100:8644-8

Bernhardt RR, Chitnis AB, Lindamer L, Kuwada JY. 1990. Identification of spinal neurons in the embryonic and larval zebrafish. *The Journal of Comparative Neurology* 302:603-16

Bezanilla F. 2000. The voltage sensor in voltage dependent ion channels. *Physiological Reviews* 80:555-92

Bezanilla F, Perozo E, Papazian DM, Stefani E. 1991. Molecular basis of gating charge immobilization in Shaker potassium channels. *Science* 254:679-83

Birnbaum SG, Varga AW, Yuan L-L, Anderson AE, Sweatt JD, Schrader LA. 2004. Structure and function of Kv4-family transient potassium channels. *Physiological Reviews* 84:803-33

Brew HM, Forsythe ID. 1995. Two voltage-dependent K^+ conductances with complementary functions in postsynaptic integration at a central auditory synapse. *The Journal of Neuroscience* 15:8011-22

Brew HM, Hallows JL, Tempel BL. 2003. Hyperexcitability and reduced low threshold potassium currents in auditory neurons of mice lacking the channel subunit Kv1.1. *The Journal of Physiology* 548:1-20

Brunt ER, van Weerden TW. 1990. Familial paroxysmal kinesigenic ataxia and continuous myokymia. *Brain* 113:1361-82

Budick SA, O'Malley DM. 2000. Locomotor repertoire of the larval zebrafish: swimming turning and prey capture. *The Journal of Experimental Biology* 203:2565-79

Burgess HA, Granato M. 2007. Sensorimotor gating in larval zebrafish. *Journal of Neuroscience* 27:4984-94

Butler A, Wei A, Baker K, Salkoff L. 1989. A family of putative potassium channel genes in Drosophila. *Science* 243:943-7

Canfield JG. 2006. Functional evidence for visuospatial coding in the Mauthner neuron. *Brain, Behavior and Evolution* 67:188-202

Casagrand JL, Guzik AL, Eaton RC. 1999. Mauthner and reticulospinal responses to the onset of acoustic pressure and acceleration stimuli. *Journal of Neurophysiology* 82:1422-37

Celio MR, Gray EG, Yasargil GM. 1979. Ultrastructure of the mauthner axon collateral and its synapses in the goldfish spinal cord *Journal of Neurocytology* 8:19-29

Chang Y, Lin J, Faber D. 1987. Spinal inputs to ventral dendrite of Mauthner cell. *Brain Research* 417:205-13

Charpier S, Behrends JC, Chang Y-T, Sur C, Korn H. 1994. Synchronous bursting in a subset of interneurons inhibitory to the goldfish Mauthner cell: synaptic mediation and plasticity *Journal of Neurophysiology* 72:531-41

Chi XX, Nicol GD. 2007. Manipulation of the Potassium Channel Kv1.1 and Its Effect on Neuronal Excitability in Rat Sensory Neurons. *Journal of Neurophysiology* 98:2683-92

Choi KL, Aldrich RW, Yellen G. 1991. Tetraethylammonium blockade distinguishes two inactivation mechanisms in voltage activated K^+ channels. *Proceedings of the National Academy of Sciences* 88:5092-5

Chong M, Drapeau P. 2007. Interaction between hindbrain and spinal networks during the development of locomotion in zebrafish. *Developmental Neurobiology* 67:933-47

Chouinard SW, Wilson GF, Schlimgen K, Ganetzky B. 1995. A potassium channel β subunit related to the aldo-keto reductase superfamily is encoded by the *Drosophila* hyperkinetic locus. *Proceedings of the National Academy of Sciences* 92:6763-7

Clarke JDW, Hayes BP, Hunt SP, Roberts A. 1984. Sensory physiology, anatomy and immunohistochemistry of Rohon-Beard neurones in embryos of *Xenopus laevis*. *Journal of Physiology* 348:511-25

Clay JR. 1984. Potassium channel kinetics in squid axons with elevated levels of external potassium concentration. *Biophysical Journal* 45:481-5

Clay JR. 1991. A paradox concerning ion permeation of the delayed rectifier potassium ion channel in squid giant axons. *Journal of Physiology* 444:499-511

Clay JR. 1998. Excitability of the squid giant axon revisited. *Journal of Neurophysiology* 80:903-13

Clay JR. 2000. Determining K^+ channel activation curves from K^+ channel currents. *European Biophysics Journal* 29:555-7

Clay JR. 2009. Determining K+ channel activation curves from K+ channel currents often requires the Goldman–Hodgkin–Katz equation. *Frontiers in Cellular Neuroscience* 3:1-6

Coetzee WA, Amarillo Y, Chiu J, Chow A, Lau D, et al. 1999. Molecular diversity of K^+ channels. *Annals of the New York Academy of Sciences* 868:233-85

Coleman SK, Newcombe J, Pryke J, Dolly JO. 1999. Subunit composition of Kv1 channels in human CNS. *Journal of Neurochemistry* 73:849-58

Coutts CA, Balt LN, Ali DW. 2009. Protein kinase A modulates A-type potassium currents of larval zebrafish (Danio rerio) white muscle fibres. *Acta Physiologica* 195:259-72

Coutts CA, Patten SA, Balt LN, Ali DW. 2006. Development of ionic currents of zebrafish slow and fast skeletal muscle fibers. *Journal of Neurobiology* 66:220-35

D'Adamo MC, Imbrici P, Sponcichetti F, Pessia M. 1999. Mutations in the KCNA1 gene associated with episodic ataxia type-1 syndrome impair heteromeric voltage-gated K^+ channel function. *Federation of American Societies for Experimental Biology* 13:1335-45

Ding S, Matta SG, Zhou FM. 2010. Kv3-Like Potassium Channels Are Required for Sustained High-Frequency Firing in Basal Ganglia Output Neurons. *Journal of Neurophysiology* 105:554-70

Dodson PD, Barker MC, Forsythe ID. 2002. Two heteromeric Kv1 potassium channels differentially regulate action potential firing. *The Journal of Neuroscience* 22:6953-61

Dolly JO, Parcej DN. 1996. Molecular properties of voltage gated K^+ channels. *Journal of Bioenergetics and Biomembranes* 28:231-53

Doyle DA, Cabral JM, Pfuetzner RA, Kuo A, Gulbis JM, et al. 1998. The structure of the potassium channel: molecular basis of K^+ conduction and selectivity *Science* 280:69-77

Dudev T, Lim C. 2009. Determinants of K+vs Na+Selectivity in Potassium Channels. *Journal of the American Chemical Society* 131:8092-101

Eaton R, Lavender W, Wieland C. 1982. Alternative neural pathways initiate fast start responses following lesions of the Mauthner neuron in goldfish. *Journal of Comparative Physiology* 145:485-96

Eaton RC, Bombardieri RA, Meyer DL. 1977. The mauthner initiated startle response in teleost fish. *The Journal of Experimental Biology* 66:65-81

Eaton RC, DiDomenico R, Nissanov J. 1988. Flexible body dynamics of the goldfish C start: Implications for reticulospinal command mechanisms. *The Journal of Neuroscience* 8:2758-68

Eaton RC, Emberley DS. 1991. How stimulus direction determines the trajectory of the Mauthner-initiated escape response in a teleost fish. *The Journal of Experimental Biology* 161:469-87

Eaton RC, Farley RD. 1975. Mauthner neuron field potential in newly hatched larvae of the zebra fish. *Journal of Neurophysiology* 38:502-12

Eaton RC, Kimmel CB. 1980. Directional sensitivity of the mauthner cell system to vibrational stimulation in zebrafish larvae. *Journal of Comparative Physiology* 140:337-42

Eaton RC, Lavender WA, Wieland CM. 1981. Identification of Mauthner-initiated response patterns in goldfish: Evidence from simultaneous cinematography and electrophysiology. *Journal of Comparative Physiology* 144:521-31

Eaton RC, Lee RKK, Foreman MB. 2001. Mauthner cell and other identified neurons of the brainstem escape network of fish.pdf>. *Progress in Neurobiology* 63:467-85

Eisen JS. 1991. Developmental neurobiology of the zebrafish. *The Journal of Neuroscience* 11:311-7

England SK, Uebeles VN, Kodali J, Bennett PB, Tamkun MM. 1995. A novel K^+ channel β-subunit (hKvβ1.3) is produced via alternative mRNA splicing. *The Journal of Biological Chemistry* 270:28531-4

Faber D, Korn H. 1975. Inputs from posterior lateral line upon goldfish Mauthner cell. II. Evidence that inhibitory components are mediated by interneurons of recurrent collateral network. *Brain Research* 96:349-56

Faber DS, Fetcho JR, Korn H. 1989. Neuronal networks underlying the escape response in goldfish. General implications for motor control. *Annals of the New York Academy of Sciences* 563:11-33

Faber DS, Korn H. 1973. A neuronal inhibition mediated electrically *Science* 179:577-8

Fetcho JR. 1992. Excitation of motoneurons by the mauthner axon in goldfish complexities in a simple reticulospinal pathway *Journal of Neurophysiology* 67:1574-86

Fetcho JR, O'Malley DM. 1995. Visualization of active neural circuitry in the spinal cord of intact zebrafish. *Journal of Neurophysiology* 73:399-406

Foray M-F, Lancelin J-M, Hollecker M, Marion D. 1993. Sequence specific ^{1}H-NMR assignment and secondary structure of black mamba dendrotoxin I, a highly selective blocker of voltage gated potassium channels. *European Journal of Biochemistry* 211:813-20

Foreman MB, Eaton RC. 1993. The direction change concept for reticulospinal control of goldfish escape *The Journal of Neuroscience* 13:4101-13

Furukawa T, Furshpan EJ. 1963. Two inhibitory mechanisms in the Mauthner neuron of goldfish. *Journal of Neurophysiology* 26:140-76

Furukawa T, Ishii Y. 1967. Neurophysiological studies on hearing in goldfish *Journal of Neurophysiology* 30:1377-403

Gahtan E, O'Malley DM. 2003. Visually guided injection of identified reticulospinal neurons in zebrafish: A survey of spinal arborization patterns. *The Journal of Comparative Neurology* 459:186-200

Gahtan E, Sankrithi N, Campos JB, O'Malley DM. 2002. Evidence for a widespread brain stem escape network in larval zebrafish. *Journal of Neurophysiology* 87:608-14

Glazebrook PA, Ramirez AN, Schild JH, Shieh CC, Doan T, et al. 2002. Potassium channels Kv1.1, Kv1.2 and Kv1.6 influence excitability of rat visceral sensory neurons. *The Journal of Physiology* 541:467-82

Glover WE. 1982. The aminopyridines. *General Pharmacology* 13:259-85

Goldberg EM, Clark BD, Zagha E, Nahmani M, Erisir A, Rudy B. 2008. K+ Channels at the Axon Initial Segment Dampen Near-Threshold Excitability of Neocortical Fast-Spiking GABAergic Interneurons. *Neuron* 58:387-400

Greene NDE, Copp AJ. 2009. Development of the vertebrate central nervous system: formation of the neural tube [Review]. *Prenatal Diagnosis* 29:303-11

Grissmer S, Nguyen AN, Aiyar J, Hanson DC, Mather RJ, et al. 1994. Pharmacological characterization of five cloned voltage gated K^+ channels, types Kv1.1, 1.2, 1.3, 1.5 and 3.1, stably expressed in mammalian cell lines. *Molecular Pharmacology* 45:1227-34

Guan D, Lee JCF, Higgs MH, Spain WJ, Foehring RC. 2007. Functional Roles of Kv1 Channels in Neocortical Pyramidal Neurons. *Journal of Neurophysiology* 97:1931-40

Gulbis JM, Zhou M, Mann S, MacKinnon R. 2000. Structure of the Cytoplasmic beta Subunit--T1 Assembly of Voltage-Dependent K+ Channels. *Science* 289:123-7

Gutman GA. 2005. International Union of Pharmacology. LIII. Nomenclature and Molecular Relationships of Voltage-Gated Potassium Channels. *Pharmacological Reviews* 57:473-508

Haddon C, Lewis J. 1996. Early ear development in the embryo of the zebrafish *Danio rerio*. *Journal of Comparative Physiology* 365:113-28

Hall A, Stow J, Sorensen RG, Dolly JO, Owen DG. 1994. Blockade by dendrotoxin homologues of voltage dependent K^+ currents in cultured sensory neurones from neonatal rats. *British Journal of Pharmacology* 113:959-67

Hallows JL, Tempel BL. 1998. Expression of Kv1.1, a Shaker-like potassium channel, is temporally regulated in embryonic neurons and glia. *The Journal of Neuroscience* 18:5682-91

Hanlon MR, Wallace BA. 2002. Structure and function of voltage dependent ion channel regulatory beta subunits. *Biochemistry* 41:2886-94

Hannemann E, Trevarrow B, Metcalfe WK, Kimmel CB, Westerfield M. 1988. Segmental pattern of development of the hindbrain and spinal cord of the zebrafish embryo. *Development* 103:49-58

Hartmann HA, Kirsch GE, Drewe JA, Taglialatela M, Joho RH, Brown AM. 1991. Exchange of conduction pathways between two related K^+ channels. *Science* 251:942-4

Harvey AL. 1997. Recent studies on dendrotoxins and potassium ion channels. *General Pharmacology* 28:7-12

Harvey AL. 2001. Twenty years of dendrotoxins. *Toxicon* 39:15-26

Harvey AL, Karlsson E. 1980. Dendrotoxin from the venom of the green mamba, *Dendroaspis angusticeps.* A neurotoxin that enhances acetylcholine

release at neuromuscular junction. *Naunyn-Schmiedeberg's Archives of Pharmacology* 312:1-6

Hashimoto Y, Nunoki K, Kudo H, Ishii K, Tairal N, Yanagisawa T. 2000. Changes in the inactivation of rat Kv1.4 K channels induced by varying the number of inactivation particles. *The Journal of Biological Chemistry* 275:5

Hatta K. 1992. Role of the floor plate in axonal patterning in the zebrafish CNS. *Neuron* 9:629-42

Heginbotham L, Abramson T, MacKinnon R. 1992. A functional connection between the pores of distantly related ion channels as revealed by mutant K^+ channels. *Science* 258:1152-5

Heginbotham L, Lu Z, Abramson T, MacKinnon R. 1994. Mutations in the K^+ channel signature sequence. *Biophysical Journal* 66:1061-7

Heinemann SH, Rettig J, Graack H-R, Pongs O. 1996. Functional characterization of Kv channel beta-subunits from rat brain. *Journal of Physiology* 493:625-33

Heinemann SH, Rettig J, Wunder F, Pongs O. 1995. Molecular and functional characterization of a rat brain Kv beta 3 potassium channel subunit. *FEBS Letters* 377:383-9

Hernandez-Pineda R, Chow A, Amarillo Y, Moreno H, Saganich M, et al. 1999. Kv3.1-Kv3.2 channels underlie a high-voltage-activating component of the delayed rectifier K^+ current in projecting neurons from the globus pallidus
Journal of Neurophysiology 82:1512-28

Hidalgo P, MacKinnon R. 1995. Revealing the architecture of a K^+ channel pore through mutant cycles with a peptide inhibitor. *Science* 268:307-10

Higashijima S, Hotta Y, Okamoto H. 2000. Visualization of cranial motor neurons in live transgenic zebrafish expressing green fluorescent protein under the control of the *Islet-1* promoter/enhancer. *The Journal of Neuroscience* 20:206-18

Hodgkin AL, Huxley AF. 1952a. Currents carried by sodium and potassium ions through the membrane of the giant axon of *Loligo*. *Journal of Physiology* 116:449-72

Hodgkin AL, Huxley AF. 1952b. A quantitative description of membrane current and its application to conduction and excitation in nerve. *Journal of Physiology* 117:500-44

Hoffman DA, Magee JC, Colbert CM, Johnston D. 1997. K^+ channel regulation of signal propagation in dendrites of hippocampal pyramidal neurons. *Nature* 387:869-75

Hollecker M, Marshall DL, Harvey AL. 1993. Structural features important for the biological activity of the potassium channel blocking dendrotoxins. *British Journal of Pharmacology* 110:790-4

Holmgren M, Jurman ME, Yellen G. 1996. N-type inactivation and the S4-S5 region of the Shaker K^+ channel. *Journal of General Physiology* 108:195-206

Hopkins WF. 1998. Toxin and subunit specificity of blocking affinity of three peptide toxins for heteromultimeric, voltage gated potassium channels expressed in *Xenopus* oocytes. *The Journal of Pharmacology and Experimental Therapeutics* 285:1051-60

Hopkins WF, Demas V, Tempel BL. 1994. Both N- and C-terminal regions contribute to the assembly and functional expression of homo- and heteromultimeric voltage gated K^+ channels. *The Journal of Neuroscience* 14:1385-93

Hoshi T, Zagotta WN, Aldrich RW. 1990. Biophysical and molecular mechanisms of Shaker potassium channel inactivation. *Science* 250:533-8

Hoshi T, Zagotta WN, Aldrich RW. 1991. Two types of inactivation in Shaker K^+ channels: effects of alterations in the carboxy-terminal region. *Neuron* 7:547-56

Hoshi T, Zagotta WN, Aldrich RW. 1994. *Shaker* potassium channel gating I: transitions near the open state. *Journal of General Physiology* 103:249-78

Hudspeth AJ. 1989. How the ear's works work. *Nature* 341:397-404

Hurst RS, Busch AE, Kavanaugh MP, Osborne PB, North RA, Adelman JP. 1991. Identification of amino acid residues involved in dendrotoxin block of rat voltage dependent potassium channels. *MOlecular Pharmacology* 40:572-6

Imbrici P, D'Adamo MC, Grottesi A, Biscarini A, Pessia M. 2011. Episodic ataxia type 1 mutations affect fast inactivation of K^+ channels by a reduction in either subunit surface expression or affinity for inactivation domain. *American Journal of Physiology Cell Physiology* 300:C1314-C22

Isacoff E, Jan YN, Jan LY. 1990. Evidence for the formation of heteromultimeric potassium channels in *Xenopus* oocytes. *Nature* 345:530-4

Ishikawa T, Nakamura Y, Saitoh N, Li W-B, Iwasaki S, Takahashi T. 2003. Distinct roles of Kv1 and Kv3 potassium channels at the Calyx of Held presynaptic terminal. *The Journal of Neuroscience* 23:10445-53

Iverson LE, Tanouye MA, Lester HA, Davidson N, Rudy B. 1988. A-type potassium channels expressed from Shaker locus cDNA. *Proceedings of the National Academy of Sciences* 85:5723-7

Jackman W, Langeland JA, Kimmel CB. 2000. *islet* Reveals Segmentation in the Amphioxus Hindbrain Homolog. *Developmental Biology* 220:16-26

Jan LY, Jan YN. 1992. Structural elements involved in specific K^+ channel functions. *Annual Review of Physiology* 54:537-55

Jerng HH, Covarrubias M. 1997. K^+ channel inactivation mediated by the concerted action of the cytoplasmic N- and C- terminal domains. *Biophysical Journal* 72:163-74

Jerng HH, Shahidullah M, Covarrubias M. 1999. Inactivation gating of Kv4 potassium channels *Molecular interactions involving the inner vestibule of the pore*. *Journal of General Physiology* 113:641-59

Jiang Y, Ruta V, Chen J, Lee A, MacKinnon R. 2003. The principle of gating charge movement in a voltage dependent K^+ channel. *Nature* 423:42-8

Jin W, Sugaya A, Tsuda T, Ohguchi H, Sugaya E. 2000. Relationship between large conductance calcium activated potassium channel and bursting activity. *Brain Research* 860:21-8

Johnston J, Forsythe ID, Kopp-Scheinpflug C. 2010. Going native: voltage-gated potassium channels controlling neuronal excitability. *The Journal of Physiology* 588:3187-200

Johnston J, Griffin SJ, Baker C, Skrzypiec A, Chernova T, Forsythe ID. 2008. Initial segment Kv2.2 channels mediate a slow delayed rectifier and maintain high frequency action potential firing in medial nucleus of the trapezoid body neurons. *The Journal of Physiology* 586:3493-509

Jow F, Zhang Z-H, Kopsco DC, Carroll KC, Wang K. 2004. Functional coupling of intracellular calcium and inactivation of voltage-gated Kv1.1/Kv 1.1 A-type K+ channels. *Proceedings of the National Academy of Sciences* 101:15535-40

Kamb A, Iverson LF, Tanouye MA. 1987. Molecular characterization of *Shaker*, a Drosophila gene that encodes a potassium channel. *Cell* 50:405-13

Kamb A, Tseng-Crank J, Tanouye MA. 1988. Multiple products of the Drosophila Shaker gene may contribute to potassium channel diversity. *Neuron* 1:421-30

Kavanaugh MP, Hurst RS, Yakel J, Varnum MD, Adelman JP, North RA. 1992. Multiple subunits of a voltage dependent potassium channel contribute to the binding site for tetraethylammonium. *Neuron* 8:493-7

Kimmel CB. 1993. Patterning the brain of the zebrafish embryo *Annual Review of Neuroscience* 16:707-32

Kimmel CB, Ballard WW, Kimmel SR, Ullman B, Schilling TF. 1995. Stages of embryonic development of the zebrafish. *Developmental Dynamics* 203:253-310

Kimmel CB, Eaton RC, Powell SL. 1980. Decreased fast start performance of zebrafish larvae lacking Mauthner neurons. *Journal of Comparative Physiology* 140:343-50

Kimmel CB, Hatta K, Metcalfe WK. 1990. Early axonal contacts during development of an identified dendrite in the brain of the zebrafish. *Neuron* 4:535-45

Kimmel CB, Powell SL, Metcalfe WK. 1982. Brain neurons which project to the spinal cord in young larvae of the zebrafish. *Journal of Comparative Neurology* 205:112-27

Kimmel CB, Sepich DS, Trevarrow B. 1988. Development of segmentation in zebrafish. *Development* 104:S197-S207

Kimmel CB, Session SK, Kimmel RJ. 1981. Morphogenesis and synaptogenesis of the zebrafish mauthner neuruon *Journal of Comparative Neurology* 198:101-20

Koch M. 1999. The neurobiology of startle. *Progress in Neurobiology* 59:107-28

Koch RO, Wanner SG, Koschak A, Hanner M, Schwarzer C, et al. 1997. Complex subunit assembly of neuronal voltage gated K^+ channels. *Journal of Biological Chemistry* 272:27577-81

Kohashi T, Oda Y. 2008. Initiation of Mauthner- or non-Mauthner-mediated fast escape evoked by different modes of sensory input. *Journal of Neuroscience* 28:10641-53

Kole MHP, Letzkus JJ, Stuart GJ. 2007. Axon Initial Segment Kv1 Channels Control Axonal Action Potential Waveform and Synaptic Efficacy. *Neuron* 55:633-47

Kopp-Scheinpflug C, Fuchs K, Lippe WR, Tempel BL, Rubsamen R. 2003. Decreased temporal precision of auditory signaling in *Kcna1*-null mice: an electrophysiological study *In vivo*. *The Journal of Neuroscience* 23:9199-207

Korn H, Faber D. 1975. Inputs from posterior lateral line nerves upon the goldfish Mauthner cell. I. Properties and synaptic localization of excitatory components. . *Brain Research* 96:342-8

Korn H, Faber DS. 2005. The Mauthner Cell Half a Century Later: A Neurobiological Model for Decision-Making? *Neuron* 47:13-28

Koyama M, Kinkhabwala A, Satou C, Higashijima S, Fetcho JR. 2011. Mapping a sensory motor network onto a structural and functional ground plan in the hindbrain. *Proceedings of the National Academy of Sciences* 108:1170-5

Kreusch A, Pfaffinger PJ, Stevens CF, Choe S. 1998. Crystal structure of the tetramerization domain of the *Shaker* potassium channel. *Nature* 392:945-8

Kuwada JY, Bernhardt RR, Nguyen N. 1990. Development of spinal neurons and tracts in the zebrafish embryo. *Journal of Comparative Neurology* 302:617-28

Lancelin J-M, Foray M-F, Poncin M, Hollecker M, Marion D. 1994. Proteinase inhibitor homologues as potassium channel blockers. *Nature Structural Biology* 1:246-50

Lee RKK, Eaton RC. 1991. Identifiable reticulospinal neurons of the adult zebrafish, *Brachydanio rerio Journal of Comparative Neurology* 304:34-52

Lee RKK, Eaton RC, Zottoli SJ. 1993. Segmental arrangement of reticulospinal neurons in the goldfish hindbrain. *Journal of Comparative Neurology* 329:539-56

Lewis KE, Eisen JS. 2003. From cells to circuits: development of the zebrafish spinal cord. *Progress in Neurobiology* 69:419-49

Li D, Takimoto K, Levitan ES. 2000. Surface expression of Kv1 channels is governed by a C-terminal motif. *The Journal of Biological Chemistry* 275:6

Li M, Isacoff E, Jan YN, Jan LY. 1993. Assembly of potassium channels. *Annals of the New York Academy of Sciences* 707:51-9

Li M, Jan YN, Jan LY. 1992. Specification of subunit assembly by the hydrophilic amino-terminal domain of the Shaker potassium channel. *Science* 257:1225-30

Liman ER, Hess P, Weaver F, Koren G. 1991. Voltage sensing residues in the S4 region of a mammalian K^+ channel. *Nature* 353:752-6

Lin J-W, Faber DS. 1988. Synaptic transmission mediated by single club endings on the goldfish mauthner cell. I. Characterisitcs of electronic and chemical postsynaptic potentials. *The Journal of Neuroscience* 8:1302-12

Lingenhohl K, Eckhard F. 1994. Giant neurons in the rat reticular formation: a sensorimotor interface in the elementary acoustic startle circuit? *The Journal of Neuroscience* 14:1176-94

Lipkind GM, Hanck DA, Fozzard HA. 1995. A structural motif for the voltage gated potassium channel pore. *Proceedings of the National Academy of Sciences* 92:9215-9

Liu H-L, Chen C-W, Lin J-C. 2005. Homology models of the tetramerization domain of six eukaryotic voltage gated potassium channels Kv1.1-Kv1.6. *Journal of Biomolecular Structure and Dynamics* 22:387-98

Liu KS, Fetcho JR. 1999. Laser ablations reveal functional relationships of segmental hindbrain neurons in zebrafish. *Neuron* 23:325-35

Liu Y, Jurman ME, Yellen G. 1996. Dynamic rearrangement of the outer mouth of a K^+ channel during gating. *Neuron* 16:859-67

Logothetis DE, Kammen BF, Lindpainter K, Bisbas D, Nadal-Ginard B. 1993. Gating charge differences between two voltage gated K^+ channels are due to the specific charge content of their respective S4 regions. *Neuron* 10:1121-9

Lopez GA, Jan YN, Jan LY. 1994. Evidence that the S6 segment of the *Shaker* voltage gated K^+ channel comprises part of the pore. *Nature* 367:179-82

MacKinnon R, Aldrich RW, Lee AW. 1993. Functional stoichiometry of Shaker potassium channel inactivation *Science* 262:757-9

MacKinnon R, Cohen SL, Kuo A, Lee A, Chait BT. 1998. Structural conservation in prokaryotic and eukaryotic potassium channels. *Science* 280:106-9

MacKinnon R, Yellen G. 1990. Mutations affecting TEA blockade and ion permeation in voltage activated K^+ channels. *Science* 250:276-9

Magee JC, Carruth M. 1999. Dendritic voltage-gated ion channels regulate the action potential firing mode of hippocampal CA1 pyramidal neurons. *Journal of Neurophysiology* 82:1895-901

Majumder K, De Biasi M, Wang Z, Wible BA. 1995. Molecular cloning and functional expression of a novel potassium channel β-subunit from human atrium. *FEBS Letters* 361:13-6

Malin SA, Nerbonne JM. 2002. Delayed rectifier K^+ currents, I_K, are encoded by Kv2 α-subunits and regulate tonic firing in mammalian sympathetic neurons. *The Journal of Neuroscience* 22:10094-105

Manganas LN, Trimmer JS. 2000. Subunit Composition Determines Kv1 Potassium Channel Surface Expression. *Journal of Biological Chemistry* 275:29685-93

Manganas LN, Wang Q, Scannevin RH, Antonucci DE, Rhodes KJ, Trimmer JS. 2001. Identification of a trafficking determinant localized to the Kv1 potassium channel pore. *Proceedings of the National Academy of Sciences* 98:14055-9

Martina M, Schultz JH, Ehmke H, Monyer H, Jonas P. 1998. Functional and molecular differences between voltage-gated K^+ channels of fast-spiking interneurons and pyramidal neurons of rat hippocampus. *The Journal of Neuroscience* 18:8111-25

Mathie A, Wooltorton JRA, Watkins CS. 1998. Voltage activated potassium channels in mammalian neurons and their block by novel pharmacological agents. *General Pharmacology* 30:13-24

McCormack K, McCormack T, Tanouye MA, Rudy B, Stuhmer W. 1995. Alternative splicing of the human *Shaker* K^+ channel β1 gene and functional expression of the β2 gene product. *FEBS Letters* 370:32-6

McKeown L, Swanton L, Robinson P, Jones OT. 2008. Surface expression and distribution of voltage-gated potassium channels in neurons (Review). *Molecular Membrane Biology* 25:332-43

Mendelson B. 1986. Development of reticulospinal neurons of the zebrafish. I. Time of origin. *Journal of Comparative Neurology* 251:160-71

Metcalfe WK, Kimmel CB, Schabtach E. 1985. Anatomy of the posterior lateral line system in young larvae of the zebrafish. *Journal of Comparative Neurology* 233:377-89

Metcalfe WK, Mendelson B, Kimmel CB. 1986. Segmental homologies among reticulospinal neurons in the hindbrain of the zebrafish larva. *Journal of Comparative Neurology* 251:147-59

Metcalfe WK, Myers PZ, Trevarrow B, Bass MB, Kimmel CB. 1990. Primary neurons that express the L2/HNK-1 carbohydrate during early development in the zebrafish. *Development* 110:491-504

Misonou H, Trimmer JS. 2004. Determinants of voltage gated potassium channel surface expression and localization in mammalian neurons. *Critical Reviews in Biochemistry and Molecular Biology* 39:125-47

Mock AF, Richardson JL, Hsieh J-Y, Rinetti G, Papazian DM. 2010. Functional effects of spinocerebellar ataxia type 13 mutations are conserved in zebrafish Kv3.3 channels. *BMC Neuroscience* 11:99-110

Moens CB, Cordes SP, Giorgianni MW, Barsh GS, Kimmel CB. 1998. Equivalence in the genetic control of hindbrain segmentation in fish and mouse. *Development* 125:381-91

Moens CB, Prince VE. 2002. Constructing the hindbrain: Insights from the zebrafish. *Developmental Dynamics* 224:1-17

Moens CB, Yan Y-L, Appel B, Force AG, Kimmel CB. 1996. *valentino*: a zebrafish gene required for normal hindbrain segmentation *Development* 122:3981-90

Moorman SJ. 2001. Development of sensory systems in zebrafish (*Danio rerio*). *ILAR Journal* 42:292-8

Morais-Cabral JH, Zhou Y, R. M. 2001. Energetic optimization of ion conduction rate by the K^+ selectivity filter. *Nature* 414:37-42

Morales MJ, Castellino RC, Crews AL, Rasmusson RL, Strauss HC. 1995. A novel beta subunit increases rate of inactivation of specific voltage gated potassium channel alpha subunits. *Journal of Biological Chemistry* 270:6272-7

Muller UK, van Leeuwen JL. 2004. Swimming of larval zebrafish: ontogeny of body waves and implications for locomotory development. *Journal of Experimental Biology* 207:853-68

Nakahira K, Shi G, Rhodes KJ, Trimmer JS. 1996. Selective interaction of voltage gated K^+ channel beta-subunits with alpha-subunits. *Journal of Biological Chemistry* 271:7084-9

Nakajima Y. 1974. Fine structures of the synaptic endings on the Mauthner cell of the goldfish. *Journal of Comparative Neurology* 156:379-402

Nakamura TY, Coetzee WA. 2008. Functional and pharmacological characterization of a Shal-related K+ channel subunit in Zebrafish. *BMC Physiology* 8

Nakamura Y, Takahashi T. 2007. Developmental changes in potassium currents at the rat calyx of Held presynaptic terminal. *The Journal of Physiology* 581:1101-12

Nakano Y, Fujita M, Ogino K, Saint-Amant L, Kinoshita T, et al. 2010. Biogenesis of GPI-anchored proteins is essential for surface expression of sodium channels in zebrafish Rohon-Beard neurons to respond to mechanosensory stimulation. *Development* 137:1689-98

Nakayama H, Oda Y. 2004. Common Sensory Inputs and Differential Excitability of Segmentally Homologous Reticulospinal Neurons in the Hindbrain. *Journal of Neuroscience* 24:3199-209

Neumeister H, Szabo TM, Preuss T. 2008. Behavioral and Physiological Characterization of Sensorimotor Gating in the Goldfish Startle Response. *Journal of Neurophysiology* 99:1493-502

Noda M, Tanabe T, Takai T, Kayano T, Ikeda T, et al. 1984. Primary structure of *Electrophorus electricus* sodium channel deduced from cDNA sequence. *Nature* 312:121-7

O'Dowd DK, Ribera AB, Spitzer NC. 1988. Development of voltage-dependent calcium, sodium, and potassium currents in *Xenopus* spinal neurons. *The Journal of Neuroscience* 8:792-805

O'Malley DM, Kao Y-H, Fetcho JR. 1996. Imaging the functional organization of zebrafish hindbrain segments during escape behaviors. *Neuron* 17:1145-55

Ogielska EM, Zagotta WN, Hoshi T, Heinemann J, Haab J, Aldrich RW. 1995. Cooperative subunit interactions in C-type inactivation of K channels. *Biophysical Journal* 69:2449-57

Pak M, Baker K, Covarrubias M, Butler A, Ratcliffe A, Salkoff L. 1991a. mShal, a subfamily of A-type K^+ channel cloned from mammalian brain. *Proceedings of the National Academy of Sciences* 88:4386-90

Pak M, Covarrubias M, Ratcliffe A, Salkoff L. 1991b. A mouse brain homolog of the *Drosophila Shab* K^+ channel with conserved delayed rectifier properties. *The Journal of Neuroscience* 11:869-80

Papazian DM, Schwarz TL, Tempel BL, Jan YN, Jan LY. 1987. Cloning of genomic and complementary DNA from Shaker, a putative potassium channel gene from Drosophila. *Science* 237:749-53

Papazian DM, Timpe LC, Jan YN, Jan LY. 1991. Alteration of voltage dependence of Shaker potassium channel by mutations in the S4 sequence. *Nature* 349:305-10

Parcej DN, Scott VES, Dolly JO. 1992. Oligomeric properties of α-dendrotoxin sensitive potassium ion channels purified from bovine brain. *Biochemistry* 31:11084-8

Pereda AE, Bell TD, Faber DS. 1995. Retrograde synaptic communication via gap junctions coupling auditory afferents to the Mauthner cell. *The Journal of Neuroscience* 15:5943-55

Perozo E, Santacruz-Toloza L, Stefani E, Bezanilla F, Papazian DM. 1994. S4 mutations alter gating currents of Shaker K channels. *Biophysical Journal* 66:345-54

Persson F, Carlsson L, Duker G, Jacobson I. 2005. Blocking characteristics of hKv1.5 and hKv4.3/hKChIP2.2 after administration of the novel antiarrhythmic compound AZD7009. *Journal of Cardiovascular Pharmacology* 46:7-17

Po S, Snyders DJ, Tamkun MM, Bennett PB. 1993. Heteromultimeric assembly of human potassium channels. Molecular basis of transient outward current? *Circulation Research* 72:1326-36

Pongs O. 1992. Molecular biology of voltage dependent potassium channels. *Physiological Reviews* 72:S69-S88

Pongs O. 2008. Regulation of Excitability by potassium channels. *Results and Problems in Cell Differentiation* 44:145-61

Prince VE, Moens CB, Kimmel CB, Ho RK. 1998. Zebrafish *hox* genes: expression in the hindbrain region of wild type and mutants of the segmentation gene, *valentino*. *Development* 125:393-406

Raible DW, Kruse GJ. 2000. Organization of lateral line system in embryonic zebrafish *Journal of Comparative Neurology* 421:189-98

Rettig J, Heinemann SH, Wunder F, Lorra C, Parcej DN, et al. 1994. Inactivation properties of voltage gated K^+ channels altered by presence of β subunit. *Nature* 269:289-94

Rettig J, Wunder F, Stocker M, Lichtinghagen R, Mastiaux F, et al. 1992. Characertization of a Shaw-related potassium channel family in rat brain. *EMBO Journal* 11:2473-86

Reyes R, Haendel M, Grant D, Melancon E, Eisen JS. 2004. Slow degeneration of zebrafish Rohon-Beard neurons during programmed cell death. *Developmental Dynamics* 229:30-41

Rhodes KJ, Keilbaugh SA, Barrezueta NX, Lopez KL, Trimmer JS. 1995. Association and colocalization of K^+ channel α- and β-subunit polypeptides in rat brain. *The Journal of Neuroscience* 15:5360-71

Ribera AB, Nguyen DA. 1993. Primary sensory neurons express a *Shaker*-like potassium channel gene. *The Journal of Neuroscience* 13:4988-96

Robertson B, Owen DG, Stow J, Butler C, Newland C. 1996. Novel effects of dendrotoxin homologues on subtypes of mammalian Kv1 potassium channels expressed in *Xenopus* oocytes. *FEBS Letters* 383:26-30

Roux B, MacKinnon R. 1999. The cavity and pore helices in the KcsA K^+ channel: electostatic stabilization of monovalent cations. *Science* 285:100-2

Rudy B, McBain CJ. 2001. Kv3 channels: voltage-gated K^+ channels designed for high frequency repetitive firing. *Trends in Neuroscience* 24:517-26

Ruppersberg JP, Schroter KH, Sakmann B, Stocker M, Sewing S, Pongs O. 1990. Heteromultimeric channels formed by rat brain potassium channel proteins. *Nature* 345:535-7

Saint-Amant L, Drapeau P. 1998. Time course of the development of motor behaviors in the zebrafish embryo. *Journal of Neurobiology* 37:622-32

Sapede D, Pujades C. 2010. Hedgehog Signaling Governs the Development of Otic Sensory Epithelium and Its Associated Innervation in Zebrafish. *Journal of Neuroscience* 30:3612-23

Schoenwolf GC, Smith JL. 1990. Mechanisms of neurulation: traditional viewpoint and recent advances *Development* 109:243-70

Schroter KH, Ruppersberg JP, Wunder F, Rettig J, Stocker M, Pongs O. 1991. Cloning and functional expression of a TEA-sensitive A-type potassium channel from rat brain. *FEBS Letters* 278:211-6

Schwarz TL, Tempel BL, Papazian DM, Jan YN, Jan LY. 1988. Multiple potassium-channel components are produced by alternative splicing at the *Shaker* locus in Drosophila. *Nature* 331:137-42

Scott VES, Rettig J, Parcej DN, Keen JN, Findlay JBC, et al. 1994. Primary structure of a β subunit of α-dendrotoxin sensitive K^+ channels from bovine brain. *Proceedings of the National Academy of Sciences* 91:1637-41

Seoh S-A, Sigg D, Papazian DM, Bezanilla F. 1996. Voltage sensing residues in the S2 and S4 segments of the *Shaker* K^+ channel. *Neuron* 16:1159-67

Serodio P, Kentros C, Rudy B. 1994. Identification of molecular components of A-type channels activating at subthreshold potentials. *Journal of Neurophysiology* 72:1516-29

Serodio P, vega-Saenz De Miera E, Rudy B. 1996. Cloning of a novel component of A-type K^+ channels operating at subthreshold potentials with unique expression in heart and brain. *Journal of Neurophysiology* 75:2174-9

Sewing S, Roeper J, Pongs O. 1996. Kvβ1 subunit binding specific for *Shaker*-related potassium channel α subunits. *Neuron* 16:455-63

Shamotienko OG, Parcej DN, Dolly JO. 1997. Subunit Combinations Defined for K+Channel Kv1 Subtypes in Synaptic Membranes from Bovine Brain†. *Biochemistry* 36:8195-201

Shao XM, Papazian DM. 1993. S4 mutations alter the single channel gating kinetics of *Shaker* K channels. *Neuron* 11:343-52

Shen NV, Chen X, Boyer MM, Pfaffinger PJ. 1993. Deletion analysis of K^+ channel assembly. *Neuron* 11:67-76

Shi G, Nakahira K, Hammond S, Rhodes KJ, Schechter LE, Trimmer JS. 1996. β subunits promote K^+ channel surface expression through effects early in biosynthesis. *Neuron* 16:843-52

Slatter CAB, Kanji H, Coutts CA, Ali DW. 2005. Expression of PKC in the developing zebrafish, *Danio rerio*. *Journal of Neurobiology* 62:425-38

Slesinger PA, Jan YN, Jan LY. 1993. The S4-S5 loop contributes to the ion-selective pore of potassium channels. *Neuron* 11:739-49

Smart SL, Lopantsev V, Zhang CL, Robbins CA, Wang H, et al. 1998. Deletion of the Kv1.1 potassium channel causes epilepsy in mice. *Neuron* 20:809-19

Smith LA, Reid PF, Wang FC, Parcej DN, Schmidt JJ, et al. 1997. Site-Directed Mutagenesis of Dendrotoxin K Reveals Amino Acids Critical for Its Interaction with Neuronal K+Channels†. *Biochemistry* 36:7690-6

Sokolov MV, Shamotienko O, Dhochartaigh SN, Sack JT, Dolly JO. 2007. Concatemers of brain Kv1 channel α subunits that give similar K+ currents yield pharmacologically distinguishable heteromers. *Neuropharmacology* 53:272-82

Song W-J, Tkatch T, Baranauskas G, Ichinohe N, Kitai ST, Surmeier DJ. 1998. Somatodendritic depolarization-activated potassium currents in rat neostriatal cholinergic interneurons are predominantly of the A type and

attributable to coexpression of Kv4.2 and Kv4.1 subunits. *The Journal of Neuroscience* 18:3124-37

Spires S, Begenisich T. 1989. Pharmacological and kinetic analysis of K channel gating currents. *Journal of General Physiology* 93:263-83

Stanfield PR. 1983. Tetraethylammonium ions and the potassium permeability of excitable cells. *Reviews of Physiology, Biochemistry and Pharmacology* 97:1-67

Starkus JG, Kuschel L, Rayner MD, Heinemann SH. 1997. Ion conduction through C-type inactivated *Shaker* channels. *Journal of General Physiology* 110:539-50

Stephens GJ, Garratt JC, Robertson B, Owen DG. 1994. On the mechanism of 4-aminopyridine action on the cloned mouse brain potassium channel mKv1.1. *Journal of Physiology* 477:187-96

Stern CD. 1992. Vertebrate Gastrulation. *Current Opinion in Genetics and Development* 2:556-61

Storm JF. 1988. Temporal integration by a slowly inactivating K^+ current in hippocampal neurons. *Nature* 336:379-81

Stuhmer W, Ruppersberg JP, Schroter KH, Sakmann B, Stocker M, et al. 1989. Molecular basis of functional diversity of voltage gated potassium channels in mammalian brain. *EMBO Journal* 8:3235-44

Svoboda KR, Fetcho JR. 1996. Interactions between the neural networks for escape and swimming in goldfish. *The Journal of Neuroscience* 16:843-52

Svoboda KR, Linares AE, Ribera AB. 2001. Activity regulates programmed cell death of zebrafish Rohon-Beard neurons. *Development* 128:3511-20

Swanson R, Marshall J, Smith JS, Williams JB, Boyle MB, et al. 1990. Cloning and expression of cDNA and genomic clones encoding three delayed rectifier potassium channels in rat brain. *Neuron* 4:929-39

Sylvain NJ, Brewster DL, Ali DW. 2010. Zebrafish embryos exposed to alcohol undergo abnormal development of motor neurons and muscle fibers. *Neurotoxicology and Teratology* 32:472-80

Szabo TM. 2006. Representation of auditory signals in the M-cell: role of electrical synapses. *Journal of Neurophysiology* 95:2617-29

Szabo TM, McCormick CA, Faber DS. 2007. Otolith endorgan input to the Mauthner neuron in the goldfish. *The Journal of Comparative Neurology* 505:511-25

Taglialatela M, Champagne MS, Drewe JA, Brown AM. 1994. Comparison of H_5, S_6 and H_5-S_6 exchanges on pore properties of voltage dependent K^+ channels. *Journal of Biological Chemistry* 269:13867-73

Taglialatela M, Stefani E. 1993. Gating currents of the cloned delayed rectifier K^+ channel DRK1. *Proceedings of the National Academy of Sciences* 90:4758-62

Takahashi M, Narushima M, Oda Y. 2002. *In vivo* imaging of functional inhibitory networks on the Mauthner cell of larval zebrafish. *The Journal of Neuroscience* 22:3929-38

Tanimoto M, Ota Y, Horikawa K, Oda Y. 2009. Auditory input to CNS Is acquired coincidentally with development of inner ear after formation of functional afferent pathway in zebrafish. *Journal of Neuroscience* 29:2762-7

Tempel BL, Papazian DM, Schwarz TL, Jan YN, Jan LY. 1987. Sequence of a probable potassium channel component encoded at Shaker locus of Drosophila *Science* 237:770-5

Triller A, Korn H. 1981. Morphologically distinct classes of inhibitory synapses arise from the same neurons: Ultrastructural identification from crossed vestibular interneurons intracellularly stained with HRP *Journal of Comparative Neurology* 203:131-55

Tu L, Santarelli V, Sheng Z, Skach W, Pain D, Deutsch C. 1996. Voltage gated K^+ channels contain multiple intersubunit association sites. *Journal of Biological Chemistry* 271:18904-11

Tytgat J, Debont T, Carmeliet E, Daenens P. 1995. The α-dendrotoxin footprint on a mammalian potassium channel. *The Journal of Biological Chemistry* 270:24776-81

Utsunomiya I, Yoshihashi E, Tanabe S, Nakatani Y, Ikejima H, et al. 2008. Expression and localization of Kv1 potassium channels in rat dorsal and ventral spinal roots. *Experimental Neurology* 210:51-8

Wang FC, Parcej DN, Dolly JO. 1999. α subunit compositions of Kv1.1 containing K^+ channel subtypes fractionated from rat brain using dendrotoxins. *European Journal of Biochemistry* 263:230-7

Waskiewicz AJ, Rikhof HA, Moens CB. 2002. Eliminating zebrafish Pbx proteins reveals a hindbrain ground state *Developmental Cell* 3:723-33

Wei A, Covarrubias M, Butler A, Baker K, Pak M, Salkoff L. 1990. K^+ current density is produced by an extended gene family conserved in *Drosophila* and mouse. *Science* 248:599-603

Weihs D. 1973. The Mechanism of Rapid Starting of Slender Fish. *Biorheology* 10:343-50

Whitfield TT, Granato M, van Eeden FJM, Schach U, Brand M, et al. 1996. Mutations affecting development of the zebrafish inner ear and lateral line. *Development* 123:241-54

Whitfield TT, Riley BB, Chiang M-Y, Phillips B. 2002. Development of the zebrafish inner ear. *Developmental Dynamics* 223:427-58

Winlove CIP, Roberts A. 2011. Pharmacology of currents underlying the different firing patterns of spinal sensory neurons and interneurons identified in vivo using multivariate analysis. *Journal of Neurophysiology* 105:2487-500

Xu J, Yu W, Wright JM, Raab RW, Li M. 1998. Distinct functional stoichiometry of potassium channel β subunits. *Proceedings of the National Academy of Sciences* 95:1846-51

Yellen G. 1998. The moving parts of voltage gated ion channels. *Quarterly Reviews of Biophysics* 31:239-95

Yellen G. 2002. The voltage gated potassium channels and their relatives. *Nature* 419:35-40

Yellen G, Jurman ME, Abramson T, MacKinnon R. 1991. Mutations affecting internal TEA blockade identify the probable pore forming region of a K^+ channel *Science* 251:939-42

Yellen G, Sodickson D, Chen T-Y, Jurman ME. 1994. An engineered cysteine in the external mouth of a K^+ channel allows inactivation to be modulated by metal binding. *Biophysical Journal* 66:1068-75

Yokoyama S, Imoto K, Kawamura T, Higashida H, Iwabe N, et al. 1989. Potassium channels from NG108-15 neuroblastoma glioma hybrid cells. Primary structure and functional expression from cDNAs. *FEBS Letters* 259:37-42

Yool AJ, Schwarz TL. 1991. Alteration of ionic selectivity of a K^+ channel by mutation of the H5 region. *Nature* 349:700-4

Zagotta WN, Hoshi T, Aldrich RW. 1989. Gating of single Shaker potassium channels in *Drosophila* muscle and in *Xenopus* oocytes injected with Shaker mRNA. *Proceedings of the National Academy of Sciences* 86:7243-7

Zagotta WN, Hoshi T, Aldrich RW. 1990. Restoration of inactivation in mutants of Shaker potassium channels by a peptide derived from ShB. *Science* 250:568-71

Zagotta WN, Hoshi T, Dittman J, Aldrich RW. 1994. Shaker potassium channel gating II: transitions in the activation pathway. *Journal of General Physiology* 103:279-319

Zhou Y, Morais-Cabral JH, Kaufman A, MacKinnon R. 2001. Chemistry of ion coordination and hydration revealed by a K^+ channel-Fab complex at 2.0A resolution. *Nature* 414:43-8

Zhu J, Gomez B, Watanabe I, Thornhill WB. 2005. Amino acids in the pore region of Kv1 potassium channels dictate cell surface protein levels: a possible trafficking code in the Kv1 subfamily. *The Biochemistry Journal* 388:355-62

Zhu J, Watanabe I, Gomez B, Thornhill WB. 2001. Determinants Involved in Kv1 Potassium Channel Folding in the Endoplasmic Reticulum, Glycosylation in the Golgi, and Cell Surface Expression. *Journal of Biological Chemistry* 276:39419-27

Zhu J, Watanabe I, Gomez B, Thornhill WB. 2003. Heteromeric Kv1 potassium channel expression: amino acid determinants involved in processing and trafficking to the cell surface. *Journal of Biological Chemistry* 278:25558-67

Zottoli S, Hordes A, Faber D. 1987. Localization of optic tectal input to the ventral dendrite of the goldfish Mauthner cell. *Brain Research* 401:113-21

Zottoli SJ. 1977. Correlation of startle reflex and Mauthner cell auditory responses in unrestrained goldfish. *The Journal of Experimental Biology* 66:243-54

6. Appendix I

6.1 Comparing methods to determine the conductance of voltage gated potassium channels

Activation curves are used to understand the conductance of Kv channels in response to changes in the membrane potential. One method of determining the conductance is by measuring the amplitude of the tail current and graphing it against the membrane potential. This is an ideal method as the tail currents are measured with respect to a constant membrane potential and do not have to be normalized (Clay, 2000) (Figure 1A). When recording from the Mauthner cell the tail currents were very small in amplitude and did not reach a maximum value. The reversal potential was calculated to be -97.2 mV, therefore several different step down potentials (-120, -70, -50 and -35 mV) were tested to alter the driving force in an attempt to increase the amplitude of the tail current; however only minimal changes were observed. Small tail currents are a common occurrence when A-type channels are present as they inactivate quickly after the cell is brought to depolarized potentials (Clay, 2009). Therefore I calculated the conductance of the Kv currents for the Mauthner cell using the GHK normalization method (John Clay 2000, 2009).

For consistency, the conductance of the Kv current in the MiD2cm cell was also calculated using the GHK normalization method. However, to my knowledge, there are 3 different methods that have been used to determine the conductance of Kv channels, 1) measuring tail currents and plotting tail current amplitude against membrane potential, 2) calculating the conductance by

normalizing the current to the driving force [$G = I_K / (V-E_K)$] (driving force normalization) and 3) using the GHK normalization equation $g_K = I_K * 25/Vm * [((e^{(Vm/25)})-1) / ((e^{((Vm-E_K)/25)}-1)]$. As I was able to record Kv tail currents from the MiD2cm cell, the midpoint of activation (V_{50}) and the slope factor (V_S) (the steepness of the curve at the midpoint of activation) calculated from these three different methods were compared to test the feasibility of the GHK normalization (Figure 1C).

To record tail currents in the MiD2cm cell a voltage protocol was run in which the cell was originally held at -90 mV (Figure 1B). The cell was then stepped to a depolarized potential for 8 ms, which ranged from -60 to 65 mV at 5 mV intervals. To produce tail currents the membrane potential was then stepped to -35 mV for 8 ms. To calculate the conductance using the GHK and driving force normalization methods, the current amplitude was measured at the end of the current trace, at time 198 ms (as per materials and methods) and substituted in for I_K. The membrane potential (Vm) was the potential at which the cell was held to elicit the currents and the reversal potential (E_K) was calculated to be -97.2 mV.

Upon plotting the conductance voltage curves, a Boltzmann function was fitted to each to determine the steady state of activation parameters, V_{50} and V_S. The three different methods gave V_{50} values that were significantly different (Figure 1C, Table 1, One Way ANOVA, $P < 0.001$). The GHK normalization curve had a $V_{50} = -8.19 \pm 1.02$ mV ($n = 15$), which was significantly more negative than that derived from the tail currents ($V_{50} = -1.03 \pm 3.09$ mV, $n = 5$, Holm Sidak, $P = 0.003$) or the driving force normalization ($V_{50} = 0.01 \pm 1.0$ mV,

n = 15, Table 1, Holm Sidak, $P < 0.001$). Yet these latter two values were not significantly different from one another (Holm Sidak, $P = 0.65$). The slope factors of all three curves were significantly different from one another (Table 1, Kruskal-Wallis, $P < 0.001$). The GHK normalization curve had the steepest slope while the slope of the tail current curve was the most shallow (Figure 1C). This leftward shift in the activation curve calculated using the GHK normalization was the same as described by John Clay (2000).

To determine if similar trends were observed for the conductance of the Kv currents in the Mauthner cell, the two different normalization methods were used to produce activation curves (Figure 1D). For both the peak and sustained currents, the GHK normalization procedure gave V_{50} values that were significantly less positive (Table 1, t-test, $P < 0.001$, $n = 8$). As for the slope factor, the GHK normalization produced curves with steeper slopes for both currents (Table 1, t-test, $P < 0.001$, $n = 8$). Therefore just as in the MiD2cm cell, the GHK normalization produced the same leftward shift in the activation curves for the Mauthner currents.

Despite these comparisons, a decisive conclusion regarding the proper method to determine Kv channel conductance cannot be inferred from the presented experimental evidence. Regarding the MiD2cm cell, the tail current and driving force normalization methods produced overlapping activation curves, suggesting the latter may be an appropriate method to substitute if tail currents cannot be recorded. However, the observed shift in the activation curves produced by the GHK normalization is consistent with previous data that reassessed

individual Kv channel conductances including that in the squid giant axon (Clay, 2000, 2009).

One of the avenues that must be further investigated is to isolate individual currents conducted by channels of the different Kv subfamilies. The existing conductance voltage plots likely represent an average conductance of all the Kv channels present in the Mauthner and MiD2cm cells. Therefore, if individual Kv subunits could be successfully expressed in oocytes, the tail currents of the homomeric channels could be recorded and the conductance calculated. These could be compared with the conductances of the *in vivo* current recordings, determined using the GHK and driving force normalization methods, to assess the method that most accurately models the steady state of activation of the Kv channels.

Figure 6.1. Conductance voltage plots of voltage gated potassium channel currents in the Mauthner and MiD2cm cells at 48 hours post fertilization

(A) Current trace of tail currents evoked in the MiD2cm cell. (B) Protocol used to evoke tail currents in the MiD2cm cell. Starting from a holding potential of -90 mV the cell was depolarized through a series of 8 ms voltage steps ranging from -60 to 65 mV in 5 mV increments. The cell was then stepped to -35 mV for 8 ms to evoke an outward tail current. (C) Conductance voltage plots of MiD2cm potassium currents derived using tail currents (●) (n = 5), GHK normalization (○) (n = 15) or driving force (DF) normalization (●) (n = 15) were fit with a Boltzmann function. Differences were observed between the midpoints of activation (V_{50}) and slope factor (V_S) values of all three methods (Table 6.1). (D) Conductance voltage plots of Mauthner potassium currents derived using GHK normalization (white symbols) (n = 8) or driving force (DF) normalization (grey symbols) (n = 8) were fit with Boltzmann functions. The values of the V_{50} and V_S were significantly different (Table 6.1).

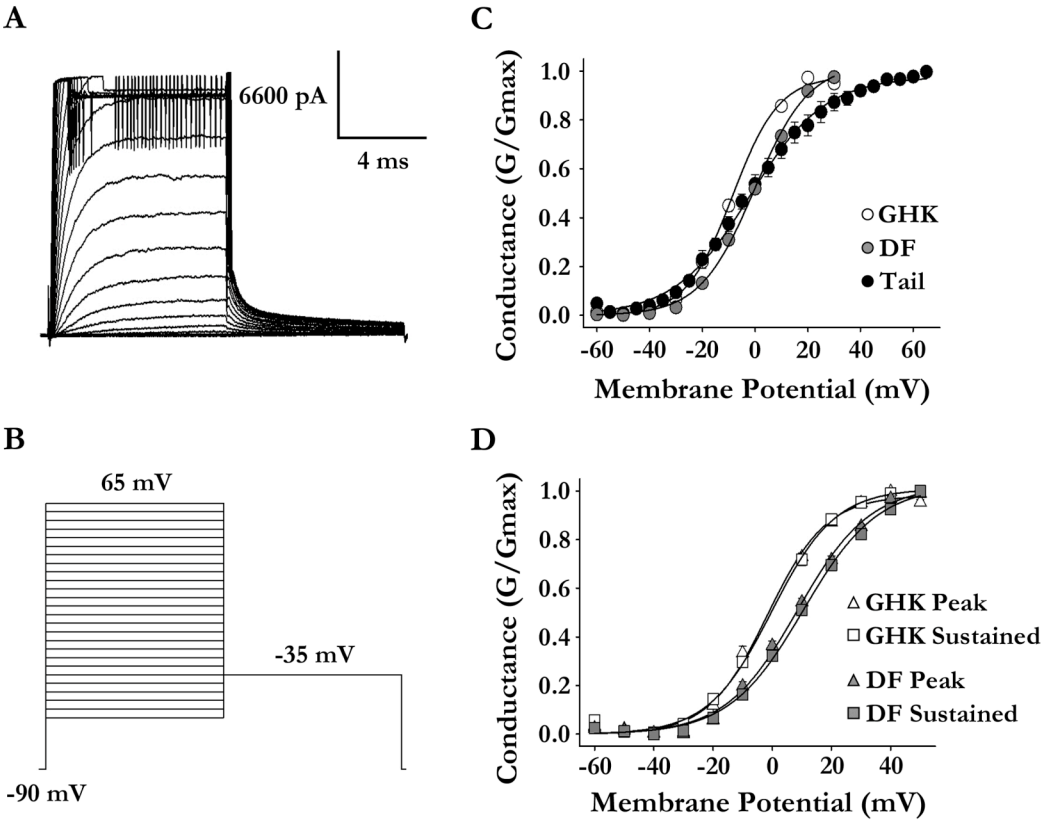
A
6600 pA
4 ms
B
65 mV
-35 mV
-90 mV
C
Conductance (G/Gmax)
1.0
0.8
0.6
0.4
0.2
0.0
-60 -40 -20 0 20 40 60
Membrane Potential (mV)
GHK
DF
Tail
D
Conductance (G/Gmax)
1.0
0.8
0.6
0.4
0.2
0.0
-60 -40 -20 0 20 40
Membrane Potential (mV)
GHK Peak
GHK Sustained
DF Peak
DF Sustained

Table 6.1. Steady state activation parameters of the Mauthner and MiD2cm cells

Cell	Current	Method	V_{50} (mV)	V_S (mV)
Mauthner	Peak	GHK	-1.8 ± 1.5	9.7 ± 0.1
	Peak	DF	8.5 ± 1.1[a]	12.1 ± 0.2[a]
	Sustained	GHK	0.0 ± 1.1	10.8 ± 0.3
	Sustained	DF	10.5 ± 0.9[a]	12.4 ± 0.2[a]
MiD2cm	Tail	Tail	-1.0 ± 3.1[c]	14.5 ± 1.7[b]
	Sustained	GHK	-8.2 ± 1.0	8.8 ± 0.5
	Sustained	DF	0.0 ± 1.0[c]	10.3 ± 0.4

Conductance voltage plots were fit with Boltzmann functions to determine the midpoint of activation (V_{50}) and the slope factor (V_S) values. Values are Mean ± SE. [a] Significantly different than the GHK normalization (t-test, $P < 0.001$, $n = 8$). [b] Significantly different than the GHK normalization (Kruskal Wallis Dunn's Method, $P < 0.05$). [c] Significantly different from the GHK normalization (One Way ANOVA, $P < 0.01$).

7. Literature Cited of Appendix I

Clay JR. 2000. Determining K^+ channel activation curves from K^+ channel currents. *European Biophysics Journal* 29:555-7

Clay JR. 2009. Determining K+ channel activation curves from K+ channel currents often requires the Goldman–Hodgkin–Katz equation. *Frontiers in Cellular Neuroscience* 3:1-6

8. Appendix II

One of the goals of my thesis was to characterize the zebrafish Kv1.1 protein using electrophysiology to determine the type and proportion of current the Kv1.1 containing channels were contributing to the total voltage gated potassium currents present in the Mauthner and MiD2cm cells. Initially my intention was to pharmacologically block the Kv1.1 channels using DTX_K, however maintaining patches for periods long enough to administer the toxin and then record proved difficult. Therefore my next approach was to clone out the zebrafish Kv1.1 channel and express it in Xenopus oocytes, whereby I would use two electrode voltage clamp to record the potassium currents. Prior molecular work had shown the zebrafish Kv1.1 protein was encoded by two different genes, G62942 and G17108, which were paralogues of one another. Syntenic relations showed G62942 to have greater conservation when compared with mouse and human, while protein encoded by G62942 showed greater amino acid similarity with human, mouse and rat (see Results section 3.1). Furthermore, my RT-PCR data showed G62942 was expressed at 48 hpf and retained in adult brain, (Figure 3.7) while in situ staining suggested it to be present in the Mauthner cell. Therefore I chose to clone out the G62942 gene and express it in oocytes first. Unfortunately I was unsuccessful in recording large amplitude currents necessary for analysis, and only observed very small amplitude currents. One explanation for the lack of current may be due to low surface expression of the protein. Mammalian Kv1.1 contains an ER retention signal in the pore region, which was conserved in the zebrafish Kv1.1 sequence (Zhu et al 2005; Zhu et al 2001; 2003).

Yet in spite of this, Dr. Gallin's lab has been able to express mouse Kv1.1 in oocytes and record currents, suggesting ER retention of the zebrafish protein is unlikely. Another possibility is that very little protein was being transcribed. To confirm the problem immunohistochemistry experiments could be performed to determine if the protein is being expressed it all and if so, where it is located.

8.1 Xenopus oocyte expression

Primers were designed to encompass the open reading frame of LOC795942 (G62942) with the forward primer having an XhoI restriction site and Kozak sequence added to it. A SpeI restriction site was added to the 5' end of the reverse primer. The primer pair was WJG2862/WJG2847 with sequences Fwd 5'- GGCTCGAGGCCACCATGACAGTTGTGGCTGGGG -3' and Rev 5'- GGACTAGTCTAGACATCGGTTAGCAGCTTACTT -3'. The PCR reaction was (in µl): 36.25 molecular grade water, 10 HF buffer, 1 10 mM dNTPs, 1 cDNA, 1.25 Fwd primer, 1.25 Rev primer, 0.5 Phusion polymerase. This was aliquoted into 4 tubes of 12.5 µl each. The PCR program was: 1. 2 min at 98^{o}C, 2. 30 s at 98^{o}C, 3. 7 s at 60^{o}C, 4. 90 s at 72^{o}C, 5. Go to step 2, repeat 30 times, 6. 7 min at 72^{o}C, 7. Hold at 4^{o}C. Immediately after, 0.5 µl of Taq 20a polymerase was added to each of the PCR reaction tubes and the tubes were incubated at 72^{o}C for 10 minutes to produce A overhangs. The PCR products were run out on a 1% agarose gel and imaged as previously mentioned. A single band at 1500 bp was cut out and extracted using the Qiagen extraction kit and eluted in 30 µl of molecular grade water.

The PCR product was cloned into the pCR 4 TOPO vector by adding 4 µl of pcr product to 0.5 µl salt solution and 0.5 µl vector and leaving it at room temperature for 5 minutes. 2.5 µl of the cloning mixture was added to 25 µl of One shot Chemically competent *E. coli* cells and placed on ice for 5 minutes. The cells were then heat shocked for 30 s at 42^{o}C before adding SOC medium to them. The cells were shaken at 240 rpm and 37^{o}C for an hour before being plated on LB + AMP plates (100 µg/ml) and left to grow overnight in a 37^{o}C incubator.

Four colonies were randomly chosen from the plates and placed in 2 ml of LB+AMP medium in a culture tube. The tubes were placed on a shaker at 37^{o}C and left overnight. The plasmids were isolated using a Plasmid Mini Kit (Qiagen) and eluted in 50 µl of elution buffer. A restriction digest was used to confirm the presence of the 1500 bp insert in the four colonies. The digestion mixture was (in µl): 5 water, 2 Buffer D, 0.5 XhoI, 0.5 SpeI, 12 plasmid. This mixture was placed in a 37^{o}C water bath for one hour then run on a 1% agarose gel. The bands at 1500 bp were cut out and extracted using a Qiagen extraction kit. The amplicon was eluted in 30 µl of molecular grade water. Pop8 plasmid, which consists of the pXT7 vector and a cloned insert, was also digested using the same procedure. The 1500 bp insert, the open reading frame of LOC795942 (G62942), was ligated into the pXT7 vector using T4 DNA ligase. The reaction was (in µl): 6 water, 1 ligase buffer, 2 insert, 0.5 vector, 0.5 T4 DNA ligase or 0 water, 1 Ligase Buffer, 8 insert, 0.5 vector, 0.5 T4 DNA ligase. The ligation reactions were placed in a 16^{o}C sandbath overnight.

The plasmids were transformed into bacterial cells using electroporation. 2 µl of plasmid was added to 54 µl of XL1-Blue *Escherichia coli* cells then placed into a cuvette. The cuvette was placed in the electroporator and pulsed with 1800 mV. Immediately after 940 µl of SOC medium was added to the cuvette. The mixture was then transferred to a 15 ml conical tube and placed in the 37^{o}C shaker/water bath for at least 45 minutes. The cells were plated on LB + AMP plates and placed in the 37^{o}C incubator overnight. Random colonies were chosen, mini-prepped using a Plasmid Mini kit (Qiagen) and the isolated plasmids were eluted in 50 µl of molecular grade water.

A colony PCR was run using the WJG2862 and WJG2847 primers and 300 ng of plasmid as template. The mixture was (in µl): 81 water, 10 10x reaction buffer, 2 10 mM dNTP, 2 WJG2862, 2 WJG2847, 1 Taq 20a Polymerase. This mixture was aliquoted into 11.5 µl and to each tube 1 µl of a different plasmid was added. The mixtures were run using the DKVPCRG PCR program (section 2.3.1) with the following modifications. The annealing temperature was set at 60^{o}C with an extension time of 1 min 30 s and run for 30 cycles. The reactions were then run out on a gel and imaged as previously described.

The colonies that contained an insert were placed in 2 ml of LB + AMP medium and placed on a 37^{o}C shaker overnight. The plasmids were isolated using a Qiagen Plasmid Mini kit and then eluted in 50 µl of molecular grade water to prepare for sequencing using Big Dye. Four sets of primers were used in both the forward and reverse direction. Two primers were vector specific WJG1174 and WJG1175 produced against the pXT7 vector with sequences 5'-

TGCTTGTTCTTTTTGCAGAAG – 3’ and 5’ –

GCTTAGAGACTCCATTCGGG – 3’ respectively. Six other internal primers were produced using the sequencing application in the Primer3plus program. The sequence for the open reading frame of LOC795942 with 68 nucleotides of pXT7 vector sequence added on either side was entered into the program. The program produced an array of primers of which 6 were chosen. The names and sequences of the three primers in the forward direction are:

629int2 5’ – GTAACCCAAAGAAGCGGATG – 3’;

629int3 5’ – TCGAATTGATAGTGCGCTTCT – 3’;

629int4 5’ – CATCGCTGGTGTGCTGAC – 3’.

The names and sequences of the three primers in the reverse direction are:

629int5 5’ – GAGGTCTCATCCATGTTGTCC – 3’;

629int6 5’ – TGACCATAACAGACACAATAGCAA - 3’;

629int7 5’ – GACGCCAATGAAGAGGAAGA -3’.

Sequencing results were blasted using NCBI then aligned to verify the sequence of the open reading frame was correct before proceeding with mRNA synthesis.

Prior to mRNA synthesis, the pXT7/62942 plasmid was linearized using the XbaI restriction enzyme in a reaction containing (in µl): 1.5 molecular grade water, 2 10x Buffer D, 15 plasmid, 1.5 XbaI. The reaction was placed in a 37^{o}C water bath and left for 1.5 hours. The mix was then run on a gel and stained as previously described. The band was cut out, extracted using the Qiagen extraction kit and eluted in 30 µl of molecular grade water. 1 µl of purified product was run

out on a 1% agarose gel alongside three standards which contained 0.1, 0.5 and 1.0 µg of linearized DNA.

The linearized plasmid was used as a template to produce mRNA using the mMessage mMachine T7 polymerase kit. The reaction was set up at room temperature with the following (in µl): 4 water, 10 T7 2x NTP/ARCA, 2 10x T7 reaction buffer, 2 linear plasmid, 2 T7 enzyme mix. The reaction was pipetted up and down, microfuged then placed in a 37^{o}C water bath for two hours.

RNA recovery was performed by lithium chloride precipitation. 30 µl of lithium chloride and 30 µl of nuclease free water were added to the RNA synthesis reaction then placed in the -20^{o}C freezer for at least 2 hours. The reaction was then centrifuged at max speed for 15 minutes at 4^{o}C after which the supernatant was aspirated off. The pellet was rinsed with 70% ethanol and centrifuged again for 10 minutes at 8500 rpm. The ethanol was aspirated off and the RNA was dissolved in 30 µl of molecular grade water. It was stored at -80^{o}C in 5 µl aliquots. To check for purity 1 µl of RNA was run on a 1% agarose gel.

Oocytes were injected with RNA, ranging in volume from 4.6 nl to 50.4 nl, then placed in a vial containing MBM or ND96 and stored at 18^{o}C.

8.2 Expressing zebrafish voltage gated potassium channel 1.1 in Xenopus oocytes

No successful recordings of Kv1.1 currents were obtained from oocytes, suggesting the channel was not able to be expressed. Several factors were altered in an attempt to find the optimal conditions for the channel to be expressed. After injections, most oocytes were incubated in MBM at 18^{o}C while some were

incubated in ND96. I also tried to alter the volumes of mRNA injected into the oocytes but this did not prove successful. A 1:10 dilution of the original RNA was made, injected into the oocytes at different volumes and incubated in either MBM or ND96 but to no avail. Procedural errors on my part were eliminated as I had colleagues produce the RNA and inject the RNA into the oocytes but this did not change the result. To rule out any problems associated with the plasmid the sequence of the Kv1.1 open reading frame was double checked to ensure the sequence was encoding a viable protein, in which case it was. There was a single polymorphism detected within my cloned sequence but it produced a silent mutation.

To record the currents of the zebrafish Kv1.1 a second expression system may be necessary, such as HEK-293 cells. Another possibility would be to clone out the open reading frame of G17108 and see if it would express in oocytes on its own or in combination with G62942.

9. Literature Cited for Appendix II

Zhu J, Gomez B, Watanabe I, Thornhill WB. 2005. Amino acids in the pore region of Kv1 potassium channels dictate cell surface protein levels: a possible trafficking code in the Kv1 subfamily. *The Biochemistry Journal* 388:355-62

Zhu J, Watanabe I, Gomez B, Thornhill WB. 2001. Determinants Involved in Kv1 Potassium Channel Folding in the Endoplasmic Reticulum, Glycosylation in the Golgi, and Cell Surface Expression. *Journal of Biological Chemistry* 276:39419-27

Zhu J, Watanabe I, Gomez B, Thornhill WB. 2003. Heteromeric Kv1 potassium channel expression: amino acid determinants involved in processing and trafficking to the cell surface. *Journal of Biological Chemistry* 278:25558-67

10. Appendix III

Figure 10.1. Determining which exponential best fits the potassium currents of the Mauthner cell

To determine the decay kinetics of the potassium current in the Mauthner cell, the currents were fit with an exponential. Currents were fit with a single, double or triple component function. To determine which best fit the current, the sum of squared errors were statistically compared using a One Way ANOVA. The exponential that gave the smallest sum of squared error value and that was significantly different from the others was considered the best fit. The graphs show that currents at -10 and 0 mV were best fit with a single exponential while the currents elicited between 10 and 40 mV were best fit with a double exponential. a denotes significantly different from the single exponential (ANOVA, $P < 0.05$, $n = 8$).

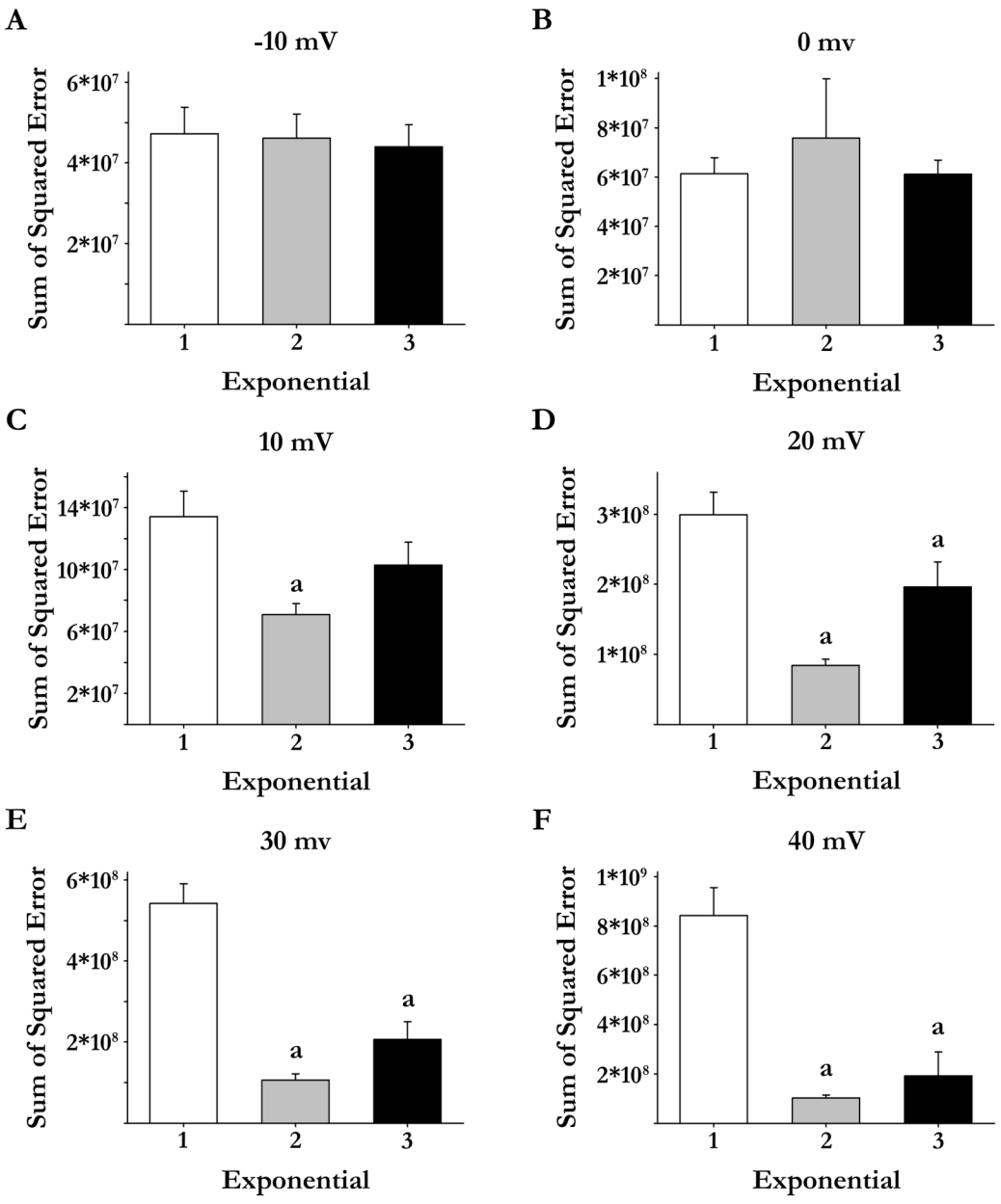
A
-10 mV
Sum of Squared Error
6*10^7
4*10^7
2*10^7
1
2
3
Exponential
B
0 mv
Sum of Squared Error
1*10^8
8*10^7
6*10^7
4*10^7
2*10^7
1
2
3
Exponential
C
10 mV
Sum of Squared Error
14*10^7
10*10^7
6*10^7
2*10^7
a
1
2
3
Exponential
D
20 mV
Sum of Squared Error
3*10^8
2*10^8
1*10^8
a
a
1
2
3
Exponential
E
30 mv
Sum of Squared Error
6*10^8
4*10^8
2*10^8
a
a
1
2
3
Exponential
F
40 mV
Sum of Squared Error
1*10^9
8*10^8
6*10^8
4*10^8
2*10^8
a
a
1
2
3
Exponential